Techniques for Communications and Geolocation using Wireless Ad Hoc Networks

A thesis
Submitted to the faculty of the

Worcester Polytechnic Institute

In partial fulfillment of the requirements for the
Degree of Master of Science
in
Electrical and Computer Engineering

By

Hasti AhleHagh

May 14, 2004

Approved by:

Dr. William R. Michalson, Thesis Advisor

Dr. Kaveh Pahlavan, Committee Member

Dr. R. James Duckworth, Committee Member

Dr. Fred J. Looft, Department Head

ABSTRACT

TECHNIQUES FOR COMMUNICATIONS AND GEOLOCACTION USING WIRELESS AD HOC NETWORKS

Networks with hundreds of ad hoc nodes equipped with communication and position finding abilities are conceivable with recent advancements in technology. Methods are presented in this thesis to assess the communicative capabilities and node position estimation of mobile ad hoc networks. Specifically, we investigate techniques for providing communication and geolocation with specific characteristics in wireless ad hoc networks. The material presented in this thesis, communication and geolocation, may initially seem a collection of disconnected topics related only distantly under the banner of ad hoc networks. However, systems currently in development combining these techniques into single integrated systems. In this thesis first, we investigate the effect of multilayer interaction, including fading and path loss, on ad hoc routing protocol performance, and present a procedure for deploying an ad hoc network based on extensive simulations. Our first goal is to test the routing protocols with parameters that can be used to characterize the environment in which they might be deployed. Second, we analyze the location discovery problem in ad hoc networks and propose a fully distributed, infrastructure-free positioning algorithm that does not rely on the Global Positioning System (GPS). The algorithm uses the approximate distances between the nodes to build a relative coordinate system in which the node positions are computed in

three-dimensions. However, in reconstructing three-dimensional positions from approximate distances, we need to consider error threshold, graph connectivity, and graph rigidity. We also statistically evaluate the location discovery procedure with respect to a number of parameters, such as error propagation and the relative positions of the nodes.

Acknowledgements

I would like to thank my advisor, Professor William R. Michalson for his support and guidance without which this work would not have been possible. He proposed several challenging research topics to work on and opened the whole new world of Ad hoc Networks and Geolocation to me and has certainly been my most memorable experience at WPI. Furthermore, I would like to sincerely thank Professor Kaveh Pahlavan not just for serving on my MS thesis committee but also for initially introducing me to Worcester Polytechnic Institute and Research. I would like to thank Professor James Duckworth for being part of my committee. Professor Levesque provides me with great support during my study and I would like to thank him. I would like to thank BEI that provided me with graduate research assistantship.

I would like to thank my friends at CARIN for providing a nice atmosphere of research. My friend Nassim provided me with great support, I would like to thank her.

Last but not least, I would like to thank my parents for their understanding, love, and support.

Table of Contents:

Table of Figures:

Table of Tables:

Chapter 1 : Introduction

1.1 The Emergence of Broadband Wireless Ad Hoc Networks with Geolocation

The maturing of communication theory, networking, geolocation, and security, as well as integrated circuitry, microelectromechanical systems (MEMS) has fomented the emergence of wireless ad hoc networks with navigation capability and precipitated the economic and computational feasibility of networks of hundreds of self-sufficient tiny ad hoc nodes.

The work in this thesis is principally motivated by the Real-Time Troop Physiological Status Monitoring project, sponsored by the US Army Telemedicine and Advanced Technology Research Center (TATRC). This project is focused on developing a system for evaluating the real-time physiological status of combat soldiers and other personnel who must work in extreme environments. These environments are characterized by a lack of pre-existing communications infrastructure and, in many cases of interest, may not have access to navigation systems such as the Global Positioning System (GPS). This system can be implemented as a multiple level hierarchy. At the lowest level are wearable sensors, capable of collecting vital sign information from individual people in real-time. Along with the sensors, tiny communication and geolocation transmitters transmit data and 3D position information to higher levels of the hierarchy for additional processing. The data exchanged can be an ultrasound image with high data rate or geolocation information with low data rate. At the top of the hierarchy

lies a communication and location infrastructure tying all of the various sensors together, thus providing a common interface mechanism for communicating information between the sensors and the emergency service providers [Mic03].

This system should be flexible, as it may be implemented unexpectedly in a desert, building, or other settings. Power consumption is an important challenge in the general development of the system. This technology may be carried into the field and other emergency situations and used by soldiers and medics under hostile conditions, so it is important to minimize power consumption of the system.

In rear combat areas, in frontline areas, or during amphibious operations or rapid mechanized advances, battlefield conditions are often chaotic. Highly mobile units, such as artillery and tanks, quickly detach from combat groups to join and support others. The number of mobile units may vary from tens to thousands. Mobility of these units may vary, or be static relative to each other in different situations or at different times. The bandwidth efficiency is also a very important factor, as combat areas tend to be low bandwidth at sometimes and high bandwidth at others. Communication and geolocation technology used in these situations should be scalable, stable, reachable, high capacity, bandwidth efficient, flexible, and robust to rapid and unpredictable changes in the network topology.

The most promising methods for data communication and geolocation in these types of environments are ad hoc networks that support both distributed data communications and localized geolocation. An ad hoc network is a collection of wireless ad hoc nodes that can communicate with each other through multi-hop routes without any dependence on a fixed infrastructure or centralized administration. In an ad hoc network

a node is both an end terminal and a router. Routing in ad hoc networks is in the multi-hop fashion, which means each node in the network helps to route the packet to the destination, and there is no centralized device to route the packets. An ad hoc network is shown in Figure 1.1.

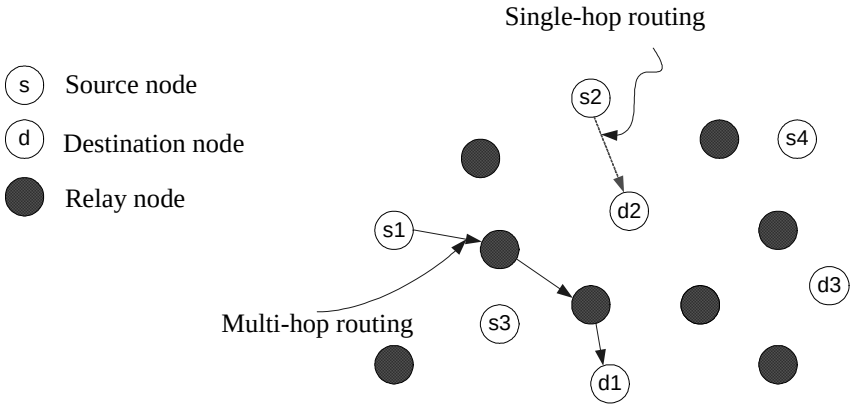

Figure 1.1: Wireless ad hoc network with multi-hop routing vs. single hop routing.

Ad hoc networks are complicated due to the routing caused by mobility and lack of centralized infrastructure, security due to the wireless environment and the fact that each node routes packets destined for other nodes, and power consumption. Numerous routing protocols have been developed to address the problem of establishing and maintaining multi-hop routing in a dynamically changing network topology. Protocols are detailed in [Per94][Per02][Bro98][Cam02][Mau01]. Several research papers have been published that compare the performance of ad hoc routing protocols [Cam02][Bro98]. Many performance studies of these routing protocols focus on higher layers and tend to ignore the effects of the other layers, particularly the effect of the channel model on routing protocol performance. There appears to be no comprehensive study that classifies ad hoc routing protocols based on the system requirements described

above. In this thesis we study physical layer effects such as path loss and fading and show that these effects alter the absolute performance of different routing protocols in different ways. We show that because physical layer effects impact different protocols differently, including these effects in protocol simulations can change the relative ranking amongst protocols for the same simulation scenario. Briefly, for the data communication part of the system under development, we study scalability, stablity, reachablity, capacity, bandwidth efficiency, and flexibility of the system as a function of a channel model, node density distribution, transmission range, mobility, and traffic load. Although each ad hoc node consists of different protocol layers that all are important in providing Quality of Service (QoS) in the network, because the routing layer is the most critical layer for ad hoc networks, we mostly concentrate our study on routing protocols and mention other layers only for their interactions with routing protocols.

For the system under development in this project providing location information along with data communication is also desired. Geolocation techniques for the system under development should be distributed, power efficient, and anchor free. There is a set of applications in mobile ad hoc networks that are location-dependent. For instance, position information can be useful in position dependent routing protocols [Bas98][Mau01][Ko98]. Localized positioning of the nodes in an ad hoc network is desirable, particularly in situations where GPS or navigation aids are either not accessible, or are not practical to use. GPS is generally not accessible in many situations, including indoors or underground, due to the GPS signal attenuation or the lack of a line-of-sight (LOS) to the GPS satellites. Similarly, navigation aids such as compasses behave erratically in the vicinity of large metal objects or electrical fields. An idea has

been recently proposed [Bah00] that uses a few fixed, base-station like, powerful long-range nodes. These beacons can communicate to all other nodes in the network and enable them to calculate their locations. This solution has several shortcomings. First, it is in contrast to the definition and nature of an ad hoc network where the infrastructure is not fixed and base stations are not consistent with the ad hoc nature of the system. Secondly, long-range beacons are significantly less fault tolerant in the presence of obstacles than ad hoc networks. Finally, the security of the whole network is reduced if one of the long-range beacons is compromised. Other alternative methods for geolocation systems are Cricket [Pri00], and Bat [War99]. These systems have been proposed mainly for indoor scenarios and used in places that GPS does not work. Generally, these systems need a large number of position beacons to provide the geolocation information. The drawbacks of these systems are due to their dependence on a fixed base and the necessity for a large number of nodes, which causes deployment issues. Figure 1.2 shows the Bat and Bah00 localization approaches.

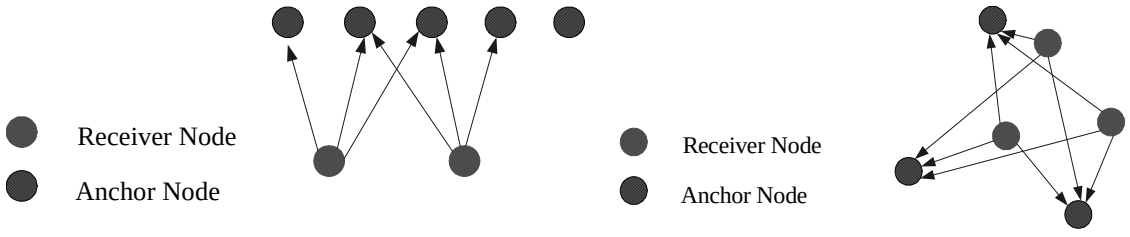

Figure 1.2: Indoor positioning approaches (a) Bat approach, (b) Bah00 approach.

Another solution to the geolocation problem that we consider in this thesis is to equip ad hoc nodes with hardware that estimates the range between the nodes, and to

employ an algorithm that can calculate the location of the nodes in a distributed manner based on the range measurements. Several distributed algorithms for geolocation have been proposed and several off-the-self technologies exist that we review in more detail in this chapter. Based on this review we justify the need for the further study of the geolocation issue in this thesis.

A number of companies offer a product that enables broadband ad hoc data communication. MeshNetworks [Mes][Sch02] introduced its Mesh Enabled Architecture (MEA) mobile broadband system that simultaneously delivers broadband data with 6Mbps data burst, high quality voice and geolocation information. The company offers a PCMCIA card that is capable of peer-to-peer routing and can be used with a laptop, PDA, or other computers. While the MEA provides peer-to-peer communication without any infrastructure, adding infrastructure can increase the coverage area, accuracy of the geolocation information, and can route data to the Internet and Public Switched Telephone Network (PSTN). Figure 1.3 shows the MEA localization and communication structure. One of the main drawbacks of this system is that it does not provide the variable bandwidth that is needed for our purpose. Nova Engineering Company [Nov] has developed a Mobile Router to maintain robust communication links in mobile ad hoc networks. This router is capable of multi-hop ad hoc routing with a burst data rate of 1Mbps. The main disadvantage of this system is that Mobile Router should be used as an external device and is not available as a card. In addition, although the Mobile Router can be attached to the GPS receiver, it doesn't provide localized positioning information. MobileRoute is software developed by the Science Research Corporation (SRC) [Mob] to

provide ad hoc peer-to-peer routing capability. MobileRoute is designed to be independent of the actual wireless interface card and radio technology.

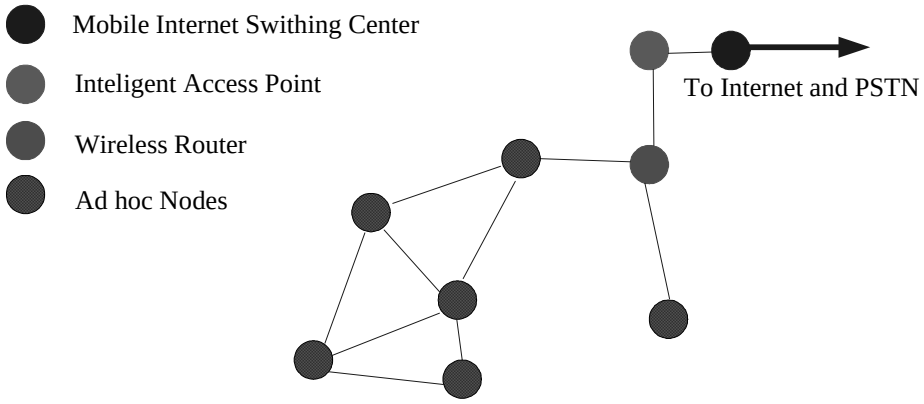

Figure 1.3: MeshNetwork localization and communication approaches.

The research documented in this thesis develops mathematical constructs to define, propose and simulate a location discovery algorithm designed for mobile ad hoc networks. We use both analytical and graph theoretic approaches to find a solution for geolocation in wireless ad hoc networks that does not impose any infrastructure on the network. Moreover, we propose a distributed infrastructure-free localization algorithm that uses distances between the nodes to calculate their location. Percolation theory is used to study scaling in the geolocation and communication algorithm. This thesis deals exclusively with simulation, and it is hoped that the algorithms will soon be tested in reality. The algorithm proposed in this thesis can be implemented on wireless cards with some modifications.

1.2 A Review of Localization Algorithms

Different types of distributed localization algorithms have been proposed so far. Some of these algorithms rely on anchor nodes, nodes with known position, and iteratively calculate the locations of the other nodes in the network based on the location of these anchor nodes. It has been shown that in these kinds of algorithms, most nodes in the network should be anchor nodes. These algorithms have been divided into two categories: One starts with a few nodes with known location, and calculates the location of the other nodes in the network gradually [Sav01], the other uses anchor nodes that are distributed throughout the network topology to calculate location of other nodes. However, the first type of algorithm may not solve the problem of location finding even when a valid coordinate system exists because errors in the local location estimates often lead to large global errors. In addition, for anchor-based algorithms [Sav01], it may be difficult to establish anchor-based nodes and also the numerical stability of these algorithms is questionable.

Another set of localization algorithms does not rely on any navigation system. These algorithms try to calculate location of the nodes based on the measured distances between them. The issues with these algorithms are a susceptibility to the local minima and propagation of error throughout the network. Local minima, shown in Figure 1.4a, occur when we start with a weight set for the network corresponding to point P. If we perform gradient descent, the minimum we encounter is the one at P_1, not that at P_2. P_1 is called a local minimum and corresponds to a partial solution for the network in response to the training data. Propagation of error occurs when the location calculation is only based on noisy range measurements. The location of the first node is error free, but

the location of the second and third nodes contains the error in the range measurements plus the error in the location of the initial node, this procedure is shown in Figure 1.4b.

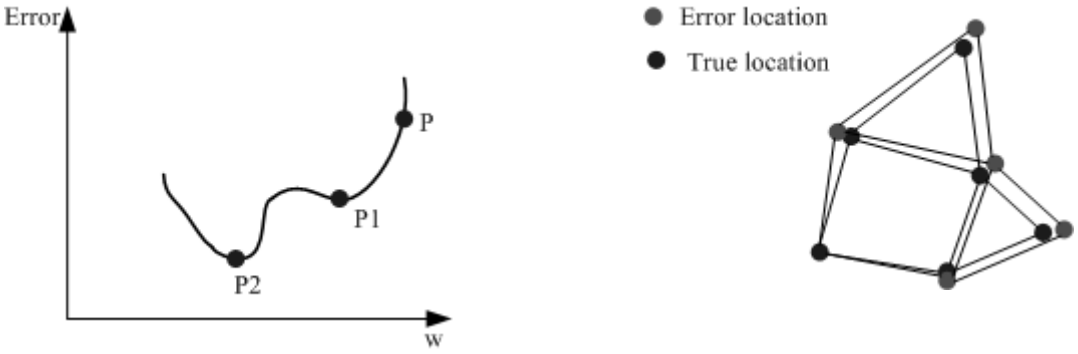

(a) **(b)**

Figure 1.4: (a) local minima, (b) Error propagation.

In this thesis we propose an anchor-free localization algorithm that relies only on the distances between the nodes, and uses heuristics to reduce the effect of error propagation throughout the network topology.

1.3 Research Goals and Approach

The two main goals of this research are:

1. To identify the best techniques for providing communication in wireless ad hoc networks. For this part we narrow our study to routing protocol performance evaluation. We classify the applicability of the DSDV, DSR, AODV, DREAM, and LAR routing protocols as a function of system parameters such as channel model, traffic load, and mobility.

2. To formulate the problem of distributed location discovery in ad hoc networks and propose a method for 3D location discovery using noisy range measurement information.

For the first part, communication, we evaluate the performance of ad hoc routing protocols using the ns-2 simulator according to performance metrics such as: packet loss, throughput, routing overhead, and delay. Specifically, we compare the performance of AODV, DSR, DSDV, DREAM, and LAR. We also present a set of factors at the channel level that are relevant to the performance evaluation of higher layer protocols. Specifically, we have extended the ns-2 to simulate urban and indoor environments, and have studied factors that include signal reception, path loss, and fading on routing protocols. We further analyze the effect of mobility and congestion on routing protocol functionality and classify routing protocols according to their physical layer parameters, congestion and mobility so that we may identify design issues important in the development of new routing protocols.

Relative to our discussion of localization algorithms, we first formulate a method for calculating node location based on measured distances. We propose a distributed, infrastructure-free positioning algorithm that does not rely on GPS. The algorithm uses the distances between the nodes to build a relative coordinate system in which positions of the nodes can be calculated in 3D. Moreover, we define the sources of error in distance measurements as well as the initial locations of nodes, and we model the errors generated by those sources. We measure the quality of a solution generated by the proposed location discovery procedure. There are situations where an assessment of the quality of a solution generated by the location discovery process may be necessary, and we examine methodologies of estimating the performances of the location discovery

process. From here, we define several objective functions and show how they maybe used in an optimization-based location discovery procedure.

1.4 Research Overview

The material presented in this thesis consists of two related topics. In Chapter 2, we introduce the concept of ad hoc communication and describe the fundamental issues in ad hoc networks. An abstract definition of a mobile ad hoc network appropriate for this work is given along with the parameters that serve to compare networks. In Chapter 3, we discuss channel issues for mobile ad hoc networks, study the quality factors, and explain the implementation of the WPI indoor channel model in ns-2. In Chapter 4, we study and compare the performance of ad hoc routing protocols in different scenarios, such as indoor, outdoor, and Rayleigh fading channels. We show that in these scenarios, the channel model has a significant effect on the performance of the ad hoc routing protocols. Chapter 5 introduces positioning in mobile ad hoc networks. In this chapter, we review the algorithms that exist for localization, and highlight some of these systems. Chapter 6 introduces our algorithm for localization in ad hoc networks and discusses the general problems that exist in this algorithm. In Chapter 7, we study performance of our proposed localization algorithm. Finally in Chapter 8, we conclude the thesis and propose a path for further study in Chapter 9.

Chapter 2 : Ad hoc Network Segments

An ad hoc network is composed of a number of ad hoc nodes deployed in an environment with or without a gateway to the Internet or PSTN. The ad hoc nodes are capable of wireless peer-to-peer communication and are characterized by their protocol stack, mobility, power management, and application. The environment refers to the region that an ad hoc network is providing service and spans a variety of environments with specific characteristics and effects on the propagation of radio signals. The characteristics of the radio channel change in different settings. While ad hoc nodes and their characteristics are discussed in this chapter, the channel issues are discussed in the next chapter.

2.1 Protocol Stack of an Ad hoc Node

Each ad hoc node consists of a data communication protocol stack as shown in Figure 2.1. Similarly to a wired network, the protocol stack for a wireless ad hoc network consists of the physical layer, data link layer, network layer, transport layer, and application layer. In addition to the stack layers, wireless ad hoc networks typically have power management and mobility management planes. Networking techniques for ad hoc networks must address the challenges imposed by the wireless environment: the need for mobility and self-sufficiency characteristics. For instance, in contrast to wired networks, the conventional layered protocol stack in not well-suited to the ad hoc wireless networking environment because it does not exploit the potential improvements in

performance that can be obtained by considering the properties of the physical and data link layers when designing and operating the Medium Access Control (MAC) protocols. An important consideration in an ad hoc routing protocol is a mechanism to account for topology changes to optimize multi-hop routing in an ad hoc network. Similarly, there are potential benefits to be obtained by developing protocols that jointly address the routing and MAC functions.

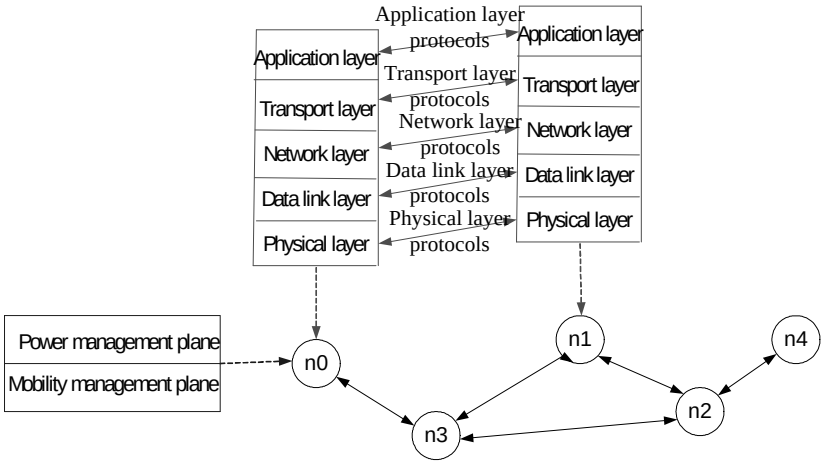

Figure 2.1: Protocol stack for an ad hoc network with power and mobility management plane.

The physical layer is responsible for frequency selection, carrier frequency generation, signal detection, modulation, and data encryption [Aky02]. Frequency generation and signal detection are primarily associated with the underlying hardware and transceiver design. Choosing a good modulation scheme is essential for reliable communication in an ad hoc network. While M-ary modulation schemes can reduce transmission time by sending multiple bits per symbol, they result in complex circuitry and increased radio power consumption [Shi01]. In [Shi01], it is shown that at low SNR environments, M-ary is more energy efficient, and at higher SNR, binary modulation is

more energy efficient. It is well known that the wireless channel can be expensive, in terms of both energy and implementation complexity. So energy efficiency in the physical layer is an important issue. In general, the physical layer addresses the needs of simple but robust modulation, transmission, and receiving techniques in ad hoc networks. It is expected that improvement in the overall performance of ad hoc networks can be obtained by considering the properties of the physical and data link layers when designing and operating the MAC protocols.

The data link layer is responsible for data stream multiplexing, as well as data frame detection, medium access and error control. It ensures reliable point-to-point or point-to-multipoint connections in a communication network. Different MAC and error control strategies exist for ad hoc networks. The major objective in MAC protocols is to develop a protocol that optimizes spectral reuse, and thus, maximizes aggregate channel utilization, as well as to fairly and efficiently share a communication resource between ad hoc nodes. Novel protocols and algorithms are needed to tackle the resource constraints and application requirements of ad hoc networks. The MAC protocol in mobile ad hoc networks is also responsible for forming the network infrastructure and maintaining it in the face of mobility. So the primary goals of MAC protocols in ad hoc networks are to provide high QoS and low battery power consumption in mobile conditions.

Different MAC protocols have been proposed both for infrastructure-free and with-infrastructure (cellular, wireless LAN) networks. In cellular systems, the base stations form a wired backbone and a mobile station is one-hop away from the nearest base station. MAC protocols in these networks are centralized and they are only responsible for QoS and bandwidth efficiency. While MAC protocols in an ad hoc

network have the task of forming the network infrastructure and maintaining it in the face of mobility. MAC protocols in ad hoc networks should be decentralized. Different MAC protocols have been proposed for wireless networks. Among those IEEE CSMA/CA 802.11 is the first Wireless LAN standard and, so far, is the only one that has achieved a significant market. IEEE CSMA/CA is based on the Carrier Sense Multiple Access/Collision Avoidance (CSMA/CA) technique. Power Controlled Multiple Access (PCMA) is decentralized and specifically designed for ad hoc networks. We use the IEEE 802.11b MAC protocol in this thesis.

The Network layer is concerned with routing the data supplied by the Transport layer. As stated before, ad hoc networks consist of autonomous nodes that collaborate in order to transfer information. Usually these nodes act as end systems and routers at the same time. Many different protocols have been proposed to solve the multi-hop routing problem in ad hoc networks, each is based on different assumptions and intuitions.

We distinguish two different routing approaches: topology-based and position-based routing. Topology-based routing protocols use link information to perform packet forwarding. They can further divide into proactive, reactive and hybrid routing protocols. Proactive algorithms employ classical routing strategies such as distance-vector routing (e.g. DSDV) or link-state routing (e.g. OLSR). They maintain routing information about the available paths in the network even if these paths are not currently used. Reactive routing protocols (e.g. DSR, TORA, and AODV) maintain only the routes that are currently in use, thereby reducing the burden on the network when only a small subset of all available routes is in use at any time. Hybrid ad hoc routing protocols (e.g. ZRP) combine local proactive routing and global reactive routing in order to achieve a higher

level of efficiency. Position-based routing algorithms eliminate some of the limitations of topology-based routing by using additional positioning information. Position-based routing algorithms require information about the physical position of the participating nodes to perform packet routing in their networks. An example for each of the routing protocols will be discussed in more detail in this chapter.

2.2 Definition of an Ad hoc Network

For this thesis, the mathematical abstraction of an ad hoc network is that of an undirected graph. Nodes of the graph represent ad hoc nodes in the network while edges represent bi-directional communication links. The latter are characterized by two nodes having the ability to send information to one another. Nodes are situated at a physical position which, in general, may be 3D.

To define an ad hoc network, we require the following information:

- $G(V, E)$: A set of n_v (often abbreviated as n) vertices and n_e edges,
- n_i, $i = 1$ to n: the node id,
- (x_i, y_i, z_i), $i = 1$ to n: the node position in 2D or 3D,
- R_{ij}: The distance between node n_i and n_j,
- R_s: The maximum transmission range of each node in the Network, and
- There exists edge E_{ij} for each pair V_i and V_j if $|R_{ij}| \leq R_s$.

The node n_j is called a one-hop neighbor of node n_i if the distance between nodes n_j and n_i is less than the transmission range, R_s. A connected graph is one wherein any

two nodes have an uninterrupted path between them following the edges of the graph. In the physical context, this means that any two nodes can communicate with a finite number of hops between them. To compare one ad hoc network with another, the following parameters are useful:

- $[x_{1\max}, y_{1\max}, z_{1\max}]$: A cubic measure of the size of the area containing the network in 3D,
- $[x_{1\max}, y_{1\max}]$: A rectangular measure of the size of the area containing the network in 2D,
- N : The number of nodes in the Network,
- R_s : The maximum transmission range of the nodes in the Network, and
- $2n_e/n$: The average connectivity of a node in the Network.

To define the locations of nodes in the network with respect to each other, the following parameters are useful:

- $K_{i,k}$ $i, k = 1$ to n : A set of k -hop neighbors of node i .

2.3 Basic Routing Protocols and Problem Formulation

Routing protocols are different from each other based on the approach they use to solve the problems associated with the routing task in the network. Given an ad hoc network with known network parameters N , $[x_{1\max}, y_{1\max}]$, R_s , and $K_{i,k}$, it is desired to find an algorithm for routing messages from a source node to a destination node. There are different criteria that result in differences between different routing protocols, for example, which path should be selected? Who decides to select the path – the source or

the intermediate nodes? Figure 2.2 shows the routing decision approach in more detail. Different routing protocols answer the above questions in different ways.

As many of the suggested ad hoc routing algorithms have a traditional routing protocol as the underlying algorithm, it is necessary to understand the basic operation of conventional routing protocols like distance vector, link state and source routing:

Link state: in link-state routing each router first obtains a view of the complete topology of the network with a cost for each link and then computes the shortest path to every other router by using, for instance, Dijkstra's algorithm [Tan96].

Distance vector: in distance vector routing every node only monitors the cost of its outgoing links and periodically broadcasts an estimation of the shortest distance to every other node in the network [Tan96]. The receiving nodes then use this information to recalculate the routing tables.

Source routing: in source routing each packet carries the complete path it has to follow around the network, which requires great overhead if the route has many hops. Given that the routing decision is made at the source, it is easy to avoid routing loops.

Routing Protocol Goal	Which Path?	Shortest path (fewest number of hops) Shortest time (lowest latency) Shortest weighted path (utilize available bandwidth)
	Who detemines Routes?	Source routing Destination routing (hop-by-hop)

Figure 2.2: Routing protocol decision approach.

2.4 Ad hoc Network Routing Protocols Studied

In this section, we briefly describe the key features of the DSDV, DSR, AODV, DREAM, and LAR protocols studied in our simulations. We also describe the particular parameters that we chose when using each of these protocols for our simulations.

2.4.1 Destination Sequence Distance-Vector (DSDV)

DSDV is a hop-by-hop distance vector protocol routing protocol. DSDV is based on the idea of the classical Bellman-Ford routing algorithm with certain improvements. The key advantage of DSDV over the Bellman-Ford algorithm is that it guarantees loop-freedom.

Every DSDV node maintains a routing table that lists the next hop for each reachable destination. DSDV tags each route with a sequence number. These sequence numbers are assigned by the destination node and are used to distinguish stale routes from new ones, thus avoiding the formation of loops. A route with a greater sequence number is newer and more favorable than one with smaller sequence number. Each node in the network periodically transmits its routing table to its immediate neighbors. Additionally it increases its own sequence number by two. A node also transmits its routing table if a significant change has occurred in its table from the last update sent. So, the update is both time-driven and event-driven. The routing table updates can be sent in two ways: a full dump or an incremental update. A full dump sends the entire routing table to the neighbors and could span many packets. Alternatively in an incremental update only the routing table entries that have changed since the last update would be sent. When the network is relatively stable, incremental updates are sent to

avoid extra traffic and full dumps are sent infrequently. In a fast-changing network, incremental packets can grow big, so full dumps will be more frequent. When a node decides that its route to the destination has broken, it advertises the route to the destination with an infinite metric (delay, cost, bandwidth…) and a sequence number one greater than its sequence number for the route that has broken. This causes any node that routes packets through the destination node to incorporate the infinite-metric route into its routing table until a node hears a route to that destination with a higher sequence number. Figure 2.3 shows routing table for the node n_4 in the DSDV routing protocol. As can be seen from the figure, each routing table maintains the number of hops to each destination in the network and sends this table to its neighbors.

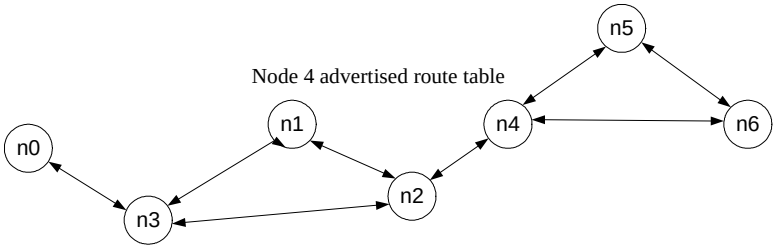

Destination	Metric (Num Hop)	Sequence Number
n0	3	S406_1
n1	2	S128_2
n2	1	S564_3
n3	2	S710_4
n4	0	S392_5
n5	1	S076_6
n6	1	S128_7

Figure 2.3: DSDV routing protocol.

2.4.2 Dynamic Source Routing (DSR)

DSR uses source routing instead of hop-by-hop routing, with each packet to be routed carrying in its header the complete, ordered list of nodes through which the packet must pass. The key advantage of source routing is that intermediate nodes do not need to maintain up-to-date routing information in order to route the packets that they forward, since the packets themselves already contain all the routing decisions. This fact, coupled with the on-demand nature of the protocol, eliminates the need for the periodic route advertisement and neighbor detection packets required by other protocols. The DSR protocol consists of Route Discovery and Route Maintenance phases. When an ad hoc node attempts to send a data packet to a destination for which it does not already know the route, it uses the Route Discovery process to dynamically determine such a route.

Route Discovery works by flooding the network with Route Request (RREQ) packets. Each node that receives a RREQ rebroadcasts it, unless it is either the destination node or it has a route to the destination in its route cache. Such a node replies to the RREQ with a Route Reply (RREP) packet that is routed back to the original source. RREQ and RREP packets are also source routed. RREQ builds up the path traversed across the network. The RREP packet routes itself back to the source by traversing this path backward. The route carried back by the RREP packet is cached at the source for future use. This process is shown in Figures 2.4a and 2.4b.

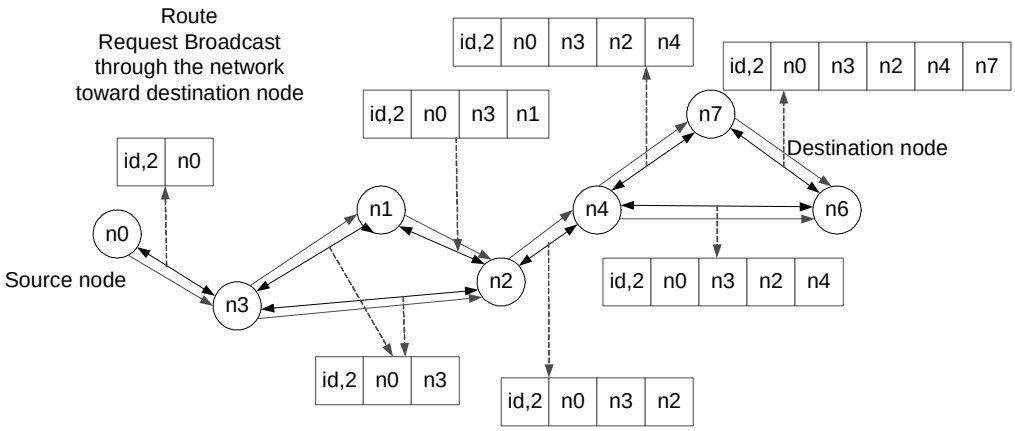

Figure 2.4a: In the Route Request phase every source node broadcasts a route request towards the destination node.

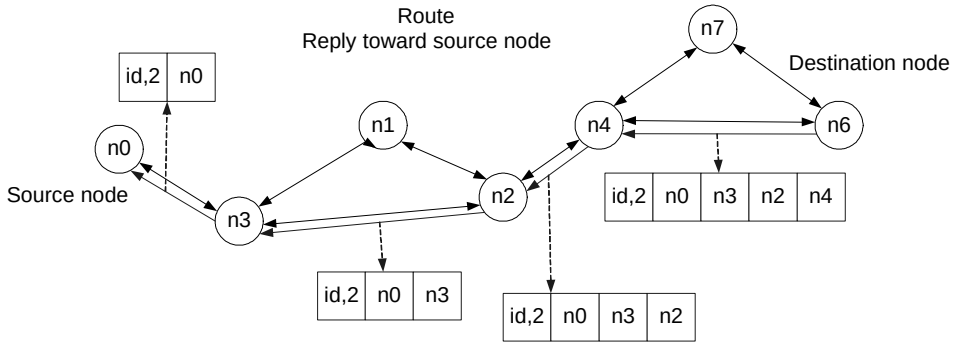

Figure 2.4b: In the route reply phase destination nodes route the packets toward the source node in the path traversed within the route request phase.

Route Maintenance is the mechanism by which the source node detects if the network topology has changed such that it can no longer use its route to the destination node. If any link on a source route is broken, the node is notified using a Route Error (RERR) packet. The source removes any route using this link from its cache and uses any other route in its cache to the destination node or initiates a new route discovery process. DSR makes very aggressive use of source routing and route caching. No special mechanism to detect routing loops is needed. Also, any forwarding node caches the source route in a packet, forwards it for possible future use.

2.4.3 Ad hoc On-demand Distance Vector (AODV)

AODV is a combination of both the DSR and DSDV routing protocols. It uses the basic on-demand mechanism of Route Discovery and Route Maintenance from DSR, plus the use of hop-by-hop routing, sequence numbers, and periodic beacons from DSDV.

When a source node needs a route to some destination, it broadcasts a Route Request message to its neighbors, including the last known sequence number for that destination. The Route Request is flooded through the network until it reaches a node that has a route to the destination. Each node that forwards the Route Request creates a reverse route for itself back to the source node. When the Route Request reaches the node with a route to the destination node, that node generates a Route Reply that contains the number of hops necessary to reach the destination node and the sequence number for the destination seen by the node generating the Reply. Each node that participates in forwarding this Reply back toward the source node creates a forward route to the destination. The state created in each node along the path from the source to the destination is hop-by-hop; that is, each node remembers only the next hop and not the entire route, as would be done in source routing.

In order to maintain routes, AODV normally requires that each node periodically transmit a Hello message, with a default rate of once per second. Failure to receive three consecutive Hello messages from a neighbor is taken as an indication that the link to the neighbor in question is down. Alternatively, the AODV specification briefly suggests that a node may use physical layer or link layer methods to detect link breakages to the nodes that it considers neighbors. When a link goes down, any upstream node that has

recently forwarded packets to a destination using that link is notified via an unsolicited Route Reply containing an infinite metric for that destination. Upon receipt of such a Route Reply, a node must acquire a new route to the destination using Route Discovery as described above. Figures 2.5a and 2.5b explain AODV in more detail. In Figure 2.5a, when the source node, n_0, wants to send a packet to the destination node, n_6, it starts a Route Request to find a route to the destination. Route Reply, as shown in Figure 2.5b, is used to set the path toward the source node.

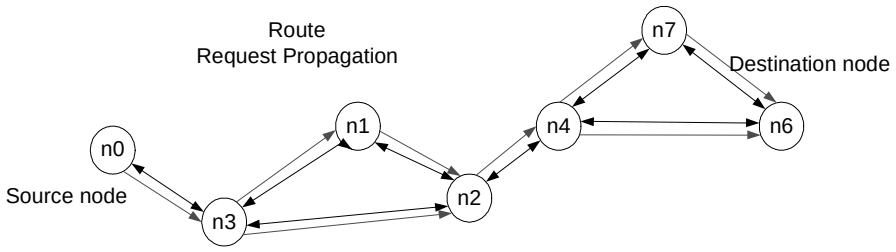

Figure 2.5a: Propagation of Route Request (RREQ) Packet.

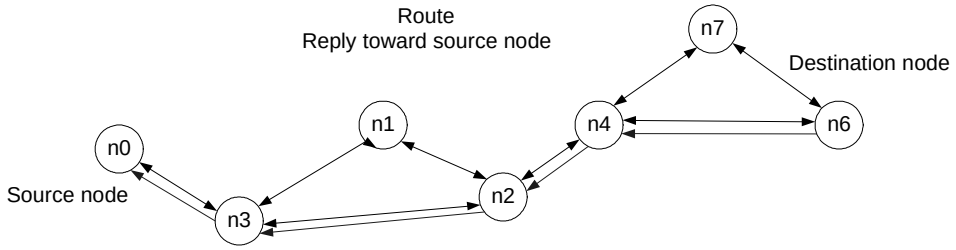

Figure 2.5b: Path taken by the Route Reply (RREP) packet.

2.4.4 Location-Aided Routing (LAR)

LAR is an on demand routing protocol that uses location information to improve the route discovery phase. On demand routing protocols usually use a flooding approach for route discovery. In LAR, location information is used to confine the flooding

procedure to a certain area. In order to send data to a destination, the source node calculates the expected zone toward the destination based on its location information. In this way rather than flooding the whole network with information, the source node only sends information toward the request zone. The set of nodes that forwards the route discovery packets are called the request zone.

The request zone usually includes the expected zone. Two types of request zone have been proposed in [Ko98]. In the first type, a rectangular geographic region is defined in which a node forwards the packet towards the destination. In this case the request zone is a rectangle with the source node in one corner and a circle, which contains the destination node in another corner. The expected zone is a circle with its center at the destination node and a radius of $R = V_{avg} \times (t_1 - t_0)$, where t_1 is the current time, t_0 is the time that this location information is updated, and V_{avg} is the average velocity of the destination node. The second type of request zone is defined using the destination coordinates and distance. In this case a node forwards the packet if it is closer to the destination than the node that it got the packet from. Each forwarding node overwrites the distance field with its own current distance to the destination. Figure 2.6 shows the request and the expected zone when the source node, n_2, sends the packet toward the destination node, n_6.

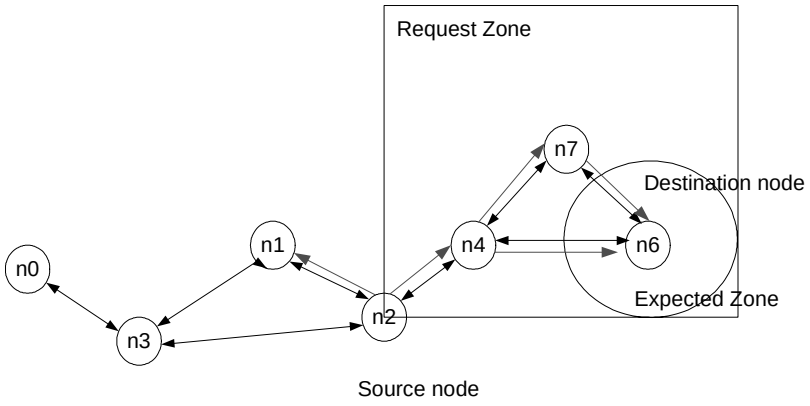

Figure 2.6: Request and Expected zones in LAR box.

2.4.5 Distance Routing Effect Algorithm for Mobility (DREAM)

DREAM is a proactive routing protocol, which uses location information to make routing decisions. In this routing protocol information is updated with respect to the mobility rate (also referred to as mobility and speed which is the rate at which a node moves in the network) and distance separating the nodes. Using these characteristics DREAM tries to limit the overhead of location packets. In DREAM, when a node wants to send a packet to a destination node, it refers to its location table to find the location information about the destination node. With this information, the source forwards the packet to its neighbors that are in the direction to the destination. To specify this direction the source calculates the expected region, which is a circle around the destination node position. However, due to the mobility of the nodes, the destination position information maybe outdated. For this reason the radius of the expected region is set to $(t_1 - t_0)v_{\max}$. Where t_1 is the current time and t_0 is the time stamp of the position information that source node has about the destination node and $v_{\max}$ is the maximum speed that a node may travel in the ad hoc network. Within the expected region the

direction towards destination will be defined as the line between source and destination with angle φ. The neighboring nodes repeat this procedure using their information of the destination's position until they possibly reach the destination node. When the destination node receives the packet, it sends an ACK packet back to the source node in the same manner that packet reaches it. If the source node does not receive an ACK packet within a timeout period it starts a recovery procedure. Figure 2.7 shows the expected region for DREAM.

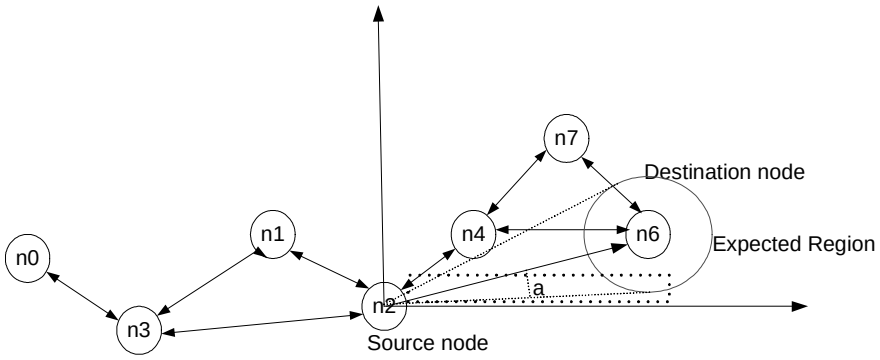

Figure 2.7: Example for the expected region in DREAM.

2.5 Mesh Enabled Architecture (MEA)

In 2001, the MEA mobile broadband solution, developed by MeshNetworks, was first implemented at Mitland, Florida. MEA simultaneously delivers broadband data, high quality voice, and precise geolocation information to mobile devices. The notable feature of MEA is that it offers an ad hoc peer-to-peer networking technology that enables point-to-point communications and high-speed access to corporate LANs or PSTN. While traveling at speeds up to 250 mph, the MEA still provides a burst data rate of 6 Mbps. Position determination methods are built into MeshNetworks' patented

Quadrature Division Multiple Access (QDMA™) radio. QDMA™ radio protocol uses Direct Sequence Spread Spectrum (DSSS) and operates in the ISM II 2.4 GHz bands. Unlike 802.11b, QDMA is optimized specifically for the wide area mobile applications. This network architecture can connect 2 to 20,000 users by a peer-to-peer routing technique with built-in positioning capability. The MEA offers integrated solutions for Emergency Response, Law Enforcement, Intelligent Transportation Systems, Mobile Wi-Fi, Military/defense, and other solutions.

In the MEA, all routing is done below the IP layer, but it supports industry standard IP applications and devices transparently - without requiring any modifications. The MEA ad hoc peer-to-peer routing technologies are “radio agnostic”.

The MEA consists of four distinct network elements: Subscriber Devices, Wireless Routers, Intelligent Access Points (IAPs), Mobile Internet Switching Controller (MiSC).

Subscriber device, shown in Figure 2.8a, either fixed or mobile, consists of MeshNetworks’ transmitter in the form of mobile broadband PC card/CompactFlash modem attached to a laptop, handheld computer or PDA. The transmitter provides access to fixed-infrastructure networks or the Internet and PSTN. The software that is ported onto an existing chip makes the PC card can act as a wireless router. With this peer-to-peer ad hoc mode, as the number of subscribers in the network increases, number of wireless routers increases and as a result the capacity of network increases.

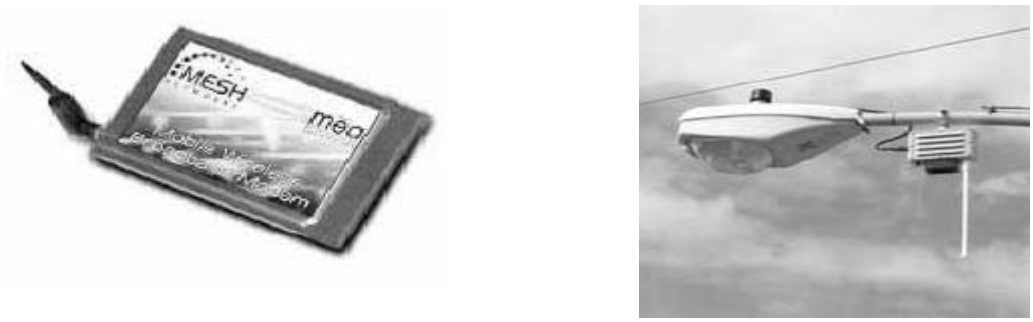

Figure 2.8: (a) Subscriber Device and, (b) Wireless Router in the MEA.

The Wireless Router, shown in Figure 2.8b, is a low-cost shoebox-sized wireless device that is primarily deployed to extend the range between IAPs and subscribers and also increases the network's efficiency. The Wireless Router is small and light which helps it to be mounted anywhere there is AC power. The Wireless Router also provides additional capabilities such as: acting as hopping point for subscribers, automatic load balancing, route selection, network capacity optimization through transmit power conservation, QoS management of the network resources, and acting as a fixed reference for geolocation services.

The IAP, shown in Figure 2.9a, connects the MEA wireless network to the wired core network. From the wired core network through media gateways, wireless network connects to the Internet or the PSTN. Each IAP offers up to 18 Mbps burst of voice, video, and data capacity to the subscribers. IAPs support up to the 10/100 base-T Ethernet interface rate. Other interfaces are supported through other commercially available media translation devices. The locations of the IAPs are not critical. IAPs provide functionalities such as local mobility management for the subscriber devices, network capacity optimization through transmit power conservation, QoS management of

the network resources, fixed reference for geolocation services, hopping points for subscriber peer-to-peer networking, and route selection.

MiSC, Figure 2.5b, i**s** responsible for network's operations, administration, management, and provides connectivity between IAPs and wired world.

Figure 2.9: (a) Intelligent Access Points, (b) Mobile Internet Switching Controller (MiSC) in MEA.

MiSC is composed of the off-the-shelf hardware components and the MeshNetworks' software. A MiSC is highly scalable and can be deployed in a distributed architecture to improve reliability and survivability. Each MiSC provides functions in the network such as: Authentication Authorization and Accounting (AAA), Billing support services and interfaces, Inter/ intra-system mobility management, Subscriber service provisioning and management, Network monitoring and reporting, and Gateway services.

Chapter 3 : Channel Issues for Ad hoc Networks

Wireless channel quality causes fundamental limitations on the performance of wireless ad hoc systems. The quality of a channel is a complex combination of effects due to path loss, multipath fading, and Doppler spread. Radio propagation can vary significantly based upon the environment, frequency of operation, node velocity, sources of interference, and other dynamic factors. For designing a wireless network, performance of the network is an important factor. Wireless channel models are used as a tool to analyze the performance of wireless communication and geolocation systems. Performance metrics depend on the system under study. This chapter presents an overview of the existing wireless channel models, and provides fundamental understanding of channel modeling and classifies models based on environment, wave characteristics and media effects.

3.1 Introduction

Three important issues in wireless communication are bandwidth limitations and unpredictable topology changes due to the characteristics of the wireless channel and the node mobility. As mentioned in Chapter 2, ad hoc networks generally use IEEE 802.11 that operates in the 2.4 GHz Industrial, Scientific, and Medical (ISM) band. Although these higher frequencies provide more bandwidth, signals at these frequencies suffer greater attenuation than lower frequencies. At these frequencies there are three basic channel effects that influence the received signal: path loss, shadow fading and multipath.

Path loss quantifies the loss in signal strength due to the distance and the absorption of the material(s) between two locations. Shadow fading characterizes the fluctuations around the average path loss. Multipath accounts for the result of multiple paths between sender and receiver combining at the receiver. The variation in the received signal strength that is due to the path loss or shadow fading is characterized as having a large-scale average value. Rapid fluctuations of the signal amplitude are referred to small-scale fading. Doppler spread contributes to rapid fluctuations of signal amplitude due to the movement of ad hoc nodes relative to each other, or movement of the surrounding objects. Multipath causes fading due to the addition of signals arriving via different paths.

While the channel effects limit the performance of infrastructure-based wireless networks to a great extent, the built in diversity in wireless ad hoc networks can improve the channel effects in some circumstances. For instance, multi-hop communication can effectively overcome shadowing and path loss effects if the node density is high enough, because it is more probable that ad hoc nodes are close to each other.

The rest of this section is organized as follows. In Section 3.2, we give a brief introduction to wireless channel models and implementation issues. In Section 3.3, we describe large-scale path loss models and describe the models proposed for different environments. In Section 3.4, we explain small-scale path loss and the effects of multipath fading and Doppler.

3.2 Wireless Channel Model

A wireless medium is an unreliable shared media that has limited bandwidth. In most radio channels the transmitted signal arrives at the receiver from various directions

as a consequence of reflecting off surfaces at various distances from the transmitter. At the receiver, each of these reflected signals might have a different phase and amplitude. A node's received signal is the sum of signals arriving along different paths and consists of both a LOS component and several non-line-of-sight (NLOS) delayed signals going through a process of reflection, transmission and/or diffraction (commonly known as "multipath"). These LOS and NLOS signals, plus random noise in the channel, affect the received signal and must be handled in the receiver. In some cases, these signals add coherently in a way that increases received power and signal to noise ratio and so enhances the channel quality. In other cases these signals add destructively causing the channel quality to degrade. Even if a node is stationary, any change in the LOS path or any reflected path will change the quality of the channel and, therefore, may change the achievable data rate. In wireless media, the dynamics of the propagated signals over the channel are constantly changing both for static and mobile nodes. There are three different types of channel models that are commonly used to account for these effects: the time-invariant channel model, the time-variant channel model and the stochastic channel model. A time-varying channel can be modeled as follows:

$$h(t,\tau) = \sum_{k=0}^{k(\tau)} a_k(t)\delta(t-\tau_k(t))e^{j\theta_k(t)} \tag{3.1}$$

In Equation 3.1, $a_k(t)$ is the random time-varying amplitude of the k^{th} path, $\tau_k(t)$ is arrival time of the k^{th} path, $\theta_k(t)$ is the random phase of the k^{th} path, τ is the channel multipath delay for a fixed value of t, and $k(\tau)$ is the number of multipath components. If variation in the channel is at a rate similar to the bit duration time, we

need to consider these variations in the channel and would therefore model the channel with the above equation. If the variation in the channel is negligible in comparison to the bit duration time, and during the bit duration time the number of paths $K \equiv E\{k(\tau)\}$, $a_k \equiv E\{a_k(t)\}$, $\tau_\kappa \equiv E\{\tau_k(t)\}$, and $\theta_k \equiv E\{\theta_k(t)\}$, we can simplify Equation 3.1 to the time-invariant (stationary) channel impulse response as follows:

$$h(t) = \sum_{k=0}^{N-1} a_k \delta(t - \tau_k) e^{j\theta_k} \tag{3.2}$$

In the above equation, path gain, phase shift, and path delay can be treated as time-invariant random variables since the variation rates are very slow compared to the transmission bit rate. The time invariant channel model is simpler than the time variant channel model due to its constant time. Almost all radio systems are narrow-band and the time-invariant channel model can be applied to them. The complete received signal is given by:

$$y(t) = \sum_{k=0}^{k(\tau)} a_k(t) x(t - \tau_k(t)) e^{j\theta_k} + z(t) \tag{3.3}$$

Where $z(t)$ is the background noise and the thermal noise of the receiver, $x(t)$ is the transmitted signal and $y(t)$ is the received signal.

Typically, physical layer algorithms (e.g. error correcting codes, channel modulation, demodulation and decoding) use the Equation 3.1, making assumptions about the effects of the variations. The performance of the physical layer implementation

is well captured by observing its packet loss rate as a function of Signal to Noise Ratio (SNR). Typically, in cases when SNR is high, there is a better chance that the received packet is error free. In most packet level simulators the received SNR is used to capture the packet level performance of any physical layer implementation. The following equation can be used to calculate the received signal power:

$$P_r(t) = \beta(t) P_t d(t)^{-\alpha} \frac{r(t)^2}{P} \tag{3.4}$$

This equation represents the effect of the distance-power gradient, rms delay spread and Doppler spread on the received signal. In Equation 3.4, $d(t)$ is the distance between the sender and the receiver at time t, $r(t)$ is the average channel gain for the packet at time t, and σ^2 is the variance of the background noise $z(t)$. β is a constant that changes with the environment and α is the distance-power gradient. P_r and P_t are the received and transmitted powers respectively. In Equation 3.4, $\frac{r^2}{P}$ is related to the Rayleigh fading of the channel and $\beta(t) P_t d(t)^{-\alpha}$ models average large-scale variation in the channel. The main part of large-scale variation is due to the path loss that relates the signal strength to the distance between two nodes. Multipath characteristics of the channel change in different environments, so various path loss models have been developed for different environments.

3.3 Large-Scale Path Loss Modeling

Given a transmitter power and a receiver requirement, the path loss model allows predicting the maximum distance between two nodes in an ad hoc network, as well as the coverage area of the base station in a fixed wireless network. Signal coverage calculation is essential for wireless network design, and is a function of the frequency of operation, environment, and the other factors. As a result, different channel models have been proposed for different environments and operating frequencies.

3.3.1 Free-space Propagation and Two-Ray Propagation Models

In free-space, the signal between transmitter and receiver travels only along one path. The signal strength at the receiver decreases as the square of the distance in the free-space. In free-space, depending upon the radio frequency, there exist additional losses due to the distance between transmitter and receiver. The relationship between the transmitted power P_t and the received power P_r in free-space is given by the Friis equation [Rap95]:

$$P_r = \frac{P_t G_t G_r \lambda^2}{(4\pi d)^2} \tag{3.5}$$

Where P_t and P_r are the transmitted and received powers, G_t and G_r are the transmitter and receiver antenna gains respectively; d is the distance between the transmitter and receiver. $\lambda = c/f$ is the wavelength of the carrier; c is the speed of light in free-space; and f is frequency of the radio carrier. If we assume that

$P_0 = P_t G_t G_r \left(\lambda / 4\pi\right)^2$ is the received signal strength at the first meter, we can rewrite Equation 3.5 as follows:

$$10\log(P_r) = 10\log(P_0) - 20\log(d) \tag{3.6}$$

In more realistic environments than free-space, the signal between the transmitter and receiver travels along several paths. A two-ray model is commonly used for modeling land mobile radio environments. For the two-ray model, the received signal power is:

$$P_r = P_t G_t G_r \frac{h_b^2 h_m^2}{d^4} \tag{3.7}$$

In this equation h_b and h_m are the base station and mobile station antenna heights respectively. If the transmitter is within the crossover distance ($\frac{4\pi h_b h_m}{\lambda}$) of the receiver, there is no reflection from the ground and the free-space model is used for the calculation of the received power; otherwise the two-ray model should be used. Figure 3.1 shows path loss for the free-space and two-ray models. The path loss in this figure is calculated for an antenna height of 1.5 m and the gain of 1. [Rap95]

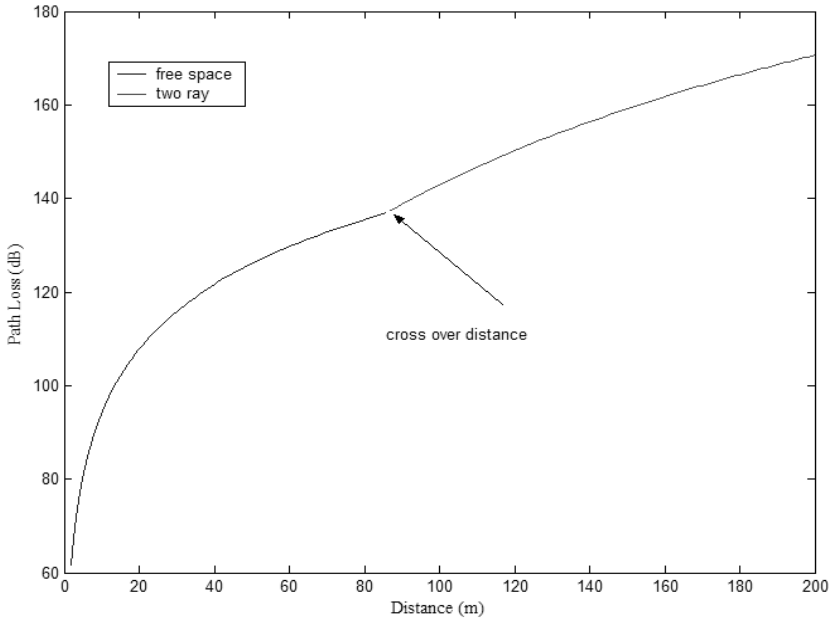

Figure 3.1: Path loss vs. Distance for free space and two-ray model

3.3.2 Path loss Models for Indoor Areas

Indoor channels are characterized as being site-specific, containing severe multipath, and having limited availability of a LOS signal propagation path between the transmitter and receiver. Two major sources of error in measuring location metrics indoors are multipath fading and NLOS conditions due to shadow fading. These characteristics have to be considered to enable the design of the wireless networks. Different measurements have been performed in the door environment to determine distance power relation in indoor environment [Rap95].

3.3.2.1 Multifloor JTC Model

The JTC multifloor model is used in situations when the propagation of signals in a multiple story building must be modeled. For multifloor attenuation the path loss is given as:

$$L_p = A + L_f(n) + B\log(d) + X \tag{3.8}$$

In Equation 3.8, n is the number of floors through which the signal passes, $L_f(n)$ represents a function that relates the path loss to the number of floors and d is the distance between transmitter and receiver in meters. A set of measurements for residential areas results the following values for the above parameters for a carrier frequency of 1.8 GHz: the constant A=38 dB, B=28, $L_f(n) = 4n \ \ dB$, and standard deviation of the Log Normal Shadowing is equal to 8 [Pah95].

3.3.2.1.1 Path Loss Model Using Building Material

This model tries to fix the free-space model by introducing losses for each partition that is encountered by a straight line connecting the transmitter and the receiver. This path loss model is given as:

$$L_p = L_0 + 20\log d + \sum m_{type} w_{type} \tag{3.9}$$

In this equation m_{type} is the number of partitions with a path loss of w_{type}. The value of w_{type} is calculated based on measurements and depends on the material of the partition

[RAP95]. For instance, in an office environment, L_0 is measured as 38dB and log Normal Shadowing of 10 dB can be added to the equation [Pah95].

3.3.3 Path loss Model for Microcell

Different path loss models are proposed for Microcellular and Macrocellular areas. Here we describe the Joint Technical Committee (JTC) model for Microcellular environments. This model is used when the structure of the environment is not available; and it applies when the distance between transmitter and receiver is less than 1 km and the height of the base station is above the rooftop. This model divides the distances into LOS region and NLOS regions. The following model is used to estimate the path loss in Microcell area [Rap95]:

$$L_p = 38.1 + \begin{cases} 25\log_{10} d, & d < d_{bp} \\ 25\log_{10} d_{bp} + 45\log_{10} \dfrac{d}{d_{bp}}, & d > d_{bp} \end{cases} \tag{3.10}$$

where d_{bp} is the Fresnel zone distance break point that describes the first LOS region, and is defined as: $d_{bp} = \left(\dfrac{4h_b h_m}{\lambda} \right)$. This Fresnel zone break point defines a region within which the power received from the LOS path dominates the total power of the other paths and the propagation loss is the same as the propagation loss in free-space. If the physical geometry is known, the JTC recommends the following path loss model:

$$L_p = 38.1 + \begin{cases} 20\log_{10} d, & d < d_{bp} \\ 20\log_{10} d_{bp} + 40\log_{10} \dfrac{d}{d_{bp}}, & d_{bp} < d < d_{cor} \\ L_{cor} + 20\log_{10} d_{bp} + 40\log_{10} \dfrac{d_{cor}}{d_{bp}} + 50\log_{10} \dfrac{d}{d_{cor}}, & d > d_{cor} \end{cases} \tag{3.11}$$

This model divides the distance into two LOS and one NLOS regions. The first region is defined by the Fresnel zone break point. The second LOS region starts from the d_{bp} and continues to d_{cor} where the mobile loses the LOS path. In the region that the mobile lost the LOS path there is an additional path loss of L_{cor} that should be added to compensate for the immediate power drop after turning the corner. Figure 3.2 shows the path loss for an unknown Microcell environment for different frequencies of f=914 Mhz, 2 GHz, and 5 GHz.

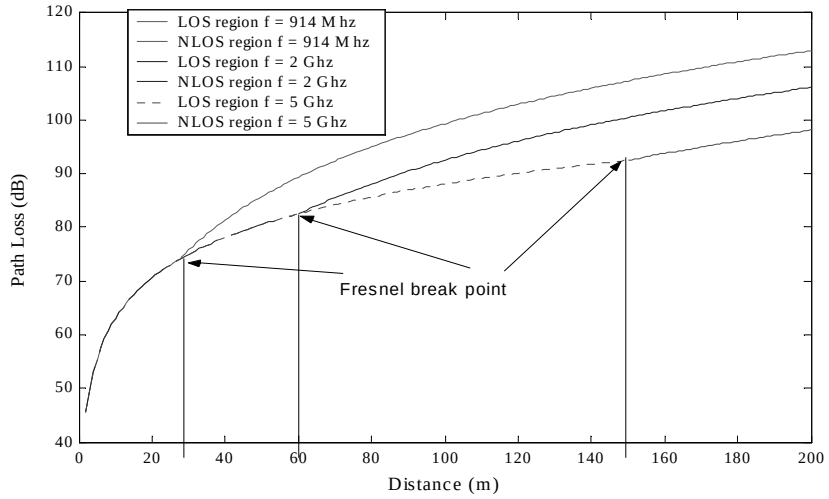

Figure 3.2: Microcell model for unknown environment structure.

3.4 Small-Scale Path Loss Modeling

As stated before, small-scale fading is used to describe the rapid fluctuations of the received signal over a short period of time. This type of fading experienced by a signal is a function of the transmitted signal and characteristics of the channel. Characteristics of the signal can be defined as bandwidth, symbol period and so on. While parameters such as rms delay spread and Doppler spread represent the characteristics of the channel. Doppler spread characterizes the movement of the transmitter, receiver, or objects in between.

The rapid fluctuation of the received signal amplitude is due to the Doppler effect and multipath fading. Doppler effect is caused by the motion of the mobile nodes toward or away from each other, while multipath fading is the addition of the signals arriving from different paths.

3.4.1 Effect of Multipath or Doppler

The Doppler effect and multipath fading, respectively due to the node or surrounding object motion and addition of signal through different paths, are the causes of rapid fluctuation of the signal amplitude. This rapid fluctuation in the received signal is called small-scale fading. A Ricean distribution is commonly used to model these fluctuations [Rap95]:

$$f_{ric}(r) = \frac{r}{\sigma^2}\exp(\frac{-(r^2+K^2)}{2\sigma^2})I_0(\frac{Kr}{\sigma^2}), \qquad ,r \geq 0, K \geq 0 \tag{3.12}$$

The random variable r corresponds to the signal amplitude, and K is a factor that determines how strong the LOS component is relative to the strength of the multipath signals, σ^2 is the variance of the multipath, and I_0 is the modified Bessel function of the first kind, order zero.

In packet level simulators, the term $\frac{r^2}{P}$, the normalized power envelope, in Equation 3.3 is attributed to this variation in the channel. In the following section we describe the way Ricean fading has been simulated in ns-2. Figure 3.3 shows the path loss for the indoor JTC, Friss model, two-ray model, and the indoor model that we have achieved based on the simulation.

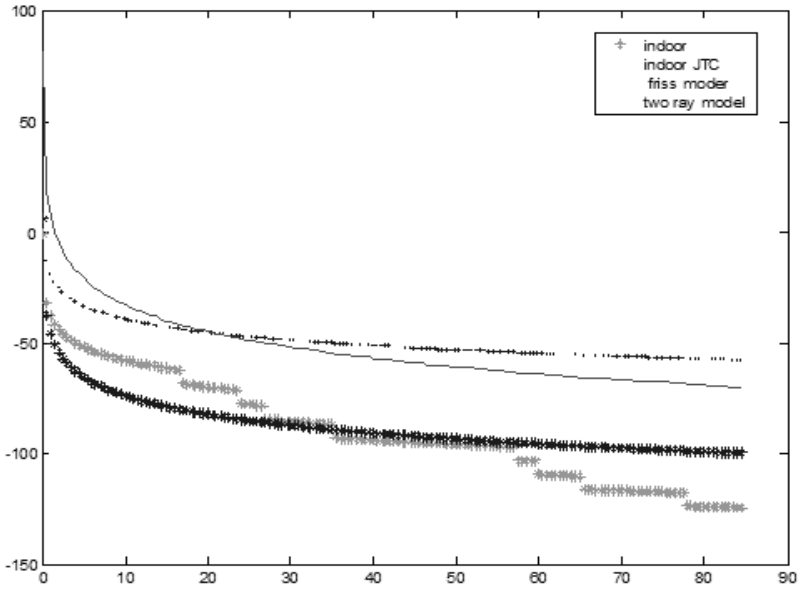

Figure 3.3: Path loss vs. Distance for indoor environment, two ray model and free space.

Chapter 4 : Performance Comparison of Ad Hoc Routing Protocols

In this chapter we investigate QoS parameters in mobile ad hoc networks via simulation. Many performance studies of ad hoc routing protocols focus on higher layer protocols and tend to ignore the effects of the other layers, particularly the effect of the channel model on routing protocol performance. In this chapter, we study channel effects such as path loss and fading and show that these effects alter the absolute performance of different routing protocols in different ways. We show that because the physical layer effects impact different protocols differently, including these effects in simulations of the protocols can change the relative ranking amongst protocols for the same simulation scenario. AODV, DSDV, DSR, LAR, and DREAM are chosen as representative of on-demand, proactive and location based routing protocols. We further study the effects of congestion, mobility, and transmission range in different scenarios. Throughput is generally accepted as one of the most important metrics to evaluate the performance of a routing protocol. Packet loss is one of the ways to study throughput, as throughput is determined by how many packets have been sent and how many packets have been lost. We study packet loss and throughput and further compare the performance of the routing protocols with the theoretical results for the capacity of the ad hoc networks.

4.1 Introduction

Several simulation-based studies of ad hoc routing protocols have been done to compare the performance of these routing protocols based on different conditions of mobility, movement, and network congestion. J. Broch et al. extended the ns-2 simulator to model ad hoc wireless networks and compared performance of AODV, DSDV, DSR, and TORA based on mobility and input traffic [Bro98]. T. Camp et al. studied the effect of mobility on performance of two location based routing protocols (DREAM and LAR) [Cam02]. The goodput (the amount of realized throughput), delay, and path length of DSR have been studied in [Ko98] as a function of mobility and traffic load. [Lu] and [Lu03] investigate packet loss in mobile ad hoc networks.

P. Gupta et al. studied the theoretical bounds for achievable data rate and bandwidth in ad hoc networks [Gup00]. They further studied the critical transmission range for maintaining connectivity in these networks. M. Takai et al. compare the physical layer implementation of ns-2 and GloMoSim (network simulator proposed by UCLA) for ad hoc networks, they also compare the simulation results for the DSR and AODV routing protocols in ns-2 and GloMoSim.

In this chapter, we study the behavior of the AODV, DSDV, DSR, LAR, and DREAM protocols for mobile ad hoc networks based on extensive simulation in ns-2 in a variety of simulated wireless channels (indoor, outdoor, and rayleigh fading), mobility scenarios, offered loads, and transmission ranges. We further compare a simulation-based study of the ad hoc networks with the theoretical bounds for the capacity and data rate. We also study power efficiency and the maximum bit rate that can be achieved per unit power in an ad hoc network.

In ad hoc networks, wireless link transmission errors, mobility, and congestion are the major factors limiting throughput in the network. Limitations in the network throughput due to the transmission errors is affected by the physical condition of the channel, the terrain where networks are deployed. Congestion in the network occurs whenever the demands exceed the maximum capacity of a communication link. Mobility has different effects on the throughput of the network. A packet may be dropped at the source if a route to the destination is not available (due to movement of one or more nodes), or a buffer that stores packets is full. Packets may also be dropped at an intermediate node if the link to the next hop has broken.

The rest of this chapter is organized as follows: in Section 4.2 we study the ns-2 simulation environment with more emphasis on the physical layer. In Section 4.3, we compare the performance of ad hoc routing protocols in different scenarios. In Section 4.4 we classify these routing protocols.

4.2 Simulation Model

For the simulations in this thesis, we used the ns-2 simulator which is a discrete event packet simulator developed by UC Berkley and extended by Carnegie Mellon University for ad hoc networks. Figure 4.1 shows the basis of ns-2 packet simulator. In ns-2, a mobile node consists of a protocol stack and has functionalities like movement, sending and receiving packets on the wireless channel. As shown in the figure, a traffic model, mobility scenario, and a wireless channel model are used as inputs to the protocol stack to test the performance of a routing protocol. After running each test, we study

performance of the routing protocol based on various performance metrics.

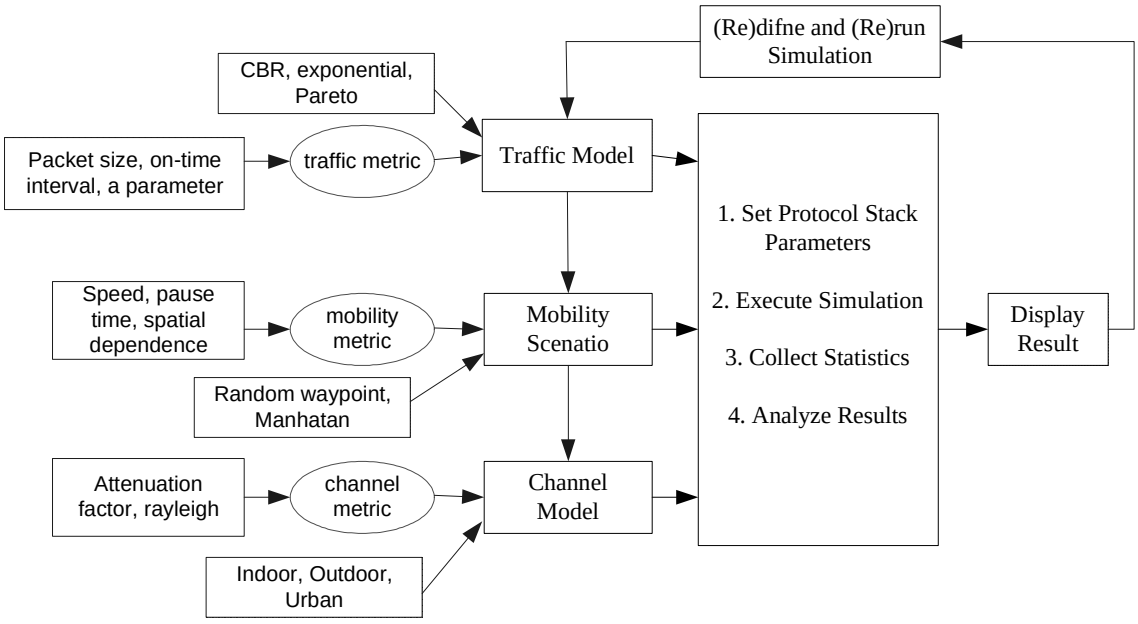

Figure 4.1: Simulation procedure of ad hoc networks.

4.2.1 Environment

Each ad hoc node is assumed to use an omni-directional antenna with the unity gain. Although 802.11 wireless interface runs at 2.4 GHz, the ns-2 wireless interface works like the 914 MHz Lucent WaveLAN direct-sequence spread spectrum (DSSS) radio interface. WaveLAN is modeled as a shared-media radio with a bit rate of 2 Mbps, and a radio transmission range of 250 meters. In this chapter for some of the simulation studies we used transmission range of 30 meters. Obtaining better performance with less power consumption is desirable in ad hoc networks. The IEEE 802.11 Distributed Coordination Function (DFC) is used as the MAC layer protocol. It is in this radio environment that we study the performance of the various routing protocols.

An office indoor channel model with the size of 87m x 36m and a free-space model with the same size are used as the channel models. The different transmission ranges used in these environments are: 20m, 30m, 40m, and 45m. Performance of ad hoc routing protocols based on different traffic models has been studied in [Ahl03].

4.2.2 Signal Reception in NS-2

Received signal strength is important in the receiver as this computation has a strong correlation with the frame error rate in the channel. Computation of interference and noise at each receiver is a critical factor in wireless communication modeling. This computation is based on SINR (Signal to Interference and Noise Ratio) or SNR (Signal to Noise Ratio). The power of interference and noise is calculated as the sum of all signals on the channel other than the one being received by the radio plus the receiver noise. The resulting power is used as the basis of SNR, which determines the probability of successful signal reception for a given frame. For a given SNR value, two signal reception models are commonly used in wireless network simulators: SNR threshold based and Bit Error Rate (BER) based models.

The SNR threshold based model uses the SNR value directly by comparing it with a SNR threshold (SNRT), and accepts only signals whose SNR values have been above SNRT at any time during the reception. The SNRT method of reception is shown in Figure 4.2. If the received signal is above the receiver sensitivity (Rx sensitivity) on the channel, the signal is considered detect and it passes to the MAC. If the power is below the receiver threshold, the radio does not receive the signal.

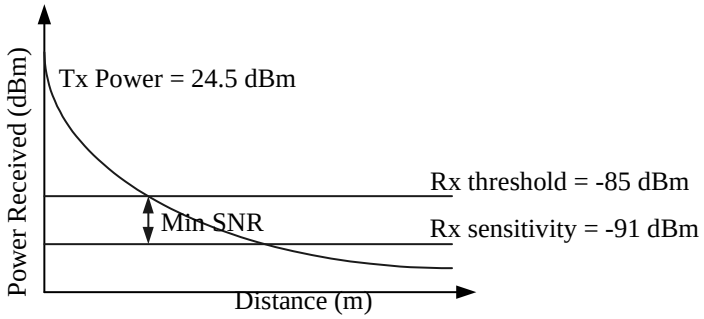

Figure 4.2: SNRT based calculation of the received signal.

The BER based model probabilistically decides whether or not each frame is received successfully based on the frame length and the BER (Bit Error Rate) deduced by the SNR and the modulation scheme used by the transceiver. As the model evaluates each segment of a frame with a BER value every time the interference power changes, it is considered to be more realistic and accurate than the SNR threshold based model. However, the SNR threshold based model has less computational cost and can be a good abstraction if each frame length is long. Simulation results with the free-space path loss model tend to have better performance than other path loss models.

4.2.3 Path Loss and Fading

Propagation models such as fading, shadowing and path loss are part of the channel model and control the input conditions given to the physical models. They have great impact on the performance of the modeled wireless ad hoc network. As cited in Chapter 3 in more detail, fading models with Rayleigh or Ricean distributions are commonly used to describe ad hoc environments. Fading having a Rayleigh distribution

is used for highly mobile conditions when NLOS paths between nodes dominate, and fading with Ricean distribution is used for the LOS path between nodes. R. Punnoose [Pun00] models the effect of Rayleigh and Ricean fading in ns-2 network simulator. Although this package does not exist in current version of ns-2 (ns-2.19b) it can be added to it.

The Additive White Gaussian Noise (AWGN) model is referred to as an idealistic channel condition where no signal fading occurs. Path loss alone can be used to model signal propagation in these conditions. The two-ray path loss model, which is the path loss model used in ns-2, is suited for LOS microcell channels in urban environments. The free-space model is used as a basic reference model and is also considered to be an idealized propagation model. With this path loss model, even nodes far from the transmitter can receive packets, which can result in fewer hops to reach the final destination in a mobile ad hoc network.

An indoor path loss model is used to model indoor conditions. Path loss in the indoor environment is complicated due to the obstacles between transmitters and receivers. We have implemented the indoor model for the ns-2. In our code, a numerical routine computes the power received on a given point of space by using the indoor model. Our channel model uses a precomputed building structure. The information regarding the location of the objects including walls, doors, windows and other obstacles is stored in a file with the specific coordinate of the objects in the environment and their material. To calculate the attenuation between transmitter and receiver, the number of obstacles between transmitter and receiver is calculated and the attenuation that the signal faces after passing through these obstacles is specified. To evaluate our model, we have

implemented the floor plan of the ATWATER KENT building at WPI as an example of the input plan (Figure 4.3). We have also implemented the path loss model for Microcellular environment discussed in Chapter 3.

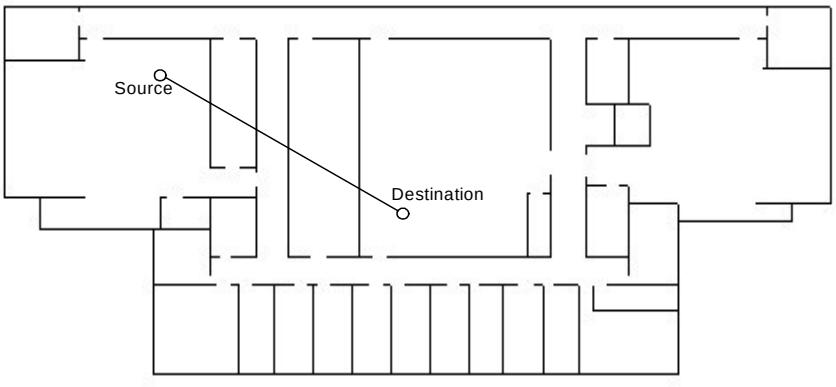

Figure 4.3: WPI third floor plan.

4.2.4 Performance Metrics

In order to quantify the differences between ad hoc routing protocols, we have used a set of performance metrics. We chose to evaluate the ad hoc routing protocols based on the following five metrics:

Packet delivery ratio: Packet delivery ratio is the ratio between the number of packets originated by the application layer and the number of packets received by the final destination. It is important that a routing protocol keep the packet delivery ratio as high as possible since efficient bandwidth utilization is important in wireless networks where available bandwidth is a limiting factor. This metric is important since it reveals the loss rate seen by the transport protocols and also characterizes the completeness and correctness of the routing protocols.

Routing overhead: Routing overhead is the total number of routing packets transmitted during the simulation. For packets sent over multiple hops, each transmission of a packet (each hop) counts as one transmission. Routing overhead reveals the bandwidth efficiency of the routing protocols. This metric shows how much of the bandwidth is consumed by the routing protocol's messages and the amount of the bandwidth that remains for the data packets. Protocols that send a large number of routing packets may increase the probability of collision and therefore will delay data packets in the Interface Queue (IFQ).

End-to-end delay: The end-to-end delay is the total delay that a data packet experiences as it travels through a network. This delay is the result of the several delays that a packet experiences as it passes through the network. These delays include the time spent in packet queues, forwarding delays, propagation delays (the time it takes for a packet to travel through the medium), and time needed to make retransmissions if a packet got lost.

End-to-end throughput: Since the available bandwidth in a network is fairly well known, it is interesting to know the actual throughput. This value shows how efficient a routing protocol is. The higher the average throughput, the less routing protocol overhead is consuming bandwidth.

4.2.5 Scenario Metrics

A scenario metric is calculated from the input data or input variable to the simulation. These values are independent of the routing protocols or the simulation process. It is important to select a set of appropriate metrics in order to provide a truthful

comparison between the different ad hoc routing protocols. The following scenario metrics are considered for our evaluation in this chapter.

Mobility: This metric measures the mobility in the network by calculating the relative node movements between all pairs of nodes in the network. The mobility metric should be proportional to the number of link changes in a model where nodes move in a random fashion.

Pause time: Pause time determines the time that a node remains stationary in the network. Each node begins a simulation by remaining stationary for pause time seconds. The node then selects a random destination at a speed specified and moves toward that destination. After reaching the destination, the node pauses again for pause time seconds, and then selects another destination and moves toward that destination. The node repeats this procedure for the duration of the simulation.

Density: The density of the network is the number of nodes in the network divided by the volume of the space. It may be inferred that the performance of the network increases as the number of nodes in the network increases. Alternatively, as the number of nodes in the network increases the MAC layer competition increases as well.

4.3 Performance Comparison of Ad Hoc Routing Protocols in Different Scenarios

In this section, we make a performance comparison of different ad hoc routing protocols based on different scenarios. Table 4.1 lists different scenarios studied in this thesis.

Table 4.1: Scenarios studied in this chapter

	Scenario 1	Scenario 2	Scenario 3	Scenario 4
Simulation time	1000s	1000s	1000s	1000s
Path loss/fading model	Free space, Two ray model	Indoor Building base model (WPI 3rf floor plan)	Free space, Two ray model	Rayleigh/Ricean
Simulation Area	87 x 36	87 x 36	400 x 800	400 x 800
Pause time	10 s ± 10%	10 s ± 10%	10 s ± 10%	10 s ± 10%
Maximum Speed	0-5.5 m/s	0-5.5 m/s	0-22 m/s	0-22 m/s
Transmission range	30m	30m	100m	100m
Movement model	Random waypoint	Indoor random waypoint	Random waypoint	Random waypoint
Data payload	64 bytes	64 bytes	64 bytes	64 bytes
Traffic pattern	Peer-to-peer	Peer-to-peer	Peer-to-peer	Peer-to-peer
Packet rate	4 packets/s	4 packets/s	4 packets/s	4 packets/s
CBR sources	20	20	20	20

4.3.1 Scenario 1: Two-Ray and Free-Space Model

This scenario consists of 50 nodes, each with a transmission range of 30m that are placed randomly in an 87m x 36m rectangle. The two-ray channel model is used to model signal propagation. 20 sources send Constant Bit Rate (CBR) packets to their peer destinations. Using peer-to-peer traffic, we intend to stress the network since traffic is concentrated in specific areas of the network. We also avoid unnecessary contention by offsetting the transmission of a data packet by 0.0001 seconds for each 20 peer-to-peer communication pairs. We used the mobgen version of the random waypoint mobility model to generate our scenarios [Cam02]. Figure 4.4 shows the average number of neighbors versus the speed for this scenario. At speed zero, the average number of neighbors is 22.5, while as the speed increases from 1 to 5, the average number of neighbors decreases from 29.7 to 27. It is because the nodes have more chance to be in transmission range of each other as the speed increases.

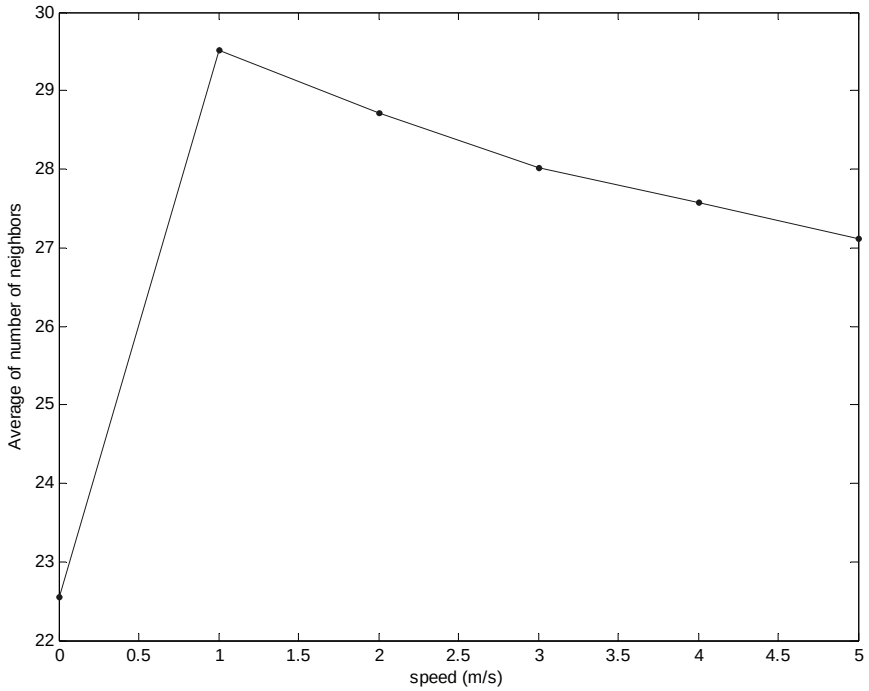

Figure 4.4: Average number of neighbors vs. speed.

Figures 4.5a-d show the data packet delivery ratio, average end-to-end delay, control packet transmissions per data packet delivered, and control byte transmission per data packet delivered for this scenario.

When the speed is zero, which means that the network is in the static condition, the average link breakages and changes are zero. In this situation, the DSDV, DSR and LAR routing protocols achieve data packet delivery ratios above 90%. All the routing protocols except DSDV have the constant packet delivery ratio as the speed increases from 1m/s to 5m/s.

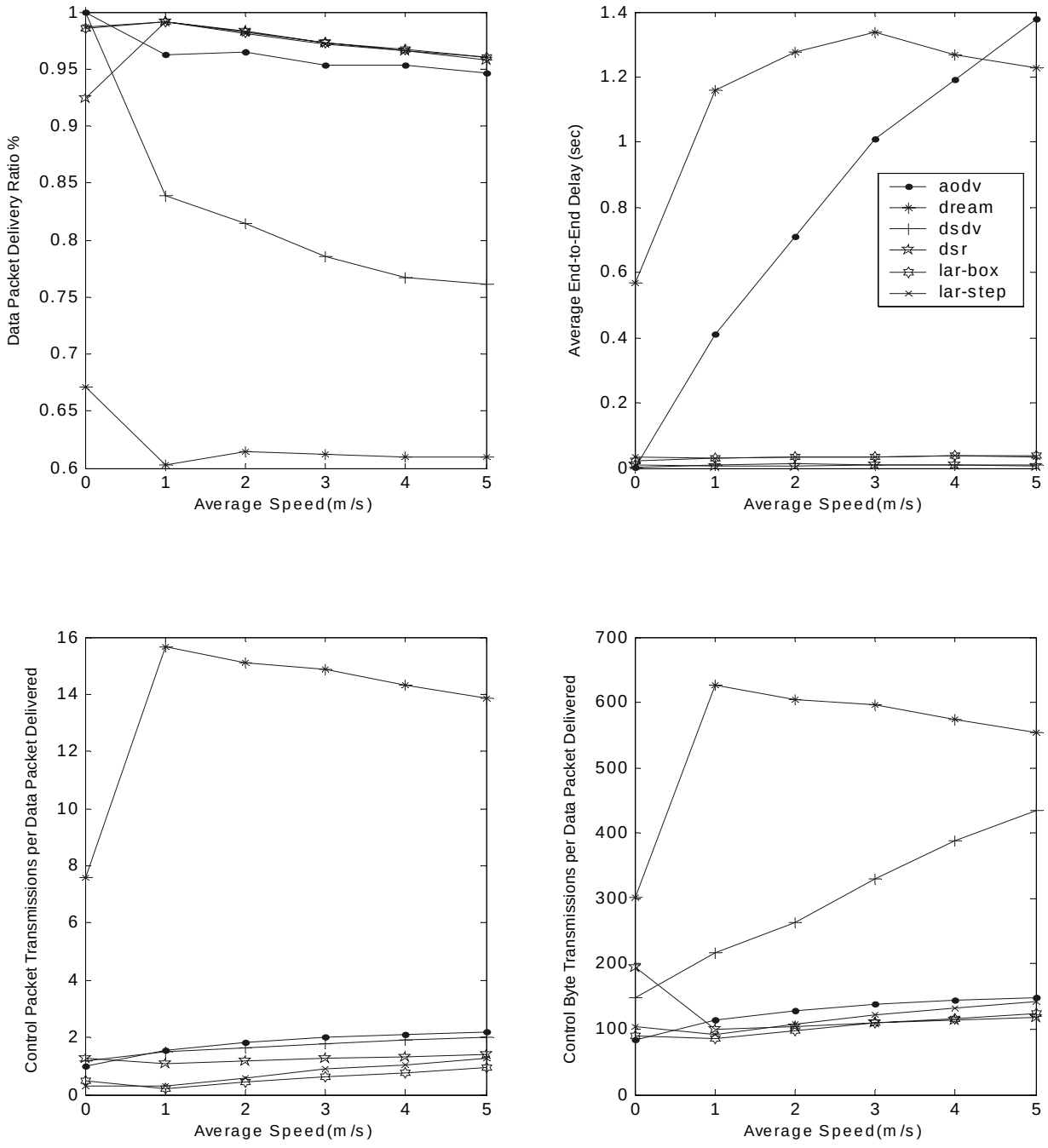

Figure 4.5: Two ray and free space channel models in a 87x36 area (a) Data Packet delivery ratio vs. speed, (b) End-to-end delay vs. speed, (c) Overhead packet transmitted vs. speed, (d) overhead byte transmitted vs. speed.

The DSDV routing protocol stores only one route to each destination and if the route is broken the node has no route to that destination and therefore all packets for that destination have to be dropped until a new route is received. DSDV uses periodic updating and it is guaranteed by the protocol design that no packet is dropped because of the "No Route" drop. The major reason for dropping packets in DSDV is the "MAC Callback" which increases from 12000 to 18000 as the speed increases from 1m/s to 5m/s. The reason for "MAC Callback" drop is the node mobility and it occurs when the next hop neighbor has moved and is not neighbor anymore. Routing discovery in DSDV is proactive and this protocol cannot adapt to the changes in the network topology when the speed increases. This is the main reason for the increase in packet loss as the speed increases.

The major reason for dropped packet in the AODV protocol in this scenario is because there is "No Route" to the destination and due to over flows "Drop IFQ". Because the node density is high in this scenario, the number of packets dropped is not significant. "No Route" drops happen when, because of the speed, source nodes cannot find any route to their destinations. "Drop IFQ"s mostly occur because of congestion in the network.

The DSR routing protocol has a packet delivery ratio above 90%. Packet drops in the DSR routing protocol are mainly because of "MAC Callback" (3 to 68 packets in this scenario) and "No Route" to the destination. The packet drops due to the "No Route" condition increase from 800 to 3000 packets.

The DREAM routing protocol cannot achieve more than 67% packet delivery ratio even at zero speed when there are no link changes in the network. Due to the

flooding nature of the DREAM routing protocol, congestion in the network increases and this increase in the network congestion is the reason for the high delay and routing packet transmission for this routing protocol in comparison with the other routing protocols. Also a greater portion of the bandwidth in this routing protocol is occupied with routing packets and this decreases the number of data packets delivered to the destinations.

LAR-box and LAR-step show the same performance as DSR. Although these routing protocols use location information to assist routing decisions, in this scenario this information does not increase the overall performance of the network.

In this scenario, the average number of neighbors is more than 27 nodes at all tested speeds. The high node density obliterates the speed effects on most routing protocols. On-demand routing protocols initiate neighbor discovery only when they want to send data to a specific destination. As most nodes are 1-hop or 2-hop neighbors of each other, node density decreases the effect of speed on the DSR, AODV, and LAR routing protocols.

As shown in Figure 4.5b, AODV and DREAM routing protocols have the highest average end-to-end delay of all the routing protocols when the speed is more than 1m/s. At zero speed, the location information of the DREAM routing protocol is accurate, but because of the contention and congestion in the network, the packets or ACKs do not reach the destination. Therefore, even at zero speed the DREAM routing protocol has an end-to-end delay close to 0.6 seconds. As the speed increases, data packet recovery is used for almost all the packets transmitted and, as a consequence, delay increases in the network. Delay increases for the AODV routing protocol as the speed increases. End-to-end delay for DSR, LAR box, and LAR step is less than 0.1 sec, and is almost constant as

the speed increases. As these protocols are on demand, when links break they just perform a “Route Repair” that does not have a large delay. From Figure 4.5b it can be concluded that the DSDV routing protocol has less than 0.1 seconds of average end-to-end delay. However, this result is not completely correct, because the data packet delivery ratio decreases as the speed increases and this implies that the delay metric is evaluated with a lesser number of samples.

Figure 4.5c shows the number of control packet transmissions per data packet delivered versus speed. This metric helps understand the power overhead for each routing protocol, which is important because power consumption is a very important factor for design of an ad hoc network. DREAM has the highest control packet and control byte transmission overhead in comparison to the other routing protocols. The reason for this is that DREAM uses small packets to transmit location information and it uses an ACK packet for every packet that is delivered from the request zone. This overhead in the DREAM routing protocol is the major reason for packet loss in this routing protocol. From the simulation we see that there are almost 16 times more than data packets delivered to the destination. LAR protocol control packet or byte transmissions are larger than DSR because these protocols send the location information in the network. The overhead for DSR and LAR protocols is less than other routing protocols as they are on-demand, only sending routing information when there is data to be transmitted. In addition these protocols use “route repair” instead of “route request” which decreases delay and routing overhead in the network.

Although DSDV uses a periodic update, control packet and byte transmissions increase with an increase in speed. This observation is partly related to the increase in

path loss. Another reason is that at high speed, the metrics of the route between destinations changes often and hence route updates are sent more frequently. At low speeds the routing update does not change frequently.

4.3.2 Scenario 2: Indoor Model

In this scenario 50 nodes are placed in an indoor environment and the transmission range of each node is set to 30m. Based on the position of the node in the selected indoor model, the signal between transmitter and receiver may face one or more degrees of attenuation. Further, obstacles in the building may decrease the number of neighbors for each node. We used our indoor version of the random waypoint mobility model to generate our scenarios. This mobility model considers the building structure and guides the node when there is an obstacle in front of it. The node movement generated with our indoor movement model for two nodes is shown in Figure 4.6a-b. The other parameters of the system are like Scenario 1. In studying this scenario, we intend to study the effect of wireless transmission errors in the various ad hoc routing protocols.

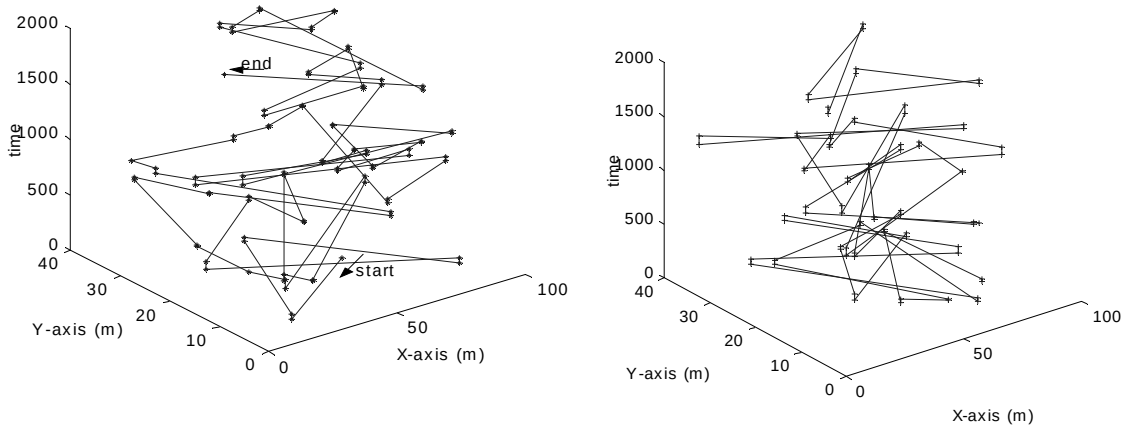

(a) **(b)**

Figure 4.6: Node movement generated by the indoor waypoint mobility (a) node n0 (b) node n49

In comparison to Scenario 1, packet delivery ratio for DSR routing protocol in this scenario decreases significantly. As the speed increases from 1 m/s to 5 m/s, data packet delivery ratio decreases from 92% to 35%. The main reasons for this drop for DSR in an indoor environment are "No Route" and "MAC Callback" errors. For DSR, wireless channel errors increase the effect of speed. Because of errors in transmissions the next hop is not necessarily a neighbor anymore and there is "No Route" to the destination. Here, "Route Repair" does not apply, because some of the nodes are isolated and packets cannot reach them. Another reason is that many of the links between nodes have loss rates low enough that the routing protocol is willing to use them, but high enough that the routing protocol throughput is consumed by retransmissions.

As shown in Figure 4.7a, the LAR routing protocols perform worse than they perform in the two-ray model, but better than the DSR routing protocol, as they use the additional information about the node's location.

Packet delivery ratio for the DSDV routing protocol decreases from 70% to 55% as the speed increases from 1 m/s to 5 m/s. The reason for this drop in performance are "MAC Callback"s which are caused because of the fact that the next hop neighbor is no longer a neighbor, or is not reachable. Because of the attenuation of the objects in this scenario the nodes are not in the transmission range of each other and therefore the number of neighbors changes more frequently.

Data packet delivery ratio for DREAM routing protocol is the same as Scenario 1. The reason is that this routing protocol floods the information through the whole network in the direction of the destination node.

AODV routing protocol performs the best among all the routing protocols. The major causes of the errors in this case are "Drop IFQ" and "No Route" conditions to the destination. In the AODV routing protocol, each node has information about its next hop unlike the source routing protocols that remember the entire route. So effect of transmission error in AODV is less that this effect in other routing protocols.

Figure 4.7b shows that average delay for the DSDV and LAR routing protocols is less than 0.1 seconds and is constant as the speed increases. This observation is partly because of metric bias, as for these routing protocols number of the packets delivered to the destination is low. While the DREAM and AODV routing protocols have the highest end-to-end delay, end-to-end delay does not show a difference for the two scenarios. However, because the number of drops and retransmissions is higher in this case, AODV has higher end-to-end delay.

As shown in Figure 4.7c-d, data packet transmission and data byte transmission for the DSR routing protocol is very high in comparison to the other routing protocols. In

DSR, whenever a link breakage occurs, it retransmits the routing information. The LAR routing protocols have lower overhead, as they use location information to route the packets throughout the network. AODV has the best byte overhead. DREAM routing protocol performance is similar to Scenario 1.

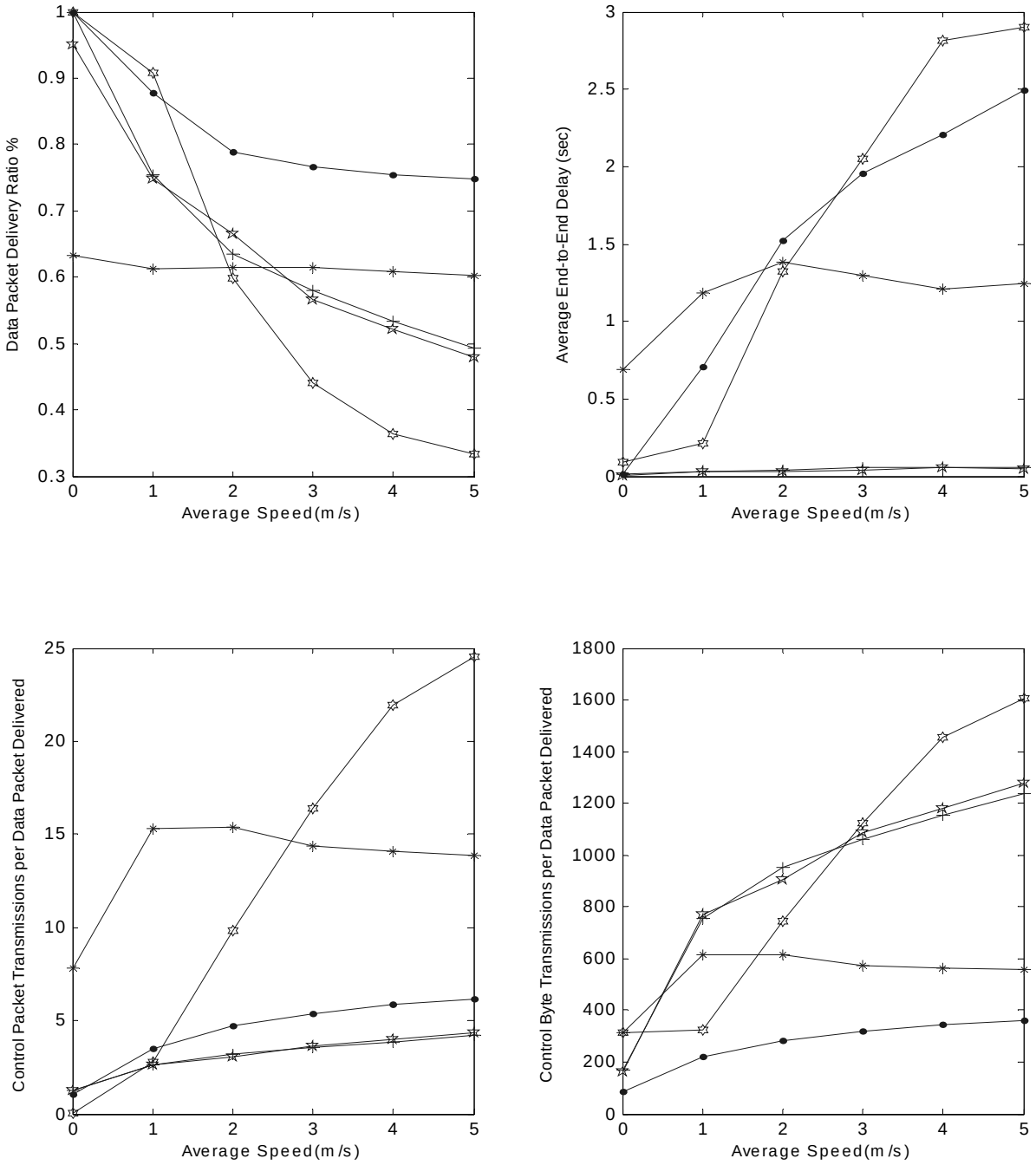

Figure 4.7: Indoor channel model in 87x36 area (a) Data Packet delivery ratio vs. speed, (b) End-to-end delay vs. speed, (c) Overhead packet transmitted vs. speed, (d) overhead byte transmitted vs. speed.

4.3.3 Scenario 3: Free-Space and Two-Ray Model 400x800

This scenario shows 50 nodes with a transmission range of 100m in a 400x800 rectangle using a two-ray channel model. The mobility model in this scenario is based on random waypoints and speed changes from 1 m/s to 20 m/s. The other system parameters are the same as in previous scenarios. As shown in Figure 4.8, the average number of neighbors changes from 4 to 6, and is far less than the average number of neighbors in Scenario 1.

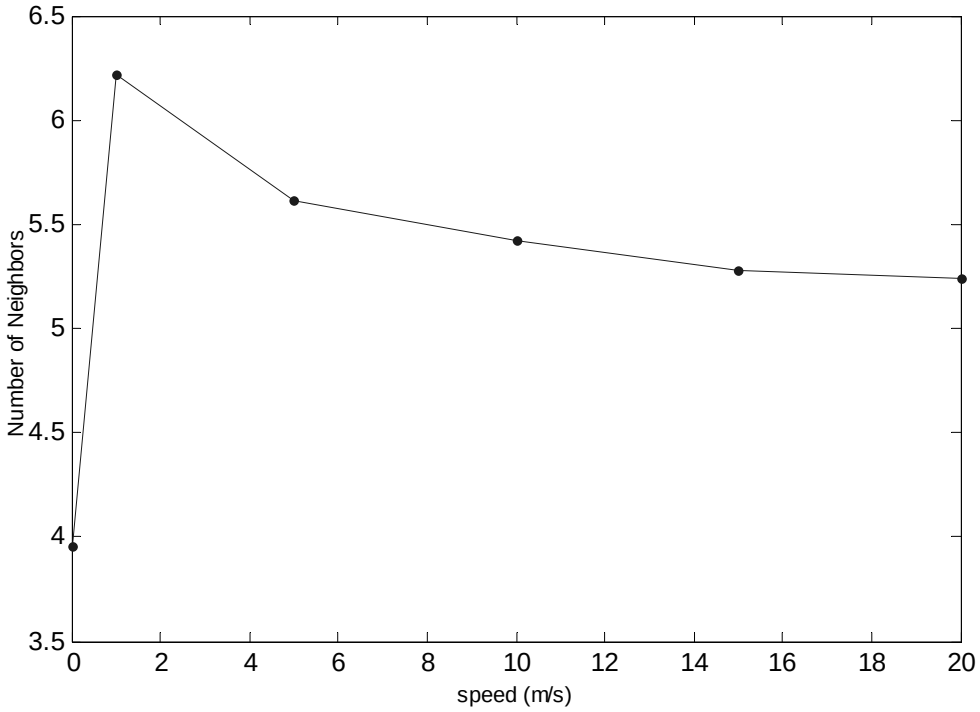

Figure 4.8: Average number of neighbors vs. speed

Figure 4.9a shows the packet delivery ratio for Scenario 3. The data packet delivery ratio for the DREAM routing protocol, because of the buffer limitation of this routing protocol, is around 30% at zero speed. As the speed increases, the packet

delivery ratio remains at 60%. Data packet delivery ratio for the DSR and LAR routing protocols decreases as speed increases. The LAR protocols perform a little better than DSR because they use location information. In this scenario, as the number of neighbors are less than Scenario 1, the probability that packets travel a longer path is higher and this is the cause of a higher number of dropped packets in this scenario. The AODV routing protocol performs the best in this scenario too, as it uses both on-demand information and also has next hop information.

Figure 4.9b shows that the end-to-end delay for the LAR-box and LAR-step routing protocols is higher than the other routing protocols, changing from 0.1 to 1.5 seconds. End-to-end delay for the DREAM protocol remains constant and changes between 0.4 and 0.6 seconds. Delay increases as the speed increases in AODV routing protocol.

As shown in Figure 4.9c-d, control byte and packet transmission per data packet delivered for the LAR routing protocols is higher than other routing protocols. Routing overhead in this scenario is higher than the routing overhead in Scenario 1, because the node density is higher in Scenario 1 than this scenario and as a result the number of hops that a node should traverse increases and this increases the routing overhead.

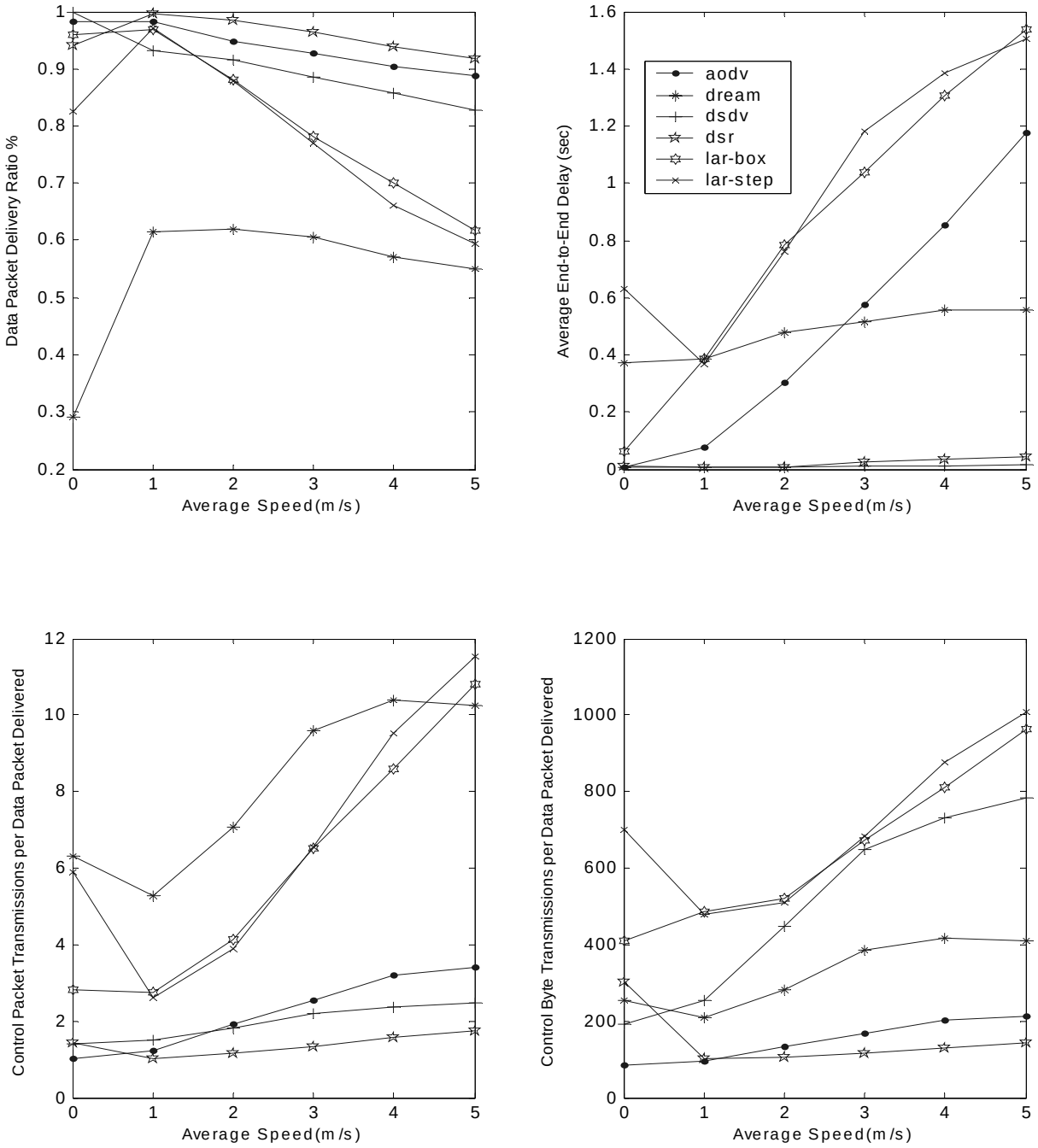

Figure 4.9: Free-space and two-ray model in 400x800 area (a) Data Packet delivery ratio vs. speed, (b) End-to-end delay vs. speed, (c) Overhead packet transmitted vs. speed, (d) overhead byte transmitted vs. speed.

4.3.4 Scenario 4: Rayleigh Fading and Two-Ray Model

This scenario contains 50 nodes with the transmission range of 100m in a 400x800 rectangle with a Rayleigh distribution with two-ray model. 20 sources send CBR packets to their peer destinations.

Figure 4.10a shows the packet delivery ratio for this scenario. As can be seen from the Figure, speed does not have any significant effect on the data packet delivery ratio and it remains constant as the speed increases. AODV and DSR perform the best among the routing protocols, while the LAR routing protocols and DREAM perform the worst. In this case, location based routing protocol does not have a good performance.

Figure 4.10b shows that end-to-end delay for the LAR routing protocols does not have a relationship with speed. End-to-end delay increases with speed for AODV from 0.9 to 2.5 seconds. End-to-end delay for DSR, DSDV, and DREAM is less than 0.5 seconds.

Figures 4.10c-d, show the control byte and control packet transmission per data packet delivered for the LAR routing protocols is higher than the other routing protocols. These routing protocols transmit location information along with the routing information and whenever a link breaks they start location discovery and route requests. The DSDV routing protocol has low control packet overhead but high control byte overhead.

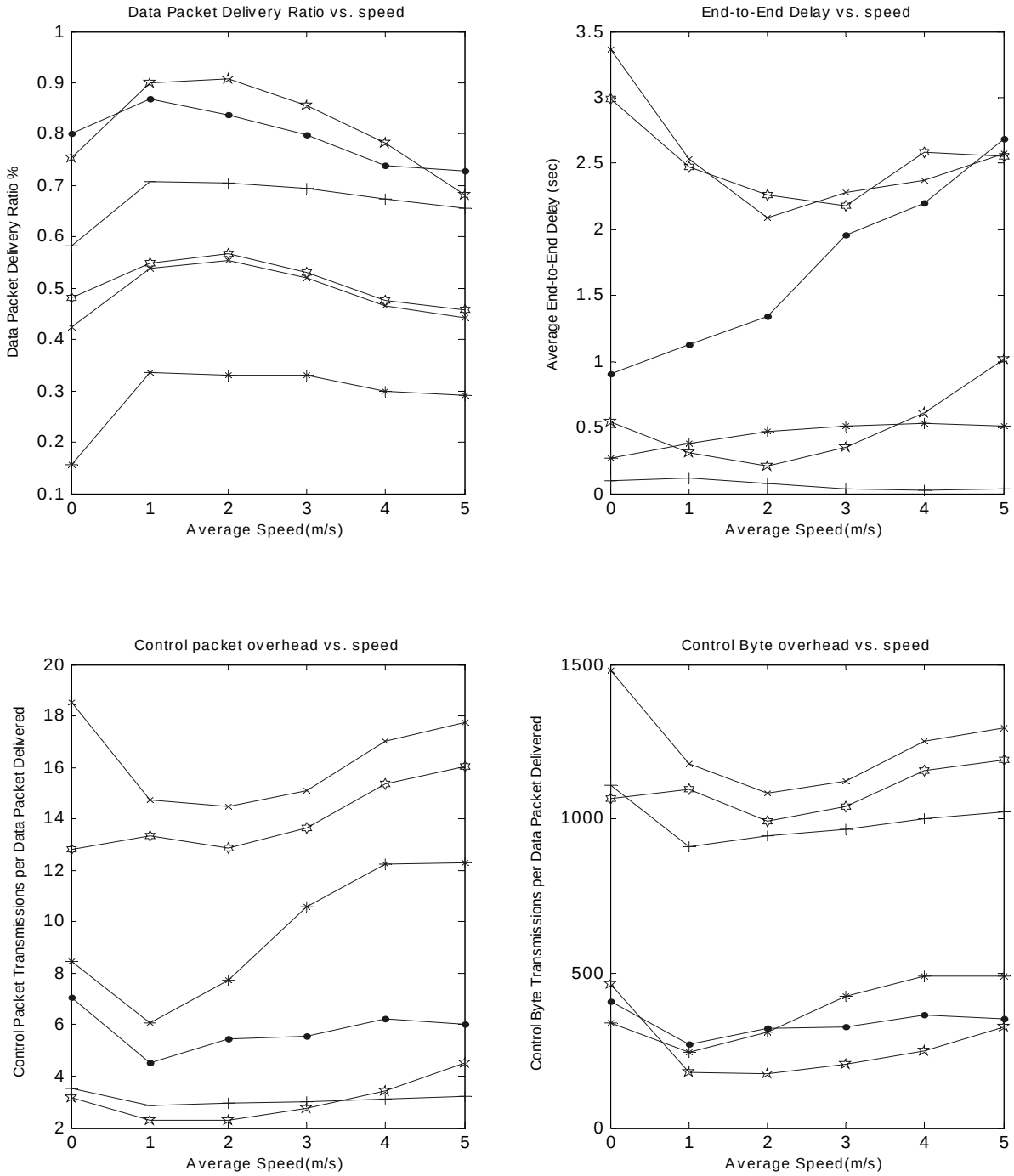

Figure 4.10: Rayleigh fading and Ricean 400x800 area (a) Data Packet delivery ratio vs. speed, (b) End-to-end delay vs. speed, (c) Overhead packet transmitted vs. speed, (d) overhead byte transmitted vs. speed.

4.4 Transmission Range Effect in Ad Hoc Routing Performance

The choice of R_s is a trade-off between full network connectivity, the reuse of available spectrum, and power consumption. It may be argued that the longer the transmission range is, the better. However, although the longer transmission range reduces the number of hops that a packet needs to transverse on its way to a destination in an ad hoc network, it also increases the number of nodes that locally compete on the shared channel, which may increase the access delay and, as a result, reduce the capacity. On the other hand, short transmission range allows better frequency reuse and longer battery lifetime. Figure 4.11 shows the effect of transmission range on packet delivery ratio and delay of the routing protocols.

The shorter transmission range can improve the network throughput, because simultaneous transmissions can co-exist in different areas of the network. But when the transmission range is very short, the chance that of network partitioning increases.

In ad hoc wireless networks, each node should transmit with just enough power to guarantee connectivity in the network. Toward this end, we show the critical power a node in the network needs to transmit in order to ensure the connectivity of the network with probability one as the number of the nodes go to infinity. In ad hoc networks, the critical requirement is that each node in the network has a path to every node in the network, i.e., the network is connected.

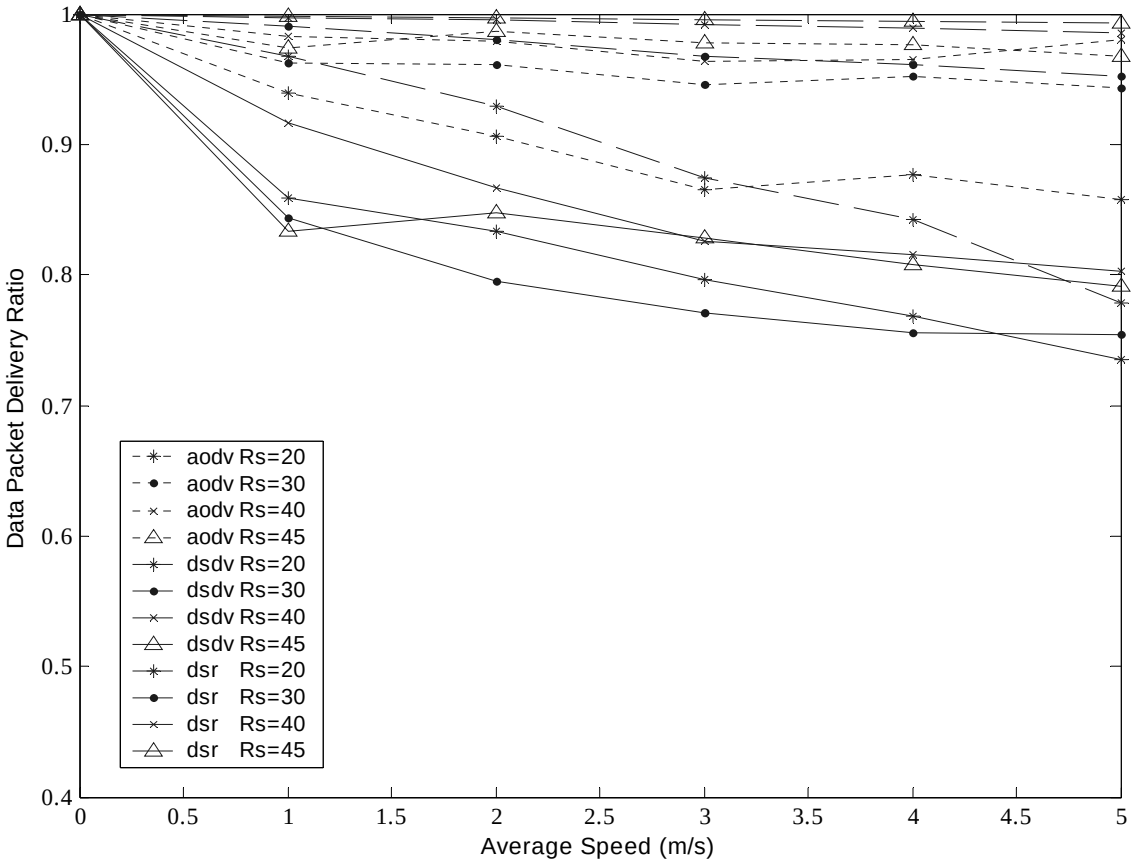

Figure 4.11: Data Packet Delivery Ratio vs. Speed for different transmission range in outdoor are

From figure 4-11, it can be implied that as the transmission range increases, the packet delivery ratio increases for the outdoor model. But there is not a very difference between transmission ranges of the nodes.

4.5 Conclusion

Using the two-ray model for propagation in an indoor channel, the DSR, LAR and AODV protocols show high and constant packet delivery ratio regardless of the speed. The DSDV and DREAM protocols show almost constant and unacceptable packet

delivery ratio at even low mobility. All routing protocols except DREAM have comparable packet overhead to data packet delivery ratios.

Control byte transmission per data packet delivered is higher for DREAM and DSDV in comparison to other routing protocols.

Data packet delivery ratio decreases for the DSR, LAR and DSDV protocols as speed increases in the indoor model. Data packet delivery ratio is constant for the DREAM routing protocol. AODV has the best packet delivery ratio amongst all the other routing protocols for the indoor model. Control packet transmission per data packet delivery ratio for all routing protocols except DREAM increases as the speed increases. Also, AODV has less control byte transmission per data packet delivery amongst all of the protocols.

In the Raleigh model, the LAR and DSR routing protocols have a constant packet delivery ratio of around 90%. The AODV and DSDV routing protocols have a constant packet delivery ratio of around 80%, while the DREAM protocol has a packet delivery ratio of 55%. The ratio of control byte transmissions per data packet delivery is almost constant for all protocols except DREAM and DSDV as the speed increases.

In general, DREAM has unacceptable, but consistent, performance for all of the compared physical layer models. The LAR protocols have the same and acceptable performance for two ray and Rayleigh fading channel models, but their performance is not acceptable for the indoor model. DSR has similar packet delivery ratio to LAR protocols but it has less control packet overhead.

AODV has packet delivery ratio of more than 75% for all scenarios, but its performance is worst in Raleigh fading scenario.

From the simulation results we understand that using location information for routing in ad hoc routing protocols does not have a great impact on the QoS parameters of the system. Although location information is used to decrease the routing overload in the network, finding location of the nodes and transferring location information increases the overhead and causes congestion in the network.

Chapter 5 : Principle of Geolocation

Geolocation can be defined as a means by which one can determine the location of a node, while navigation would be the process of updating the node's location. Navigation and geolocation methods can be classified into six categories: Piloting, Dead Reckoning, Celestial Navigation, Inertial Navigation, Proximity Method, and Radio Geolocation [Beu99][Par96]. Piloting guides an object by frequent references along fixed waypoints. Dead Reckoning is based on accurate measurements of an object's acceleration, velocity, and direction of movements using various inertial or magnetic sensors. Celestial Navigation uses the observation of the celestial bodies to determine the position of an object on the surface of the Earth. Inertial Navigation is done by using gyroscopes or of integrating accelerometers mounted on stabilized platforms. Radio Navigation employs characteristics of the electromagnetic waves for navigation and geolocation. The focus of this thesis is on radio geolocation.

5.1 Radio Geolocation

The location discovery process in a radio geolocation system consists of a distance or angle estimation phase and a distance or angle combining phase. This procedure is shown in Figure 5.1.

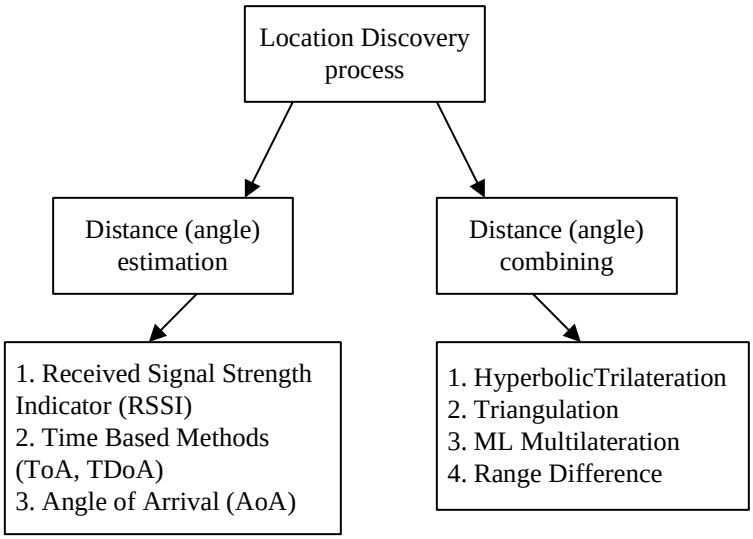

Figure 5.1: Location discovery process

Distance and angle estimation methods can be based on measuring a Received Signal Strength Indicator (RSSI), Angle of Arrival (AoA), Time of Arrival (ToA), or Time Difference of Arrival (TDoA). The RSSI method measures distance based on signal power at the receiver, the known transmission power, and known *a priori* channel model. This method has been used for RF signals. The AoA method estimates the angle at which the signals are received and uses simple geometric relationships to calculate node positions. The AoA method is usually measured by using directional antennas or more often, using antenna arrays.

ToA and TDoA methods record time of arrival or time difference of arrival. The propagation time can be directly translated into distance based on known signal propagation speed. These methods can be applied to many different signals, such as RF, acoustic, infrared, and ultrasound. Table 5.1 summarizes these range measurement methods.

Table 5.1: Comparison of distance (angle) estimation methods

Range Measurement	RSS	TOA	TDoA	AoA
Observed information	Received signal strength	Propagation time of received wave	Arriving time of waves emitted in same time	Incidence angle of received wave
Suitable Environment	Urban & Indoor	Urban & Suburban	Urban & Suburban	Rural & areas where LOS is available
Example of application	RF ID tags	Satellite Positioning (GPS, GLONASS)	Positioning for ship (LORAN, Decca)	Phased array radar
Advantages	- Simple computation - Low cost - Independent of radio system - No synchronization for Base Station is required	- In the case of coherent detection, high accuracy is possible	- In the case coherent detection, high accuracy is possible - Time of transmission is not needed by Receiver.	-Simple computation -Independent of radio system -No synchronization for Base Station is required
Disadvantages	- Low accuracy in large cells	- Synchronization is required - Expensive	- Complex calculation - Expensive - Synchronization required	- Array antenna required - Low accuracy in large cells

The most popular distance and angle combining methods include Hyperbolic Tri-lateration, Triangulation, Maximum Likelihood (ML) estimation, and Range Difference estimation. These methods are illustrated in Figure 5.2. The Hyperbolic Tri-lateration method locates a node by calculating the intersection of three circles in 2D or four spheres in 3D (Figure 5.2a) and is commonly used with the RSSI range estimation method. Triangulation locates a node by using the trigonometry laws of sins and cosines (Figure 5.2b) and this method is commonly used with the AoA estimation method. When there are more than three range measurements available we can use the Multilateration method. The Maximum Likelihood Multilateration method (Figure 5.2c) calculates the position of a node by selecting the position that minimizes the difference between the measured and estimated distances to neighboring nodes. The Range Difference method (Figure 5.2d) uses the range difference between the nodes with known location to estimation the location of the unknown node.

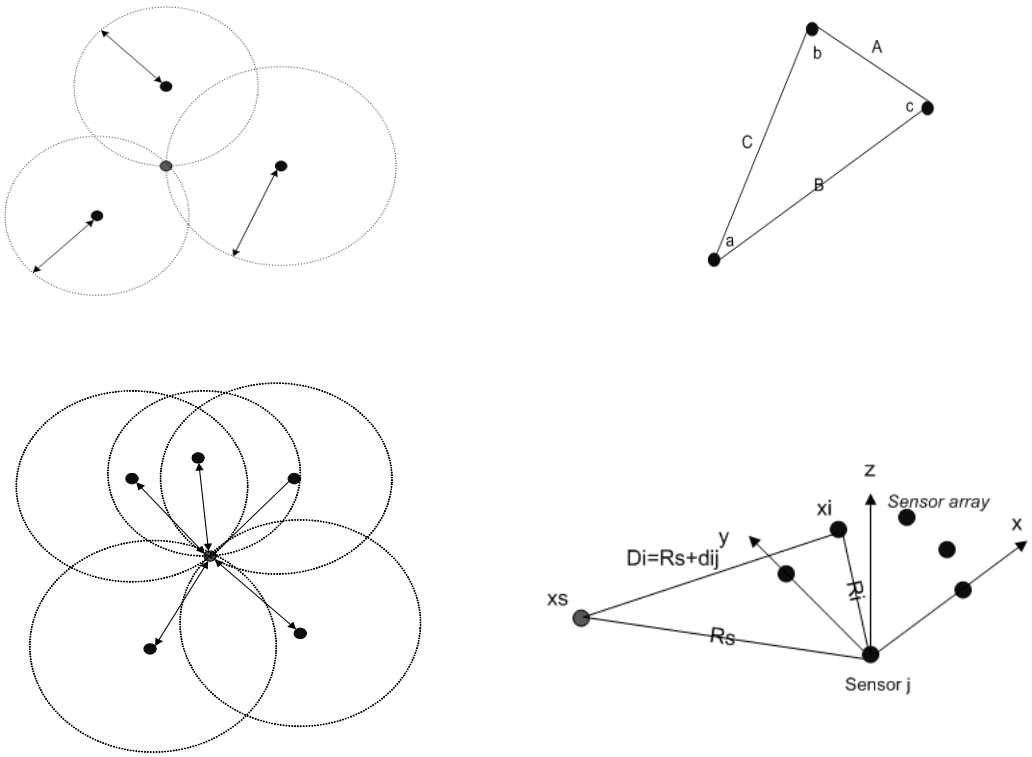

Figure 5.2: Combining phase methods (a) Hyperbolic Tri-lateration, (b) Triangulation method $\frac{A}{\sin(a)} = \frac{B}{\sin(b)} = \frac{C}{\sin(c)}$**, (c) ML Multilateration, (d) Range Difference method.**

5.2 Metrics for Comparing Geolocation Systems

Radio geolocation systems are evaluated by a set of parameters that are dependent of the technology or techniques a system uses and cannot be applied to all positioning systems. These metrics are:

- **Physical Position and Symbolic Location:** A location system can provide physical or symbolic information. For example a building is located at 12°E, 43°N by 12°W, at a 20m elevation. In contrast, a symbolic location indicates where something is located. For example “in the kitchen” or “next to the mailbox”.

- **Absolute versus Relative:** An absolute location system uses a shared reference grid for all located objects. For example, all GPS receivers use latitude, longitude, and altitude. In a relative system, each object can have its own frame of reference.
- **Accuracy and Precision:** A location system should report locations accurately and consistently from measurement to measurement. Some inexpensive GPS receivers can locate positions to within 10 meters for approximately 95% of measurements. More expensive differential units usually do much better, reaching 1 to 3-meter accuracies 99% of the time.
- **Scale:** A location-sensing system may be able to locate objects worldwide, within a metropolitan area, throughout a campus, in a particular building, or within a single room. Further, the number of objects the system can locate with a certain amount of infrastructure or over a given time may be limited. For example, GPS can serve an unlimited number of receivers worldwide using 24 satellites plus three active spares.
- **Cost:** We can assess the cost of a location-sensing system in several ways. Time costs include factors such as the installation process's length and the system administration needs. Space costs involve the amount of installed infrastructure and the hardware's size and form factor.
- **Limitations:** Some systems will not function in certain environments. This limitation has implications for the kind of applications we can build.

5.3 Geolocation Systems Overview

In the past few decades, wide ranges of localization applications and technologies have been developed. In this section, we survey some of the research and commercial location systems. Table 5.2 summarizes the properties of these technologies. In the 1970s, automatic vehicle location (AVL) systems were implemented to determine the position of a vehicle. In these systems, a set of stationary base stations acted as observation points and used ToA and TDoA techniques to generate distance estimates [Fri87]. The multilateration technique and Taylor Series expansion was used to transform the resultant non-linear least squares problem to a linear problem. Similar approaches can also be found in military applications for determining the position of airplanes [Par96]. In 1993, the well-known GPS system was deployed, which is based on the NAVSTAR satellite constellation (24 satellites). LORAN operates in a similar way to GPS but uses ground-based beacons instead of satellites. In 1996, the Federal Communications Commission (FCC) required all wireless service providers to provide location information to Emergency 911 services by October 2001. Following this requirement, localization algorithms have merged with communication applications such as cellular phones. In cellular networks, base stations transmit a beacon signal, while mobile stations reply back to the base station. TDoA is used to estimate the distance between mobile station and base station. Multilateration techniques using least squares methods are used to locate mobile handsets.

The RADAR [Bah00] system has been developed by Microsoft Research for indoor localization. This system uses RF signal strength measurements from fixed base stations that can track the location of users within a building. The RADAR system works

in two phases. First, a comprehensive set of received signal strength measurements is obtained in an offline phase to build a set of signal strength maps. The second phase is an online phase during which the location of users can be obtained by observing the received signal strength from the user stations and matching that with the readings from the offline phase. With this method multipath and shadowing effects are eliminated.

Table 5.2: Related work in Geolocation

Technology Name	Geolocation Technique	Abs/ Rel	Accuracy	Scale	Limitation
GPS	Radio ToA Multilateration-least square methods	Abs	1-5 meters (95-99%)	24 satellites worldwide	Non indoors
AVL	ToA-TDoA Multilateration-non linear least square	Rel			Non indoors
LORAN	Ground-base beacons Multilateration-least square methods	Abs	100m	Coastal system	Non indoors
E-911	TDoA Multilateration-least square methods	Abs	150-300m(95%)	Density of cellular infrastructure	Where cell coverage
RADAR	RSSI Multilateration		3-4.3m(50%)	3 bases per floor	Wireless NICs required
Cricket	Proximity, lateration	Rel	4x4 ft. regions (~100%)	~1 beacon per 16sq. ft.	No central management, receiver computation
Bat	Multilateration	Abs	9cm (95%)	1 base per $10\,m^2$	Required ceiling sensor grids
Badges	Ultrasound TOA/TDoA lateration	Abs	Room size	1 base per room	Sunlight & fluorescent interference

Bat [War99][War97] is another localization system developed for indoor geolocation. In the Bat system, signals from an ultrasound transmitter are collected by an array of receivers placed on the ceiling. Location of a Bat transmitter can be calculated via multilateration with a few centimeters of accuracy. An RF base station coordinates

the ultrasound transmissions such that interference from nearby transmitters is avoided. The Bat system relies heavily on a centralized infrastructure.

An outdoor localization technique has been proposed for sensor nodes in ad-hoc situations. In the method proposed by [Savv01], the location of a node is given as a centroid. This centroid is generated by counting the beacon signals transmitted by a set of beacons pre-positioned in a mesh pattern. PicoRadio [Beu99] presented by UC Berkeley is based on RSSI and pre-calculated signal strength maps. The Cricket campus [Pri01] system proposed by MIT uses several ultrasound sensors and one RF receiver to calculate sensor node's location. AHLoS [Sav02] is designed for ad hoc situation and uses RF and ultrasound transmissions to calculate location of the node. Unlike Cricket and Bat, AHLoS is a fully ad-hoc system with distributed localization algorithms running at every node.

5.4 Location Discovery Algorithms

Different distributed localization algorithms have been proposed for localized and distributed position calculations. Distributed algorithms developed for localization can be divided to two different approaches. The first characterization is according to whether or not they rely on anchor nodes, which are nodes that are preconfigured with their true position with the help of GPS or any other navigation devices. The second is based on whether they are incremental or concurrent algorithms.

Anchor-based algorithms [Pri01] rely on anchor nodes and assume that a certain minimum number of the nodes know their position, e.g., by manual configuration or using some other navigation devices. The final coordinate assignment of individual

nodes will therefore be valid with respect to another possibly global coordinate system. Any positioning scheme built around such algorithms has the limitation that it needs another positioning scheme to bootstrap the anchor node positions, and cannot be easily applied to any context in which another location system is unavailable. It turns out that in practice a large number of anchor nodes are needed for the resulting position errors to be acceptable.

Anchor-free algorithms [Pri01][How01] use only local distance information to determine node coordinates and no nodes have preconfigured positions. Of course, this coordinate system will not be unique and can be embedded into another global coordinate space in different ways, depending on global translation, rotation, and possibly flipping. This limitation is fundamental to the problem specification, and is not a limitation of the algorithm. If the coordinate assignments must conform to another coordinate system such as GPS, any algorithm that does not use anchor nodes can easily be converted to a one that uses a small number of anchor nodes by adding a final transformation where all the node coordinates are transformed using three (in 2D) or four (in 3D) anchor nodes.

Incremental algorithms usually start with a core of three or four nodes with assigned coordinates. Then they repeatedly add appropriate nodes to this set by calculating the node's coordinates using the measured distances to previous nodes with already computed coordinates. These coordinate calculations are based on either simple trigonometric equations or some local optimization scheme. One of the drawbacks of these algorithms is error propagation, which may result in poor overall coordinate assignments. Some incremental approaches apply a later global optimization phase to balance such errors [Pri01].

In concurrent algorithms, all the nodes calculate and refine their coordinate information in parallel. Some of these algorithms use an iterative optimization scheme that reduces the difference between measured distances and the calculated distances based on current coordinate estimates. Concurrent optimization schemes have a better chance of avoiding local minima compared to incremental schemes, especially in the presence of measurement errors, because they continually balance global error and thereby try to avoid error propagation.

5.5 Detailed Description of Existing Geolocation Systems

To help understand how the problem of indoor positioning has been approached, this section describes the Cricket and Bat geolocation systems in more detail.

5.5.1. Cricket

Cricket is an indoor location system for pervasive computing environments [Pri00]. Cricket uses a combination of RF and ultrasound technologies to provide geolocation service to users and applications. Wall-mounted and ceiling-mounted beacons are spread through the building, broadcasting information on an RF signal operating in the 418 MHz AM band. With each RF advertisement, the beacon transmits a concurrent ultrasonic pulse. Listeners attached to devices and mobiles listen for RF signals, and upon receipt of the first few bits, listen for the corresponding ultrasonic pulse. When this pulse arrives, they obtain a distance estimate for the corresponding beacon. The listeners run maximum-likelihood estimators to correlate RF and ultrasound samples and to pick the best one.

The Cricket Compass provides 3D positioning information and orientation information. Cricket uses multilateration to calculate the position.

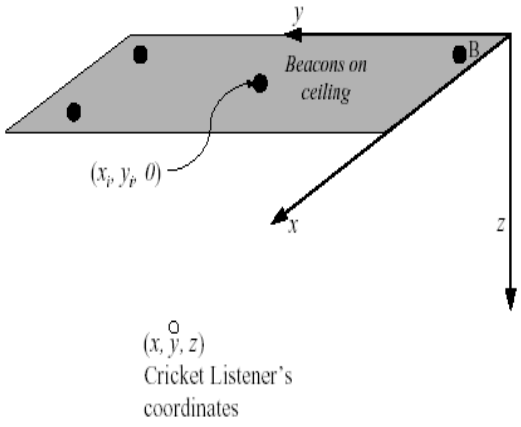

Figure 5.3a

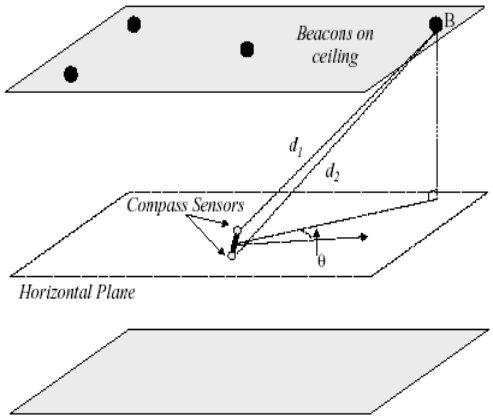

Figure 5.3b

Figure 5.3: Cricket location estimation method (a) Cricket Listener's coordinates, (b) Location calculation.

5.5.1.1 Cricket Location Measurement

Let v be the speed of the sound, d_i be the actual distance to each beacon B_i at known coordinates (x_i, y_i, z_i), and $\hat{t}_i$ be the measured time-of-flight to beacon B_i. The following distance equations hold:

$$(x - x_i)^2 + (y - y_i)^2 + (z - z_i)^2 = d_i^2 = \left(v\hat{t}_i\right) \qquad (5.1)$$

If the beacons are installed on the same *x*-*y* plane, we can set $z_i = 0$. Thus, the coordinate system defined by the beacons has a positive z-axis that points downward inside a room, as shown in Figure 5.3a. Consider *m* beacons installed on the ceiling, each broadcasting their known coordinates $(x_i, y_i, 0)$. We can eliminate the z^2 variable in the

distance equations and solve the following linear equation for the unknown listener coordinate $P = (x, y, z)$ if the speed of sound v is known:

$$A \vec{x} = \vec{b} \tag{5.2}$$

Where the matrix A and vectors $\vec{x}$, $\vec{b}$ are given by

$$A = \begin{bmatrix} 2(x_1 - x_0) & 2(y_1 - y_0) \\ 2(x_2 - x_0) & 2(y_2 - y_0) \\ \cdots & \\ 2(x_{m-1} - x_0) & 2(y_{m-1} - y_0) \end{bmatrix}, \qquad \vec{x} = \begin{bmatrix} x \\ y \end{bmatrix}, \tag{5.3}$$

$$\vec{b} = \begin{bmatrix} x_1^2 - x_0^2 + y_1^2 - y_0^2 - v^2\left(\hat{t}_1^2 - \hat{t}_0^2\right) \\ x_2^2 - x_0^2 + y_2^2 - y_0^2 - v^2\left(\hat{t}_2^2 - \hat{t}_0^2\right) \\ \vdots \\ x_{m-1}^2 - x_0^2 + y_{m-1}^2 - y_0^2 - v^2\left(\hat{t}_{m-1}^2 - \hat{t}_0^2\right) \end{bmatrix}, \qquad m \geq 3 \tag{5.4}$$

When $m \succ 3$, the system is over-constrained. In the presence of time-of-flight measurement errors, there may not be a unique solution for (x, y). We can still solve for an estimated value (x', y') by applying the least-squares method. For a general system of linear equations, the least squares method finds a solution $\vec{x}'$ that minimizes the squared error value δ, where

$$\delta = \left(A\vec{x}' - \vec{b} \right)\left(A\vec{x}' - \vec{b} \right)^T, \qquad \vec{x}' = \begin{bmatrix} x \\ y \end{bmatrix}, \tag{5.5}$$

the least-squares approach basically gives the best-fit approximation to the true position (x, y).

5.5.2. The Bat System

The Bat ultrasound location system as implemented by Cambridge University provides fine-grained 3D location and orientation information. The Bat is a 3D ultrasonic location system, which consists of transmitters attached to tracked objects and mobile units (see Figure 5.4), and an array of calibrated receivers deployed at known locations on the ceiling [War99] [War97]. RF and ultrasonic signals are transmitted simultaneously from the transmitters. The receiver measures the delay of the ultrasonic signal to infer its time of arrival from the mobile unit.

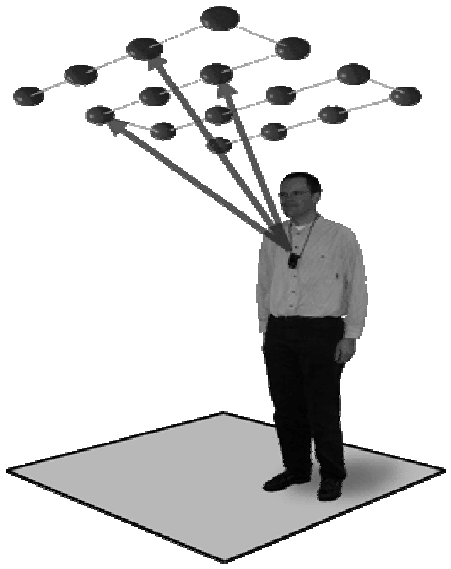

Figure 5.4: Bat location estimation method

By multiplying the measured time of arrival with the speed of sound, one can calculate the distance between a receiver and the mobile unit. A different distance estimate is obtained for each of the receivers deployed on the ceiling. The known positions of the receivers and their estimated distance from the mobile unit are used to calculate the mobile unit's position. Also, the use of ultrasound in these systems would imply that they are only good if there is an unobstructed path from the ultrasonic transducer to the receiver.

5.5.2.1 Bat Location Measurements

Bat uses multilateration with nonlinear regression as its combining phase method. In this method a set of receivers are placed at points on a horizontal ceiling. It is assumed that a mobile transmitter is placed at location (x, y, z) and its distance from the receiver at coordinate system $(x_i, y_i, 0)$ is R_i:

$$R_i = \sqrt{\left(x_i^2 + y_i^2\right) + \left(x^2 - 2x_i x\right) + \left(y^2 - 2y_i y\right) + z^2} \tag{5.6}$$

This relationship can be viewed in a setting where an estimate of the mobile unit position is to be determined. This position is calculated based on a set of distances $R_1, R_2, ..., R_n$ that are simultaneously measured from the mobile unit to a corresponding set of non-collinear receivers at positions $(x_1, y_1, 0), ..., (x_n, y_n, 0)$ where $n \geq 3$. The distance measurements and positions of the receivers will be subject to experimental error, and so Equation 5.7 must be extended, as below:

$$R_i = \sqrt{\left(x_i^2 + y_i^2\right) + \left(x^2 - 2x_i x\right) + \left(y^2 - 2y_i y\right) + z^2} + \varepsilon_i \qquad (i = 1,\ldots,n) \qquad (5.7)$$

This equation is a nonlinear model. A nonlinear regression method can be used to fit the collected values of $R, x,$ and y to the model, where $\hat{x}, \hat{y}, \hat{z}^2$ are estimated parameters of x, y and z^2. The estimates will minimize the sum of the squares of the residuals given by

$$\begin{aligned} e_i &= R_i - \hat{R}_i \\ \hat{R}_i &= \sqrt{\left(x_i^2 + y_i^2\right) + \left(\hat{x}^2 - 2x_i\hat{x}\right) + \left(\hat{y}^2 - 2y_i\hat{y}\right) + \hat{z}^2} \qquad (i = 1,\ldots,n) \end{aligned} \qquad (5.8)$$

For $n \geq 4$, the standard deviation of the mobile unit distance measurements around the ideal relationship of Equation 5.8 can also be estimated, using the standard error of the estimate, s, where

$$s = \sqrt{\frac{\sum_{i=1}^{n} e_i^2}{n-3}} \qquad (5.9)$$

The standard error of the estimate provides an approximate measure of the overall predictive value of the nonlinear model, and hence indicates the extent to which the data set fits that model.

5.6 Summary

In this chapter we studied the location finding problem and, as an example we studied in more detail some of the geolocation systems that have been developed for indoor geolocation. One disadvantage of these systems is the expensive wiring infrastructure used to relay information. Also, in many situations of interest, deploying a fixed infrastructure may not be possible. Many of these systems need a central computer to calculate the location of an object and that maybe costly from the time perspective. These systems are mainly proposed for calculating location of the nodes in 2D and they don't provide location information in 3D. In the case of 3D, there is an ambiguity in the location of the nodes in space. In addition, these systems do not scale well with the number of objects being located in the system. As the number of locatable object increases, the level of contention among transmitters increases.

With this background, we justify the need for better solution to the geolocaiton information and in the next section we proposed our location discovery algorithm that tries to solve some of these problems.

Chapter 6 : Position Fixing for Mobile Ad Hoc Networks

This chapter presents a method to facilitate large-scale deployment of location-aware ad hoc networks. The main idea of this chapter is to show that large networks of location-aware ad hoc nodes can be made cooperatively self-configuring, that is, that each sensor can run an algorithm locally, interacting only with neighboring nodes, such that after a number of iterations all sensors will have reached a consensus about their coordinates in some coordinate system. This chapter solves the following problem: *Given a set of nodes with unknown location coordinates, and a mechanism by which a node can estimate its distance to a few nearby (neighbor) nodes, determine the position coordinates of every node via local node-to-node communication.* This problem is known as graph realization from a graph theory perspective.

Our solution to this problem is a distributed, infrastructure-free, three-dimensional positioning algorithm that does not rely on any external geolocation system. The algorithm uses the distances between the nodes to build a relative coordinate system for every node and converges to a coordinate assignment that is consistent with the distance estimates by exchanging only local information. The resulting coordinate assignment has translational and orientational degrees of freedom, but is correctly scaled. Post-processing could incorporate absolute location information into four or more nodes as a means to remove the translational and orientational degrees of freedom. To formulate a location discovery algorithm, we have developed a geometric and graph theoretical approach. We also propose necessary and sufficient conditions for location discovery.

In Section 6.1, we propose a general flow of our geolocation algorithm and in the subsequent sections we explain detail of each step of the algorithm. And finally we propose the algorithm in Section 6.8.

6.1 Generic Flow of the Algorithm

To reconstruct a three-dimensional set of points using noisy information about the distance between the nodes, we propose a distributed algorithm that gradually calculates the location of the nodes in the network. We assume that error in distance measurements lies within a certain tolerance. In this algorithm each node sends a Hello message to find its number of neighbors and, each node periodically sends its location table to the other nodes in its transmission range to find its k-hop neighbors. In this way, nodes can update their information about the network topology. As we will describe later in this chapter, each node builds its own graph theoretic model of the network and tries to calculate location of the nodes in its own local coordinate system. If a node has less than four neighbors, it cannot establish its coordinate system. If the node has greater than or equal to four neighbors, it can calculate its coordinate system. Also a node should have four neighbors that are in the transmission range of each other. At the end of running this algorithm, each node knows the topology of the whole network and location of the other nodes in its local coordinate system. We also use a mechanism to reduce the propagation of position errors in the network.

6.2 Location Estimation Methods

In this section we describe the location estimation technique we used for the localization algorithm. The problem can be stated as:

Given a set of nodes with known location coordinates, and a mechanism by which a source node with unknown location can estimate the distance to a few nearby (neighbor) nodes, determine the location coordinate of the source node.

Different methods have been proposed in the literature to answer the above question. Here, in addition to a general background, the range difference method is explained.

6.2.1 Background and Related Work

TDOA can be estimated by two methods: subtracting the TOA measurements from two nodes, or correlating two versions of the acknowledgement signals at two synchronized nodes. Two approaches can be found in literature for producing a location estimate from TDOA measurements: geometrical and statistical. The first approach is based on the geometrical relationship between the node locations and TDOA measurements. The geometrical approach for calculating the position of a node is to solve for the intersection of the circular or hyperbolic lines of position. The statistical approach is based on Least squares, Maximum likelihood estimation and other optimization methods.

A common method for estimating a source location from the measurements derived from TDOA, is based on finding a hyperbolic line of positions. Each range (or time) difference determines a hyperbola. The point at which these hyperbolas intersect is the estimated source position. Another approach is based on the idea that three nodes

with their set of range differences determine a straight line of position. This line is the major axis of a general conic section that passes through the nodes. These two methods are shown in Figures 6.1a and 6.1b. When more than three nodes are available, several lines of position are generated and their intersection provides an estimate of the source location. The method proposed in [Sch72] computes the intersection point from a set of $\binom{N}{3}$ linear equations, where N is the number of nodes.

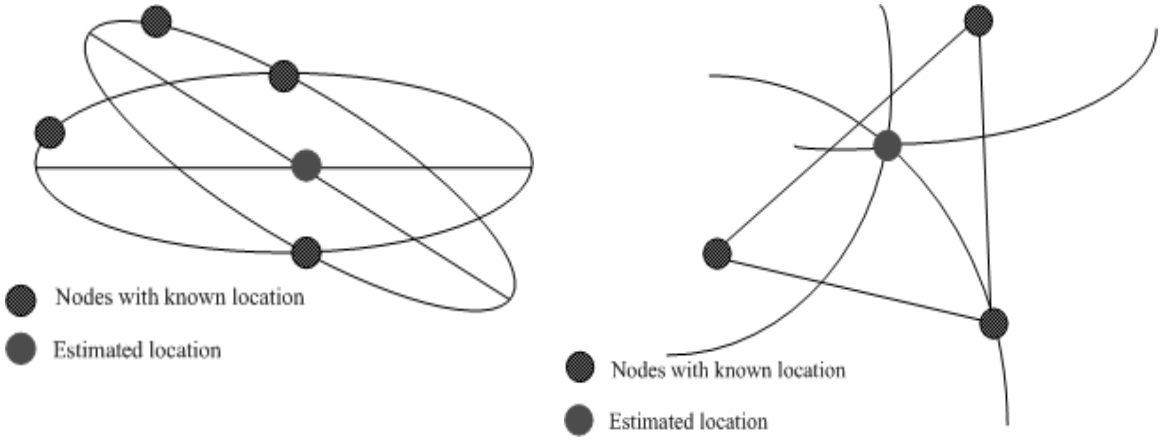

(a) **(b)**

Figure 6.1: (a) Location on the conic axis, (b) Hyperbolic lines of position.

A different approach is proposed by [Del80] based on the straight line of position approach, which leads to a set of N equations. These equations contain all the relevant node information without redundancy. But there is nonlinearity between certain variables in these equations and this causes computational difficulty. The method proposed in this section is based on a set of either $(N-1)$ or $(N-2)$ linear equations. This method is

called the range difference method and we discuss in more detail this section. A similar method has been proposed in [Fri87].

6.2.2 Range Difference Method

The range difference method (or, a passive localization algorithm) presented in [Fri87] calculates the location of a node based on the solution of a set of either $(N-1)$ or $(N-2)$ linear equations. For this method we need $N \succ (n+1)$ nodes, where n is the dimension of the coordinate system. For instance, in three-dimensions N should be greater than 4. In some practical situations, no more than $N = n+1$ nodes with known locations are available. In this section we derive explicit equations for these situations.

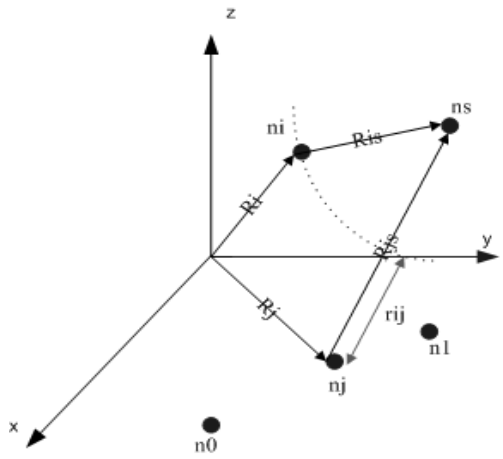

Figure 6.2: Range difference method.

Let $n_i = [x_i, y_i, z_i]$ denote the (x, y, z) coordinate of the *ith* node, $n_s = [x_s, y_s, z_s]$ denote the source location and R_{is} and R_{js} be the measured distances

between a node with unknown location, n_s, and the nodes n_i and n_j respectively (see Figure 6.2). The range difference in the distance of nodes n_i and n_j, r_{ij}, is equal to:

$$r_{ij} = R_{is} - R_{js} = \|n_i - n_s\|^2 - \|n_j - n_s\|^2 \tag{6.1}$$

There are $\binom{N}{2} = \frac{N!}{(N-2)!2!}$ distinct range differences. However, all of these range measurements can be completely determined from $(N-1)$ range measurements (e.g., $\{r_{i1},\ i = 2,...,N\}$). The square of the distance between the source and the ith node can be written as:

$$R_{is}^2 = (r_{ij} + R_{js})^2 = r_{ij}^2 + 2R_{js}r_{ij} + R_{js}^2 \tag{6.2}$$

We also have:

$$R_{is}^2 = \|n_i - n_s\|^2 = n_i^2 - 2n_i n_s^T + n_s^2 \tag{6.3}$$

If we set the left terms of Equations 6.2 and 6.3 to be equal to each other, we have:

$$2n_i n_s^T = n_i^2 + n_s^2 - r_{ij}^2 - 2R_{js}r_{ij} - R_{js}^2 \tag{6.4}$$

For $i = j$, we can rewrite Equation 6.4 as:

$$2n_j n_s^T = n_j^2 + n_s^2 - R_{js}^2 \tag{6.5}$$

Subtracting Equation 6.5 from Equation 6.4 we have:

$$2\left(n_i - n_j\right)n_s^T = n_i^2 - n_j^2 - r_{ij}^2 - 2R_{js}r_{ij} \tag{6.6}$$

Equation 6.6 can also be written in matrix form as:

$$A_j n_s^T = B_j - R_{js}C_j \tag{6.7}$$

Where

$$A_j = \begin{bmatrix} \left(x_1 - x_j\right) & \left(y_1 - y_j\right) & \left(z_1 - z_j\right) \\ \vdots & \vdots & \vdots \\ \left(x_{j-1} - x_j\right) & \left(y_{j-1} - y_j\right) & \left(z_{j-1} - z_j\right) \\ \left(x_{j+1} - x_j\right) & \left(y_{j+1} - y_j\right) & \left(z_{j+1} - z_j\right) \\ \vdots & \vdots & \vdots \\ \left(x_N - x_j\right) & \left(y_N - y_j\right) & \left(z_N - z_j\right) \end{bmatrix}, \ \left(N-1\right)\times 3 \tag{6.7a}$$

$$B_j = \frac{1}{2}.\begin{bmatrix} n_1^2 - n_j^2 - r_{1j}^2 \\ \vdots \\ n_{j-1}^2 - n_j^2 - r_{j-1j}^2 \\ n_{j+1}^2 - n_j^2 - r_{j+1j}^2 \\ \vdots \\ n_N^2 - n_j^2 - r_{Nj}^2 \end{bmatrix}, \ \left(N-1\right)\times 1 \tag{6.7b}$$

$$C_j = \begin{bmatrix} r_{1j} \\ \vdots \\ r_{j-1j} \\ r_{j+1j} \\ \vdots \\ r_{Nj} \end{bmatrix}, \ (N-1)\times 1 \tag{6.7c}$$

Given the range measurements $\{r_{ij}, \ i = 1,...,N\}$, matrices A_j, B_j and C_j are known, as they depend only on the known node locations and range measurements. Location vector n_s can be computed by using a least squares equation solver. A closed-form solution that is useful for some subsequent derivations is given by:

$$n_s^T = \left(A_j^T A_j\right)^{-1} A_j^T \left(B_j - R_{js} C_j\right) \tag{6.8}$$

In solving Equation 6.8, we can calculate the coordinates of the source node. To verify different range based positioning algorithms and study the effect of errors in distance measurement or the error in the node location, we ran a set of Monte Carlo simulations for two different scenarios. First, we purely study the effect of error in the measured distances between the nodes on the location of an unknown node with the assumption that all nodes are located in their exact positions. In the second scenario, we assume that both the locations of the nodes, and the measured distances between the nodes are erroneous and we study these error effects on the node location [Ho04].

Figure 6.3 shows the location error obtained from the range difference algorithm versus the standard deviation of the measurement noise. In case 1, six nodes are located at (distances in meters)

$$r_0 = (0,0,0) \quad r_1 = (40,0,0) \quad r_2 = (-40,0,0)$$

$$r_3 = (0,0,40) \quad r_4 = (0,-40,0) \quad r_5 = (0,0,-40)$$

In the second case, five nodes are located at distances

$$r_0 = (0,0,0) \quad r_1 = (40,0,0) \quad r_2 = (-40,0,0)$$

$$r_3 = (0,0,40) \quad r_4 = (0,-40,0)$$

In the third case, seven nodes are located at distances

$$r_0 = (0,0,0) \quad r_1 = (40,0,0) \quad r_2 = (-40,0,0)$$

$$r_3 = (0,0,40) \quad r_4 = (0,-40,0) \quad r_5 = (0,0,-40) \quad r_6 = (20,20,20)$$

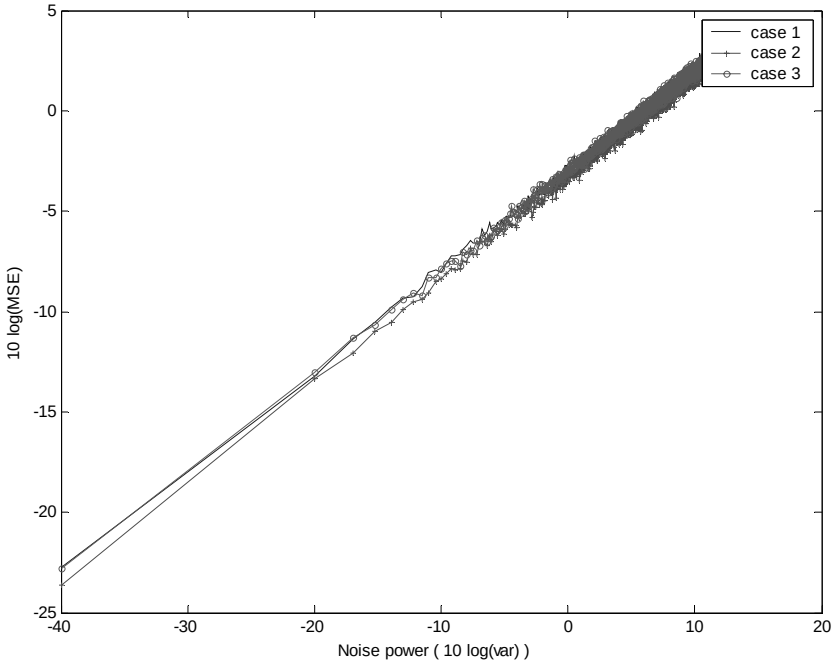

Figure 6.3: Error in Location Estimation versus Error in Distance.

As can be seen in Figure 6.3, there is not much difference in the estimated location error when the number of receivers changes. Figure 6.4a shows the situation where both the node locations and range measurements have error. The variance of error in position is proportional to: [1 2 2 4 3 2 5].

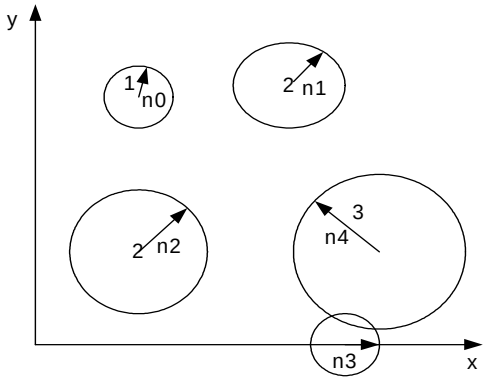

Figure 6.4a: True node location and variance of the location error

The locations of the nodes in case 1, case 2, and case 3 is the same as locations of the nodes in the above example, but the variance of error in location for case 4 is proportional to [1 2 2 4 3 22 9]. It can be infered from Figure 6.4b that error in location for case 1 and case 2 is almost the same while error in case 4 is higher than the other situations.

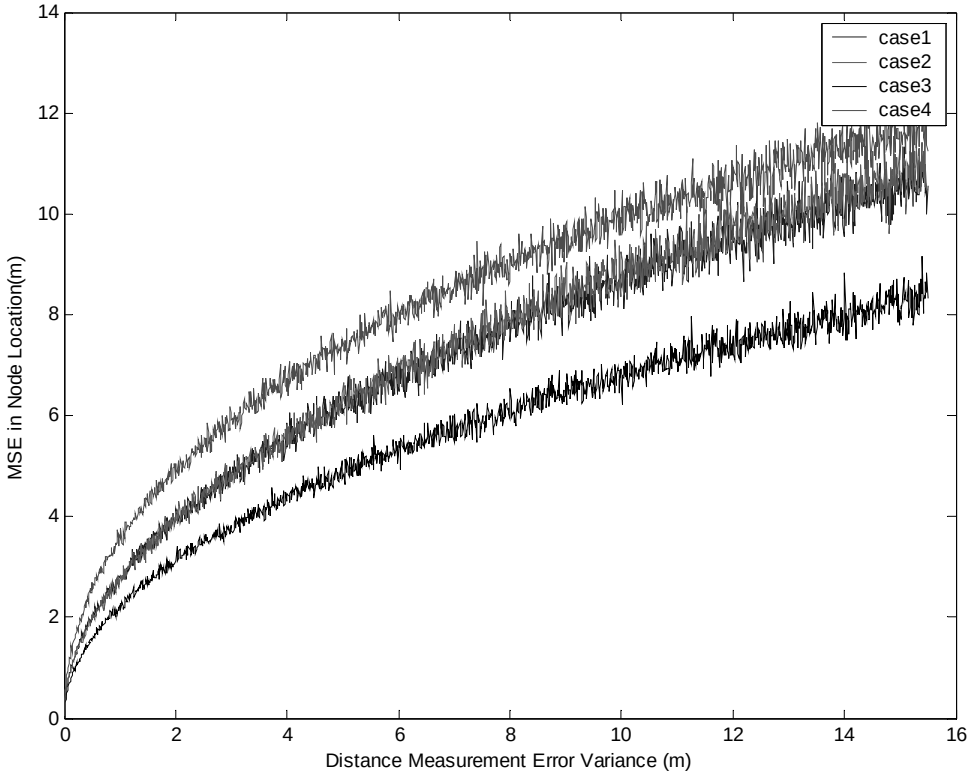

Figure 6.4b: Error in Location Estimation vs. Error in distance and receiver's location.

6.3 Distance Error Model

In time-based range estimation, the distance calculation is corrupted by error sources such as measurement error, time synchronization, NLOS propagation, and received signal strength. All of these types of errors can degrade the positioning accuracy. However, the major sources of error in time-based localization are measurement noise and NLOS propagation error. Measurement noise is usually modeled as a zero-mean Gaussian random variable, while NLOS error usually has an unknown distribution with a positive mean. Recently it has been shown that the NLOS error in TOA measurements can be modeled by the combination of zero mean Gaussian and Exponential distribution [Bar03]. To protect location estimation from NLOS error corruption, NLOS identification and reconstruction techniques have been investigated.

In our simulation we only consider the NLOS and measurement noise error and ignore the other types of error. Without considering other errors, range measurements of a source node n_s that receives distance information from N other beacon nodes is shown as:

$$r_{js} = d_{js} + n_{js} + NLOS_{js} \qquad j = 1,..., N \tag{6.9}$$

Where r_{js} is the range measurement to the jth node, d_{js} is the real distance between the two nodes, n_{js} is the measurement noise, and $NLOS_{js}$ is the NLOS error.

The measurement noise has a zero mean Gaussian distribution with a standard deviation of σ_n:

$$f(n)=\frac{1}{\sqrt{2\pi}\sigma_n}e^{-\frac{n^2}{2\sigma_n^2}} \tag{6.10}$$

The $NLOS_{js}$ error has an exponential distribution with the following distribution:

$$f(n)=ne^{-\lambda n} \tag{6.11}$$

NLOS error results from the blockage of direct signals and the reflection and diffraction of multipath signals. We use an error mitigation method to identify and eliminate the error caused by the NLOS conditions.

6.4 Building the Local Coordinate System

In this section we describe how every node builds its local coordinate system in three-dimensions. We assume that node n_0 becomes the center of its own local coordinate system with the coordinates (0,0,0); node n_1 lies on the assumed X-axis and has coordinate of $(R_{10},0,0)$. The location of the next node, n_2, which is in the transmission range of both nodes n_0 and n_1, is assumed to be in the plane of triangle $\Delta n_2 n_0 n_1$ with coordinate $(R_{20}\cos(\alpha), R_{20}\sin(\alpha),0)$, where α is the angle $\angle(n_2,n_0,n_1)$ in the triangle $\Delta n_2 n_0 n_1$. This angle can be calculated using the cosine rule for triangles: $\alpha=\cos^{-1}\left(\frac{R_{10}^2+R_{20}^2-R_{12}^2}{2R_{10}R_{20}}\right)$. As α can be clockwise or counter clockwise, there is

uncertainty about the coordinates of the node n_2. It could be one of two possible locations that have exactly the same distance to n_0 and n_1 respectively but are mirror images of each other with respect to the $n_0 - n_1$ line. This procedure has been shown in Figure 6.5. The location of node n_3 can be solved as:

$$x_3 = \frac{R_{10}^2 + R_{30}^2 - R_{13}^2}{2R_{10}} \tag{6.12}$$

$$y_3 = \frac{R_{20}^2 - R_{10}^2 - R_{23}^2 + R_{13}^2 + x_3\left(2R_{10} - 2R_{20}\cos(\alpha)\right)}{2R_{20}\sin(\alpha)} \tag{6.13}$$

$$z_3 = \sqrt{R_{30}^2 - x_3^2 - y_3^2} \tag{6.14}$$

In this way, n_3 has uncertainty between two locations that are symmetric to the plane of triangle $\Delta n_2 n_0 n_1$. Also we had two uncertainties concerning the location of node n_2 from the previous step. The location of this node is one of four possible locations in the plane. Similar calculations are used to find the location of the fourth node. Similarly to the other nodes, the location of this node now has eight degrees of uncertainty. The remaining nodes calculate their location based on the range difference method explained in Section 6.2.1. From this point, the degree of uncertainty remains eight. This is because we used the range difference method that uses more information to estimate the node location. Figure 6.6 shows the effect of uncertainty on the derived topology.

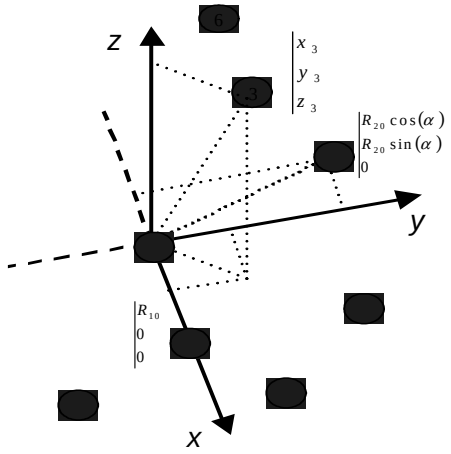

Figure 6.5: Establishing the coordinate system.

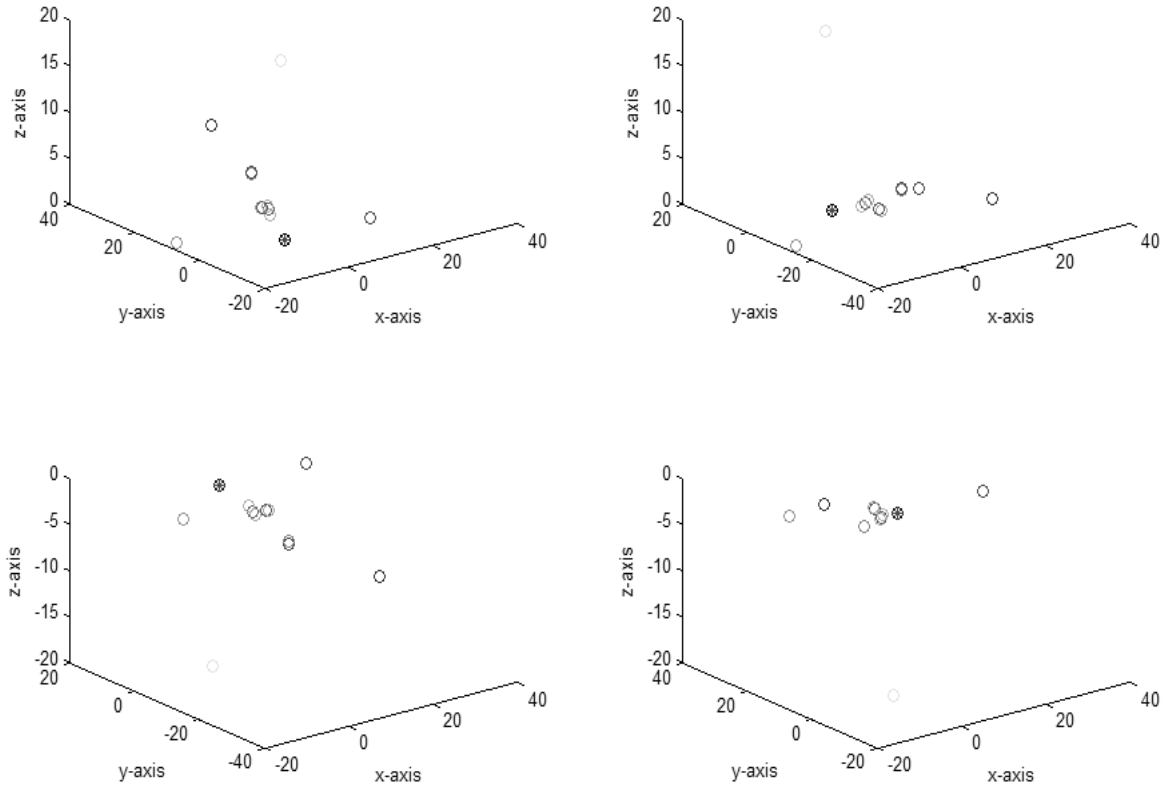

Figure 6.6: Effect of Uncertainty in the location estimation (a) sin(a) and z2 are positive, (b) sin(a) is negative z2 is positive, (c) sin(a) is positive z2 is negative, (d) sin(a) and z2 are negative.

A necessary condition for each node to calculate its local coordinate system is to have four neighboring nodes that are all within transmission range of each other. From a graph theory perspective, there should be a complete subgraph in the network topology for which node n_0, the center of the coordinate system, is one of the vertices. As all the nodes in the network topology calculate their local coordinate system, there should be enough nodes common to the various subgraphs that nodes can calculate the positions of other nodes relative to their coordinate system and their position in other coordinate systems.

6.4 Coordinate System Rotation and Position Computing

To adjust the direction of the coordinate system of the node n_j to have the same direction as the coordinate system of node n_i, node n_j has to rotate, and possibly mirror, its local coordinate system. The necessary conditions for two nodes to adjust their local coordinate system in 3D are:

- $n_i \in NNG_{n_j} \bigcap n_j \in NNG_{n_i}$
- $\exists\ n_k, n_q, n_p \neq n_i, n_j \quad \bigcap \quad n_k \neq n_q \neq n_p \quad \bigcap \quad n_k, n_q, n_p \in NNG_{n_i} \quad \bigcap$ $n_k, n_q, n_p \in NNG_{n_i}$

Two coordinate systems have the same direction if the directions of their X-axis, Y-axis and Z-axis are the same. To calculate the position of a two-hop node, we adjust the direction of the local coordinate systems of the nodes so that they are oriented in the same direction.

In the local coordinate system of the node n_i we consider its neighbor, n_k. To adjust the direction of coordinate system of the node n_k to have the same direction as the coordinate system of node n_i, node n_k has to rotate and possibly mirror its coordinate system. To make two coordinate systems, node n_i and n_k, have the same direction, the location of node n_i must be known in the coordinate system of node n_k and vise versa. Also, there must be at least two other nodes within a common transmission range of both nodes.

To calculate the location of a node, which is in the coordinate system of node n_k, in the coordinate system of node n_i, we rotate the coordinate system of node n_k to have the same direction as the coordinate system of node n_i, as shown in Figure 6.7. For example, node is in the XYZ coordinate system and node is in the X′Y′Z′ coordinate system. For rotation in 3D, we may use the following procedure:

1- In the X′Y′Z′ coordinate system of node n_k we calculate the angle between the Z′-axis and $\vec{ik}$ vector, β, and use it as a rotation angle. The cross product of the Z′-axis and $\vec{ik}$ is the rotation vector. We rotate the Z′-axis, and all the nodes in the coordinate system of node n_k around this arbitrary vector. The overall rotation matrix is:

$$R_m = R_{x'}(\phi)R_{y'}(\varphi)R_{z'}(\beta)R_{y'}(-\varphi)R_{x'}(-\phi) \tag{6.15}$$

$R_{x'}(\phi)$ And $R_{y'}(\varphi)$ are the rotation matrices around the X'-axis and Y'-axis. φ is the projection angle of rotation vector on Y′Z′ plane and ϕ is the angle between Z'-axis and projection of rotation vector on Y′Z′ plane. (this is shown in Figure 6.7a). After rotation, the Z''-axis is in the direction of vector $\vec{ik}$ so the orientation of the Z''-axis is known in the coordinate system of node n_i.

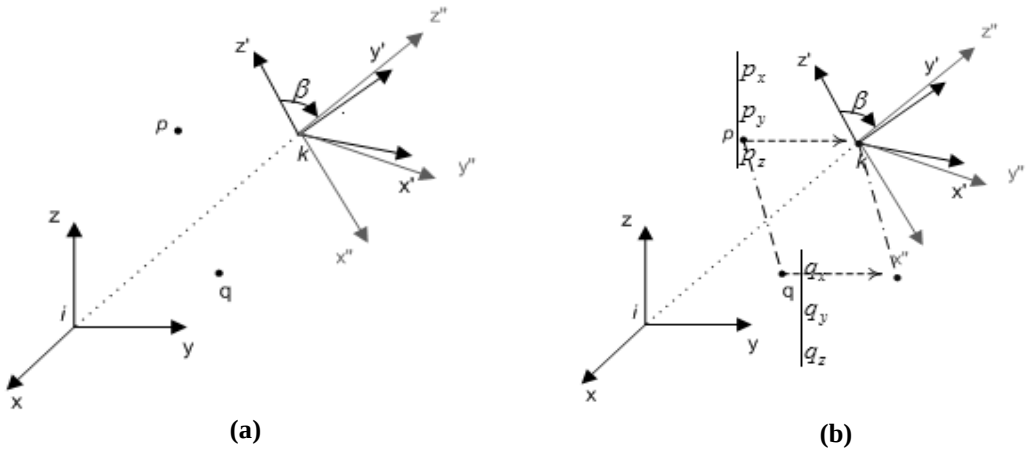

Figure 6.7: (a) Rotation of the coordinate system of node n_k with rotation angle β, (b) transfer of nodes p and q to the origin.

2- Next we translate node n_p to the origin of the coordinate system of node n_k and node n_q to the corresponding point in both the coordinate systems of node n_i and the coordinate system of node n_k. The projection of the node n_q in the X″Y″ plane can be calculated both in the coordinate system of node n_i and n_k. We then rotate the X″-axis and all the nodes in the coordinate system of node n_k

around the Z″-axis with angle α. Therefore X″-axis lies in the coordinate system of node n_i. The orientation of the Y″-axis can be determined using the right hand rule.

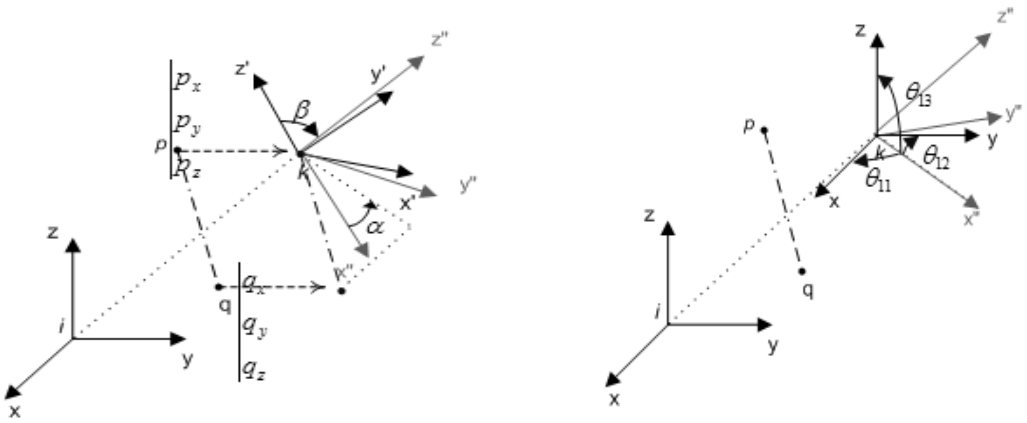

Figure 6.8: (a) Adjusting coordinate system of the two nodes, (b) finding the angle between two coordinate system.

3- Finally, we calculate the angle between the XYZ axes of two the two coordinate systems. When the angle between the two coordinate systems is known, we can calculate the rotated location of the node with the following matrix:

$$\begin{bmatrix} p_x \\ p_y \\ p_z \end{bmatrix} = \begin{bmatrix} \cos\theta_{xx'} & \cos\theta_{xy'} & \cos\theta_{xz'} \\ \cos\theta_{yx'} & \cos\theta_{yy'} & \cos\theta_{yz'} \\ \cos\theta_{zx'} & \cos\theta_{zy'} & \cos\theta_{zz'} \end{bmatrix} \begin{bmatrix} p_x'' \\ p_y'' \\ p_z'' \end{bmatrix} \tag{6.16}$$

With the above procedure, all the nodes obtain their locations within one coordinate system. If the coordinate system of node n_i is chosen to be the reference coordinate

system, all the nodes in the network have to adjust the directions of their coordinate systems to the same direction and every node has to compute its position in this system.

After node n_j adjusts its coordinate system to the coordinate system of node n_i, it can calculate the locations of its neighbor nodes in the coordinate system of node n_i. Here we explain how nodes can compute their positions in the coordinate system of node n_i. If node n_j knows its location in the coordinate system of node n_i, node n_l, which is a one-hop neighbor of node n_j and a two-hop neighbor of the node n_i, can calculate its location in the coordinate system of node n_i. As the coordinate systems of nodes n_i and n_j have the same direction, the position of the node n_l is simply obtained as a sum of two vectors.

$$\vec{il} = \vec{ij} + \vec{jl} \tag{6.17}$$

This is illustrated in Figure 6.9. The same is applied to the 3-hop neighbors of node n_i that are within the transmission range of node n_l, if the coordinate system of n_l has the same direction as the coordinate systems of n_i and n_k. By receiving the position of node n_l in the coordinate system of node n_i, and adding this vector to their vector in the coordinate system of node n_l, they obtain their position in the coordinate system of node n_i. As shown in the following formula:

$$\vec{ij} = \vec{ik} + \vec{kl} + \vec{lj} \tag{6.18}$$

The same procedure is repeated for all nodes in the network, in order to compute their positions in the coordinate system of node n_i. The nodes that are not able to build their local coordinate system, but which communicate with at least three nodes that have already computed their positions in the reference coordinate system, can obtain their position in the reference coordinate system by triangle rules.

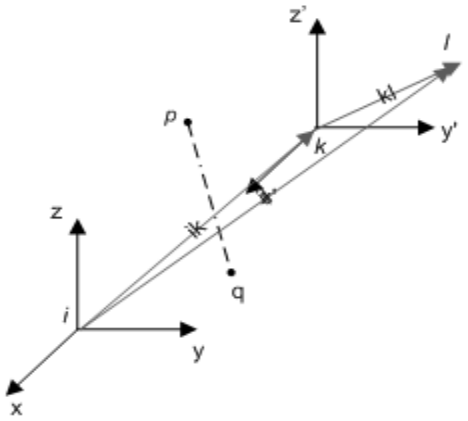

Figure 6.9: Location calculation in the second coordinate system.

6.5 Global Rigidity in Coordinate System Rotation

In the previous section we proposed a method to compute the relative locations of a set of nodes placed in the three-dimensional space, relying only upon the distances between the nodes. This problem is known as graph realization from the graph theory perspective. In this section we are concerned with the problem of determining if the

graph has a unique realization. For our purposes, translation, rotation and reflection of the entire graph are not considered to be different realizations.

The graph realization problem has been proven to be an NP-hard problem [Pri03]. Saxe has shown that the graph realization problem is a strongly NP-complete problem in one-dimension and a strongly NP-hard problem for higher dimensions [Ber96]. In other words, it is unlikely to find an efficient general algorithm to solve the problem.

The graph that is generated by the graph realization can be flexible, rigid, or globally rigid. A graph that continuously deforms, while still satisfying all the conditions is called a flexible graph; otherwise it is rigid. A rigid graph can still have more than one realization and may not be unique. A globally rigid graph is a graph that has a unique embedding. Figure 6.10, shows the flexible, rigid, and globally rigid graphs.

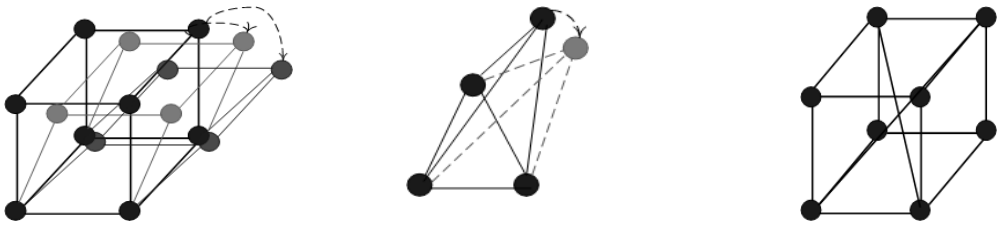

Figure 6.10: (a) Flexible graph, (b) Rigid graph, (c) Globally rigid graph.

Apparently, graphs with many edges are more likely to be rigid than those with only a few. Intuitively, the edges are constraining the possible movements of the vertices. In 3D space a set of n vertices has 3n possible independent motions.

It has been shown that for a graph to be globally rigid in d dimensions it must be (d+1)-connected and the removal of any edge must leave the graph rigid too. It is proven

that while these two conditions are necessary for a graph to be rigid, they are not sufficient.

To study the rigidity of the graph we can study the rigidity matrix. Each row in the matrix corresponds to an edge while each column corresponds to a coordinate of a node. Each row has 2d nonzero elements, one for each coordinate of the node connected by the corresponding edge [Ber96]. The non-zero values are the differences in the coordinate values of the two nodes. The rank of this rigidity matrix can be used to predict if a graph is rigid or not. It is shown that an obtained graph is rigid if and only if its rigidity matrix has a rank equal to the result of Equation 6.19 [Ber96].

$$\begin{cases} nd - d(d+1)/2 & \text{if} \quad n \geq d \\ n(n-1)/2 & \text{otherwise} \end{cases} \tag{6.19}$$

It has also been shown that a graph with $2n-3$ edges is rigid in two dimensions if and only if no subgraph G' has more than $2n'-3$ edges [Ber96]. Although this is a necessary condition for rigidity in three-dimensions, it is not a sufficient condition. There are different algorithms for testing rigidity in 2D that run in $O(n)$, $O(n^2)$ time. In three-dimensions, there is no graph theoretic characterization of rigidity. One approach to determine rigidity is to calculate the rank of the rigidity matrix by symbolically constructing the determinant [Pri03]. The determinant of this matrix can have an exponential number of terms, so this calculation requires an exponential amount of time. If the graph is rigid then almost any realization will generate a rigid graph. We can simply select a random realization of the graph, construct the rigidity matrix and

determine its rank. If the rigidity matrix rank is equal to Equation 6.19, then the graph is rigid. A lower rank determines that the graph is flexible.

6.6 Node Placement

As noted before, the success of the location discovery algorithm depends on network connectivity and, as a result, on node density. Node density is the number of nodes in unit area (2D) or space (3D). If N nodes are deployed in volume V the node density is: $\frac{N}{V}$. In node deployment one of the main metrics of interest is the probability that any node in the network has four or more neighbor nodes. Assuming that nodes are uniformly distributed in the cube of surface L and height of h, the probability that a node has n neighbors is:

$$p(n) = \binom{N-1}{n} P_{R_s}^{n} \left(1 - P_{R_s}\right)^{N-n-1} \tag{6.20}$$

$$P_{R_s} = \frac{4\pi R_s^3}{3L^2 h}$$

Where N is the total number of nodes deployed in a cubic field of volume $L^2 h$. The probability that a node has n_{thresh} or more is:

$$p(n \geq n_{thresh}) = 1 - \sum_{i=0}^{n_{thresh}-1} p(i) \tag{6.21}$$

As N approaches infinity, equation 6.21 converges to a Poisson distribution.

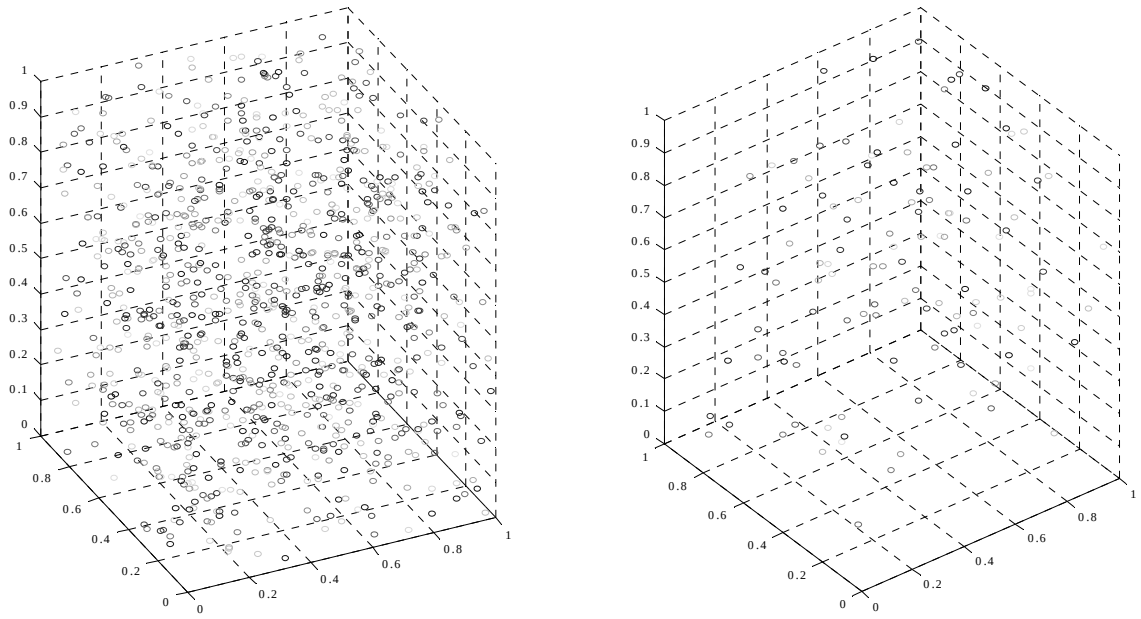

Figure 6.11: When the density of the nodes increases, the number of neighbors increases.

6.7 Objective Function Selection

The overall performance of the distributed location discovery algorithm depends on the quality of the node position calculation in each stage of location estimation. To optimize node locations, we define a set of objective functions that provide metrics for determining the likelihood that a particular estimated location is a promising choice.

Objective functions are formed for both the average and the maximum location error to evaluate quality of the node position in each step in the location discovery process.

The objective function used to estimate the average location error is expressed as:

$$E_{d,avg} = \frac{1}{N}\sum_{i=1}^{N}\left|R_{is} - \left\|p_i - p_s\right\|\right| \tag{6.22}$$

And the objective function used to estimate the maximum location error is:

$$E_{d,\max} = \max_{i=1\ldots N}\left|\frac{R_{is} - \left\|p_i - p_s\right\|}{R_{is}}\right| \tag{6.23}$$

In the above equations, N is the number of neighbor beacon, nodes with previously estimated locations, that node n_s uses to estimate its location. The overall error function used to evaluate the overall quality of the solution is:

$$E_{overall,avg} = \sum_{i=1}^{N}\sum_{j=1}^{i-1}\left|D_{ij} - \left\|p_i - p_j\right\|\right| \tag{6.24}$$

This objective function calculates the sum of the differences between the measured distance from node n_i to the node n_j, and the distances between the estimated locations of nodes n_i and n_j in the solution.

For the results presented in this paper we used the overall error in node location to evaluate error in our positioning algorithm.

6.8 Algorithm Description

To reconstruct a three-dimensional set of points using noisy measurement information about the distances between points, we propose the following algorithm. Here, we assume that errors in the distance measurements lie within a certain tolerance.

1. **Find-number-of-neighbors();**
2. **Build-topology-graph();**
3. **Rank-graph-nodes();**
4. **Build-localCoordinate-for-each-node();**
5. **Find-location-of-1hop-neighbors-ineach-coord();**
6. **Rotate-CoordinateSystems();**
7. **Find-location-of-khop-for-each-node();**
8. **Use-optimization-to-find-the-solution();**

Figure 6.12: Global flow of the algorithm

The first step in our localization algorithm is to find the number of neighbors for each node. Breadth-first Search (BFS) is used for neighbor discovery at this point in the algorithm. The total running time of BFS is O(V+E), where V is the total number of nodes in the network and E is the number of connections between them. Each node

periodically sends its neighbor table to the other nodes in its transmission range. In this way, nodes can update their information about the network topology. Nodes also exchange their local table and find their k-hop neighbors. It is assumed that all the messages are exchanged correctly. Neighbor information may be obtained using radio links, while range information may be obtained using radio coupled with ultrasound or acoustic signals.

The second step is to build a graph theoretic model for the ad hoc network. As explained before, each node in an ad hoc network is represented as a node, or vertex, V, in a graph. There is an edge, E, between two vertices if two nodes are 1-hop neighbors of each other.

In the third step, nodes in the network set a variable to inform their neighbors about their status. If a node has less than four neighbors, it cannot establish its location, and sets its stray flag to be true. If the node has greater than or equal to four neighbors, but it has not previously calculated its location, it sets its getFinal flag to true and its getLocation to false. If the node has already calculated its location in the coordinate system of another node, it sets getLocation to true and specifies the ID of the node that it calculated its location relative. A node may calculate its location in the coordinate system of more than one node.

In the fourth step, each node establishes its local coordinate system. For a node to calculate its local coordinate system, it should have more than four neighbors in the transmission range of each other. Further, the node should be a vertex of a full mesh subgraph. If a node has more than one set of four nodes that establish a full mesh, there are different sets of selection between these nodes. In this case, selection of the nodes

should be based on two different criteria. The first is motivated by the fact that when the distances between the nodes are greater, the coverage of the nodes is greater. Although the error in distance is larger for larger distances but as for the first node error is almost linear with distance it is not a very important condition. The second criterion is that we select the nodes with the highest number of 1-hop and 2-hop neighbors. With this selection we increase the coverage range of the localization algorithm. Although both of the above arguments are correct but by running some simulations we get the conclusion that to have the best performance from the network we should consider both of these fact. So in our algorithm, we select the nodes with higher number of 1-hop and 2-hop neighbors and the larger distances from the center node. After selection of the nodes, we use the same procedure described in Section 6.2 to calculate local coordinate system of the nodes in the network.

In the fifth step, we calculate location of the nodes based on the range difference method that is discussed in Section 6.2. As each node calculates its location, it sets the getLocation flag and specifies the local node that it uses to calculate its location.

In the sixth step, all 1-hop neighbors in the network calculate their location. In this step, the center node finds its 2-hop neighbors. It searches for 1-hop neighbors of its neighbors and identifies one that has not calculated its location in its coordinate system. For this purpose, a 1-hop neighbor of the center node should rotate its coordinate system to the coordinate system of the center node and calculates its 2-hop neighbors in its local coordinate system. This procedure is explained in Section 6.4. We repeat the same process to calculate location of the k-hop neighbors.

Throughout the location calculation in the sixth step the error propagates in the network as the k-hop neighbor calculates its location based on the k-1-hop neighbor that contains error in the location and the distances between them.

During the location calculation, we specify the order in which nodes in a network should estimate their locations such that the location error is minimized. Instead of accepting the first calculation of location as the final location, a node continues to accept location information from other nodes and adjusts its position estimate accordingly.

If a node has N neighbors with previously calculated locations, in 3D there are:

$$M = \sum_{i=4}^{N} \binom{N}{i} = \binom{N}{4} + \binom{N}{5} + \ldots + \binom{N}{N} \tag{6.25}$$

possible choices for its location (M is the total number of intersections). If we have N>4 distance measurements to a set of N nodes, we can combine this information into different groups, or subsets, in which each group represents a possible set of nodes which can be used for calculating position. In our algorithm, we consider all of these combinations and run the objective function for each one to select the one with the best solution. In each of the steps described above a node checks its objective function to verify the accuracy of the location calculation. If the threshold is less than the one specified the node cannot calculate its location and it should restart the location calculation in another way. In each step, error location estimation will be done to calculate the objective function to be smaller than an appropriate value. This procedure is explained in more detail in Section 6.7.

Before any coordinate system rotation we check for the graph rigidity. We explain the need for the graph rigidity in Section 6.5.

At the end of running this algorithm, each node knows the topology of the whole network and location of the other nodes in its local coordinate system.

Chapter 7 : Performance Analysis of Localization Algorithm

In this section, we study performance of the proposed location discovery algorithm. Different parameters affect the performance of the location discovery procedure such as the magnitude and distribution of the measurement errors and transmission range. This section is organized in the following way. We first discuss the methods to evaluate performance of a location estimation method. In Section 7.3, we study performance of the proposed location discovery algorithm based on the performance metrics that we describe on Section 7.1.

7.1 Performance Evaluation of the Location Estimation Method

Location estimation performance can be measured by Circular Error Probability (CEP), Dilution of Precision (GDOP), Mean Square Error (MSE), Cramer-Rao Lower Bound (CRLB), and Graph Rigidity Ratio.

CEP is based on the variances of the location estimate in the x, y, and z directions. This gives an overall measure of the location estimator accuracy. GDOP is a measure of the location estimation performance depending on the actual location of a node relative to others. Every location estimation performance can be evaluated by comparing the position estimator's MSE to the Cramer-Rao Lower Bound (CRLB). CRLB is the theoretical limit for the variance of the estimator's output. Graph Rigidity Ratio provides

information about the structural error of the graph. We briefly consider the definition and value of each of these performance measures.

7.1.1 Circular Error Probability (CEP)

If an estimator is unbiased, CEP describes the scattering of the location estimate around the true location of the node. CEP is defined as the radius of a circle around the estimator's location bias that contains half of the generated estimates. CEP, within an accuracy of 10%, is given as: $CEP \cong 0.75\sqrt{\sigma_x^2 + \sigma_y^2 + \sigma_z^2}$, where σ_x^2, σ_y^2, and σ_z^2 are the variance of the location estimates $\hat{x}$, $\hat{y}$, and $\hat{z}$ respectively.

7.1.2 Geometric Dilution of Precision (GDOP)

GDOP is the standard deviation of the range measurements [6]. Mathematically, it is defined as the ratio of the RMS position error to the RMS ranging error, that is:

$$GDOP = \frac{\sqrt{\sigma_x^2 + \sigma_y^2 + \sigma_z^2}}{\sigma_s} \tag{7.1}$$

From the above equation, it is evident that the GDOP is directly proportional to CEP, which means that if the scattering of the position estimate around the true position of the unknown node is small the estimator's output variance will be small as well. The smaller the Root Mean Square (RMS) position estimate error, the better the performance of the estimator.

7.1.3 Mean Square Error (MSE)

MSE is the square of the distance between a true node position and an estimated node position. For most of the results in chapter 5 and 6, we will use RMS error as the performance measure of interest.

$$MSE = (x - \hat{x})^2 + (y - \hat{y})^2 + (z - \hat{z})^2 \tag{7.2}$$

$$RMS = \sqrt{MSE} \tag{7.3}$$

7.2 Error Effects in the Positioning Algorithm

In this section we are trying to assess the effects of error in the distance measurement on the overall performance of the localization algorithm. As discussed in Section 6.2, with the range difference method studied in this thesis, the error in the node location increases as the error in distance increases. In cases that the initial node locations are also erroneous, the error in unknown node location increases to the higher extent. As our localization algorithm is distributed, each node calculates its location based on the location of previously calculated nodes and the erroneous distances. In this way error propagates throughout the network.

Figure 7.1 shows the propagation of error in the network when the standard deviation of error is v=0.005m, the dimension of the area is [87, 36, 4] meters, the transmission range is Rs=50m, and the number of nodes in the network is equal to 40. In this condition the density of the nodes is high and most of the nodes are 1-hop or 2-hop neighbors of each other. As shown in the figure, the first four nodes in the network have

smaller errors in their locations in comparison with the other 1-hop neighbors. These nodes are the ones that were used to set up the local coordinate system. As shown in the X-axis of Figure 7.1, Hop Number (Hop Hierarchy) defines the order in which the nodes calculate their local coordinate system. In this figure, hop number 1 and hop number 2 which correspond to origin of the coordinate system, and establish the X-axis, have a location error almost equal to zero. Mean location error increases for hop number 3 and 4, which respectively correspond to the node that establishes the XY plane and the node that specifies the direction of the Z-axis. Location error for the other nodes in the network, nodes 5 through 8, have almost the same value. The mean location error for 2-hop neighbors is more than the location error in the 1-hop neighbors and they almost have the same value. Briefly, this is because these nodes estimate their location based on the distances between them and the error in the measured distance is the main source of error. For the other nodes, error in the location is due to error in the measured distance and in the initial locations of the nodes.

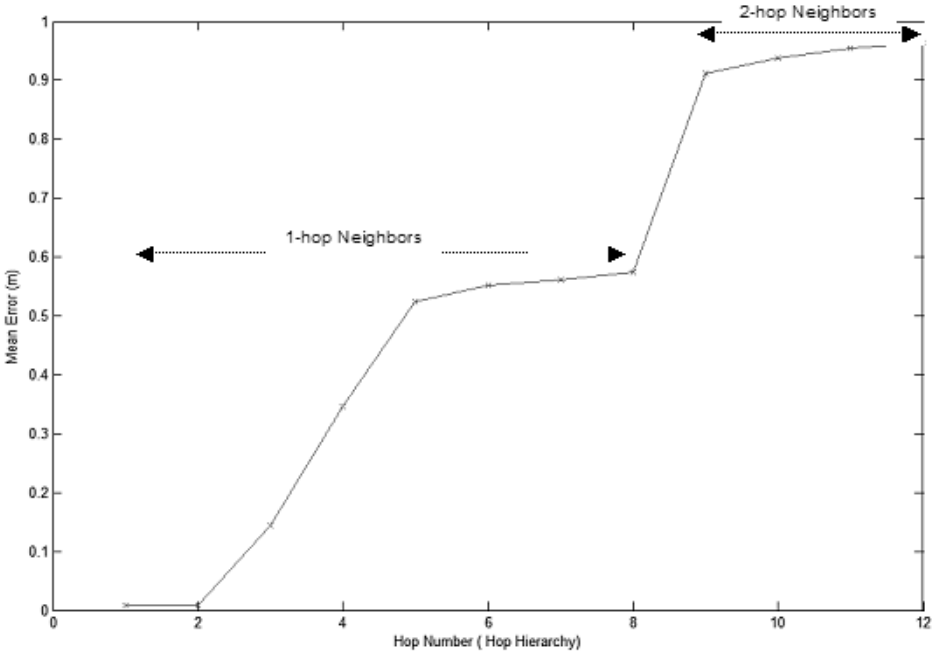

Figure 7.1: Error propagation in the node location.

Figure 7.2 shows the error propagation in the network when the node density is lower than the case shown in Figure 7.1. This case is for a situation where 35 nodes are placed in a [110, 50,4] meter volume with a transmission range of Rs=50. In this case, the error is larger, and propagates more quickly. It can be seen that no more than 3-hop neighbors are shown in the figure. The reason is that for higher order nodes, in addition to the error in the node location and distances between the nodes, there is an error associated with the rotation of the coordinate system. So the amount of error is high and the objective function that we used is no longer satisfied. All the results in this chapter are based on Monte Carlo simulation with more than 200 runs.

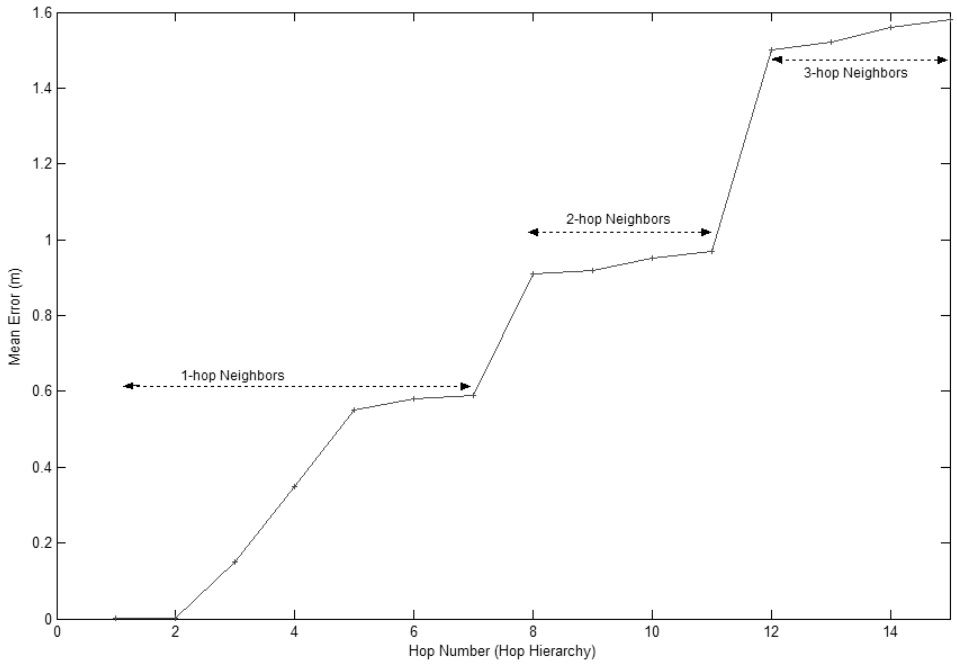

Figure 7.2: Error propagation in the node location.

Figure 7.3 shows the Cumulative Distribution Function (CDF) of the error variance (m) when the variance of the measurement error in the distance differs. It has been shown that when the standard deviation of error is 0.0001m, the CDF of the MSE is very close to zero. In this case we do not have out of range nodes and almost all the nodes can calculate their location in the network. If the measurement error increases, the error in the location estimation increases more rapidly. As variance of error in the distance measurements increases from to 0.0001 to 0.001 the probability of the error in location estimation increases from 0.0001 to 0.0006. In some cases it is not possible to calculate location of the nodes because they are out of range in the network. In many other conditions the error in the distance is so high that the lines do not intersect each other. These conditions are identified by the objective function and eliminated. In this

way error does not propagate in the network more slowly. Figures 7.3 and 7.4 show the CDF of the variance of error when the variance of error in distance is different.

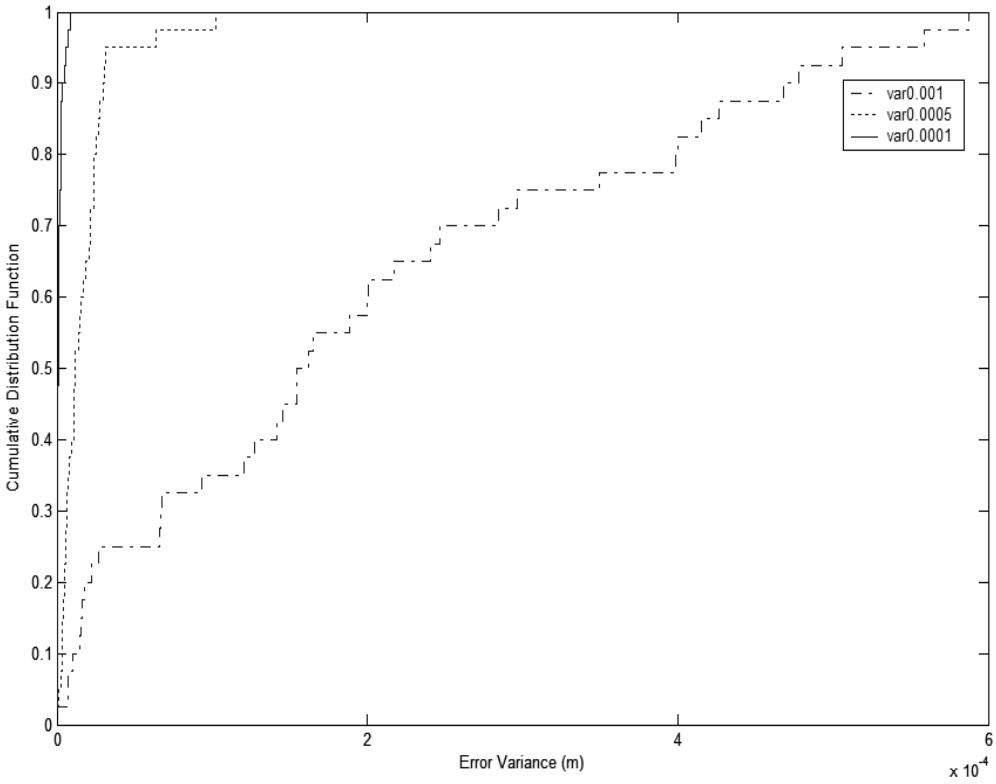

Figure 7.3: Cumulative distribution of the error.

Figure 7.4 shows the CDF of the error variance when the variance of the measurement error in the distance differs. It has been shown that when the standard deviation of error is 0.05m, we have large errors. If the measurement error increases, the error in the location estimation increases with a greater amount. The threshold variance of 0.05 is used for these calculations.

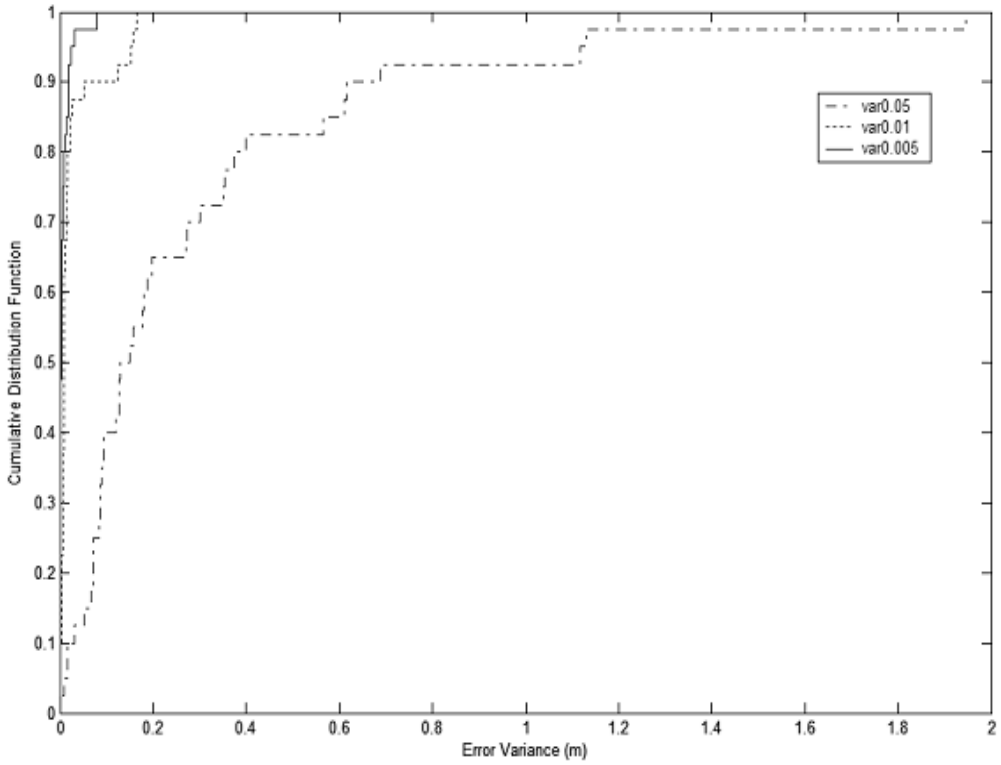

Figure 7.4: Cumulative Distribution of error.

Figures 7.5, 7.6, and 7.7 show the CDF of the Error variance for the distance measurements when the density of the nodes in different areas is different from each other. The first case in these figures is for a condition where 70 nodes are placed in a cube of 105m, 43m, and 10m with the transmission range of 50m. In case 2, 98 nodes are placed in a cube with dimensions 118m, 49m, and 11m with the transmission range of 50m for each node. The third case is where 120 nodes are placed in a cube with dimensions 151m, 62m, and 14m with the transmission range of 50m. The fourth case is

the same we studied before where 40 nodes are placed in a cube of the dimensions 87m, 36m, and 4m with the transmission range of each node equal to 50m. All these conditions represent different node density. In Figure 7.5, where the density of the variance of error is 0.00001, the probability of error for case 4 is smallest and is equal to 0.00001. Density of the nodes for case one is 7.98 that is the larger than the other cases.

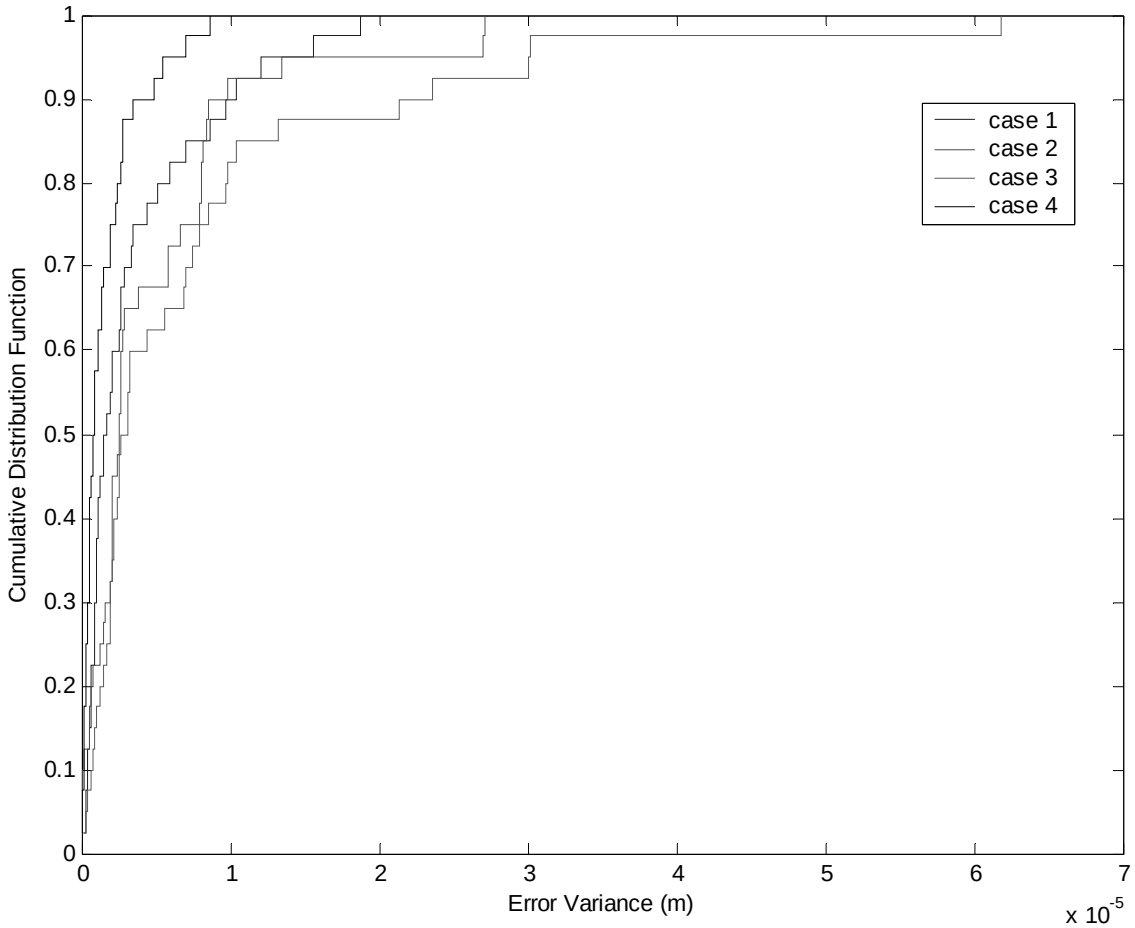

Figure 7.5: Cumulative Distribution of error with the distance error variance of 0.0001

In this figure case 3 with the node density of 2.29 has the probability of error equal to 0.00006, which is higher than the other cases.

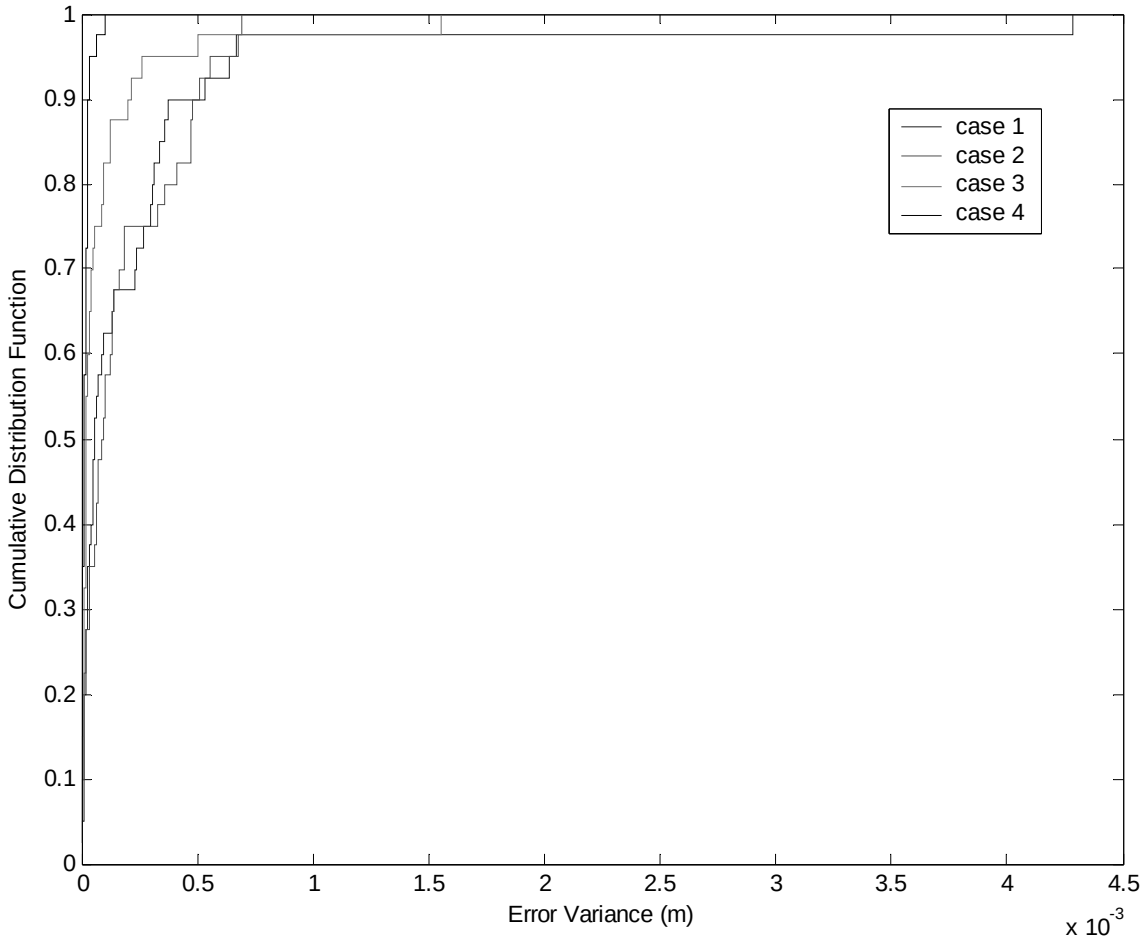

Figure 7.6: Cumulative Distribution of error with the distance error variance of 0.0005

Figure 7.6 shows the probability of error where the variance of error in distance is 0.0005. In this figure the same as Figure 7.5 variance of error for case 4 with the highest density is smaller then the other case.

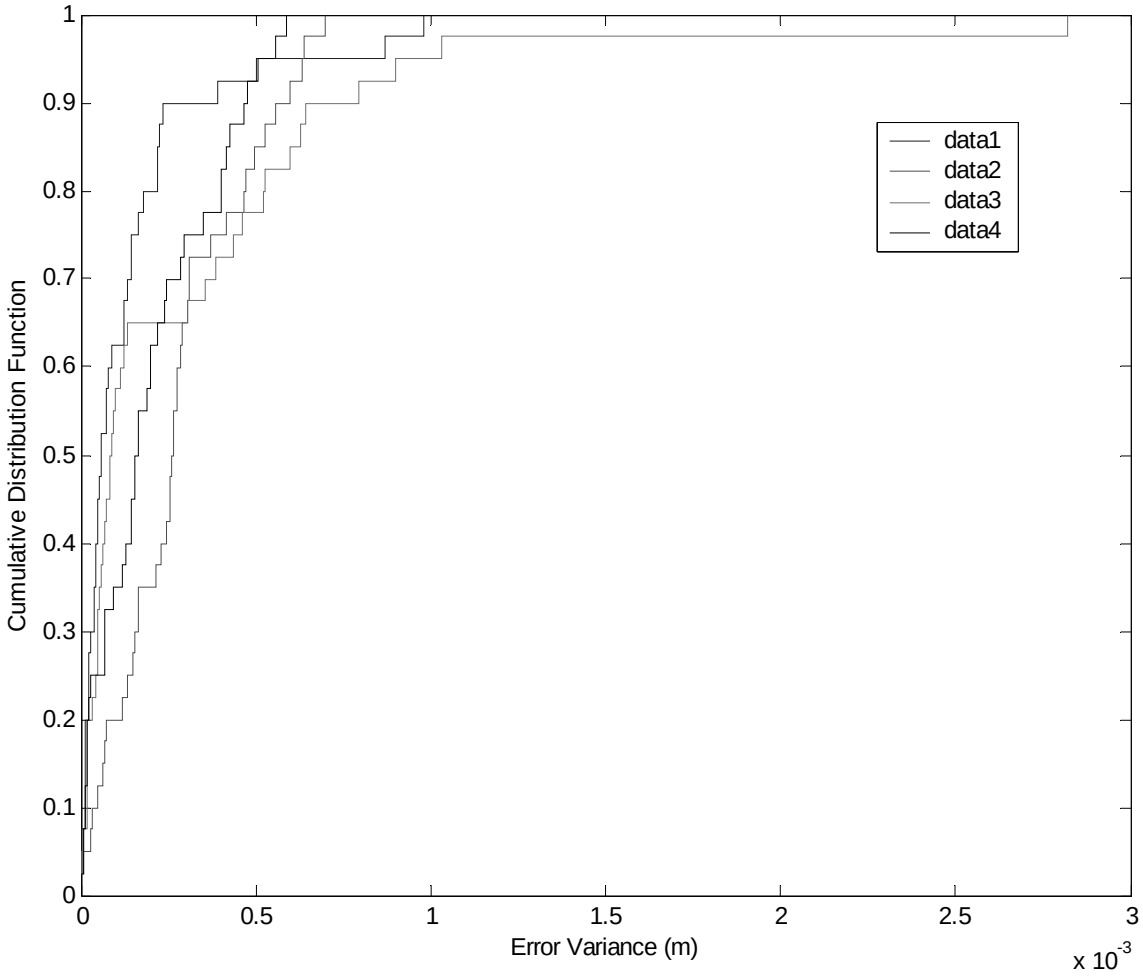

Figure 7.7: Cumulative Distribution of error with the distance error variance of 0.001

Figure 7.8 shows the coverage of the proposed location discovery algorithm. This figure shows the percentage of ad hoc nodes that are able to find their physical location after running the location discovery procedure. Figure 7.8 shows the number of located nodes when the transmission range differs from 5m to 60m and number of nodes differs from 20m to 60m. When the density of the nodes is smaller, with the same transmission range the number of located nodes is less than the case when the node density is higher. As shown in Figure 7.8, the transmission range is more important in determining connectivity than node density.

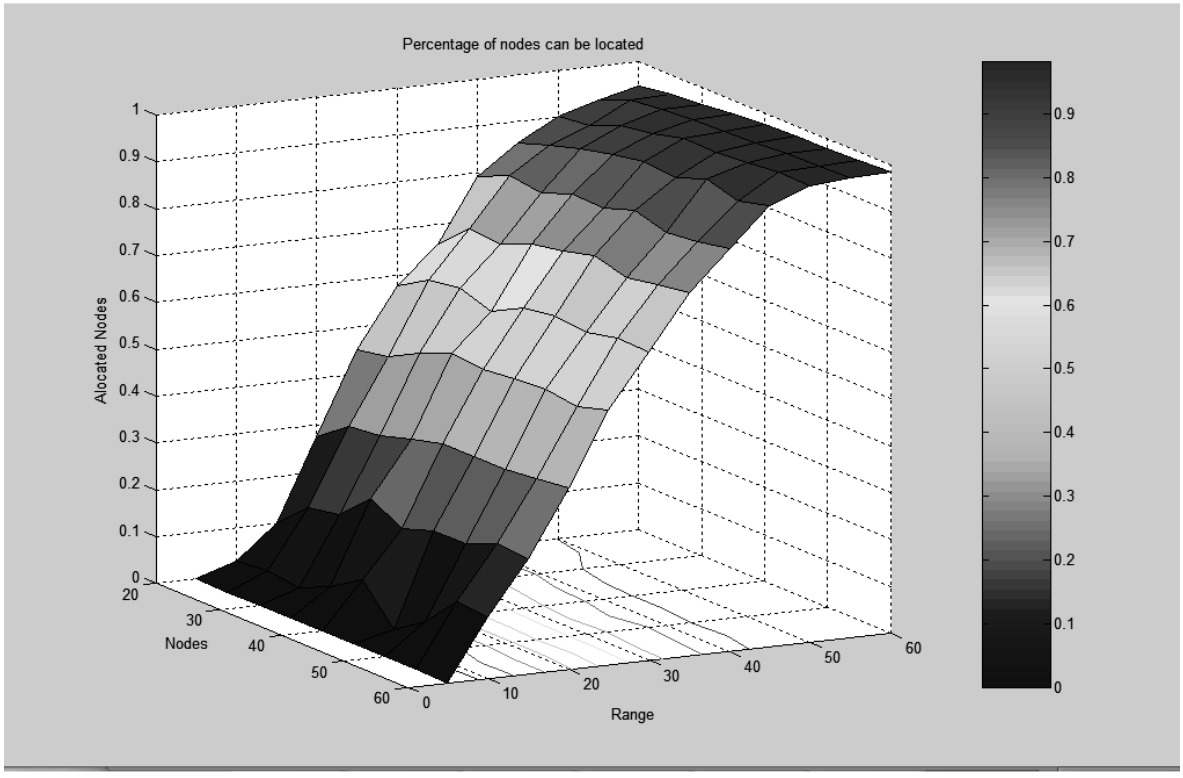

Figure 7.8: Percentage of nodes that can find their location with the distributed algorithm

7.3 Summary

In this section we evaluated the location discovery algorithm proposed in this thesis. From the results of simulation, we see that error propagates in the network and this leads to global errors. To reduce this effect we use an objective function to avoid accumulation of error. We also showed that when the variance of the error increases, the error in the location of the nodes increases. Our algorithm has good performance with the variance of error up to v=5cm. In this case the variance of error in the location is up to 2m. While in the case that variance=1cm or less the variance of the error in the location estimation is less that 20cm.

As the density of nodes increase in the network the probability of the error decreases with node density. In this algorithm coverage increases as the transmission range increases and this is because the density of the nodes increases with the coverage.

Chapter 8 : Conclusion

Providing reliable communication and geolocation in wireless ad hoc network is one of the most important tasks in wireless ad hoc networks. Almost all applications required reliable communication in different environments and accurate information about the physical location of the nodes in the network. In this thesis we addressed multi-hop communication in different wireless channels and location discovery problem in wireless ad hoc networks, by developing geometric and graph theoretic abstractions of the problem.

For the communication section, we first classified routing protocols based on the channel characteristics. We implemented an indoor channel model for ns-2 simulator and studied the results of simulation in indoor, outdoor, and Rayleigh fading with two-ray model condition. Our results reveal the fact that in general for our simulation parameters, the AODV routing protocol performs the best among the other studied routing protocols. We also concluded that the studied routing protocols assume that a wireless link is either good or bad and that if a link is useful for delivering routing packets, then the link is useful for delivering data. This assumption is the major source of drops in these routing protocols since AODV uses both hop-by-hop and on-demand methods, it performs a little better than the other routing protocols. We also indicate that the main reasons for packet drops in wireless ad hoc routing protocols are mobility, congestion, and wireless channel. It was assumed that design of the routing protocols only could reduce the effect of mobility and congestion, while our results shows that design of the routing protocol can

also overcome the effects of the wireless transmission error. The reason for this conclusion is that the same channel model effects routing protocols.

For geolocation, we proposed a fully decentralized and distributed 3D geolocation algorithm that uses distances between the nodes to calculate the location of the nodes in a setting. In this algorithm, nodes start from a completely random initial coordinate assignment and converge to a consistent solution using only local interaction. We discussed the error propagation problem that results in bad overall position calculation and uncertainty in node locations. We used an objective function to calculate the solution at each step of a process which minimizes error propagation in network. We also studied the rigidity of the solution. We further simulated the algorithm and studied the performance of our proposed algorithm. Our results show that when the variance of error in distance measurement is 5 cm or less, we can determine the location of a node to within 2m. When the variance of error in the range measurements is less than 0.0001 m the error in the estimated location in less than 0.0001m.

Chapter 9 : Future work

In this section, we briefly outline some of potential directions for future research related to ad hoc routing protocols and location discovery in wireless ad hoc networks. In addition to the improvements and generalizations, such as improving the algorithm used in this thesis and more accurate statistical modeling, there are some major research opportunities:

- Using anchor nodes along with the numerical analysis to improve the performance of the geolocation algorithm,
- Writing a common software for testing different geolocation algorithms with a wireless channel model close to reality,
- Improving ad hoc routing protocols with a layer that predicts the channel characteristics and improves the routing protocols QoS,
- Calculating the GDOP for our decentralized localization algorithm,
- Calculating the Cramer-Rao Lower bound for this algorithm.

Publications:

[Aky02] Akyildiz, I.F., Su, W., Sankarasubramaniam, Y., and Cayirci, E., ``A Survey on Sensor Networks, IEEE Communications Magazine," Vol. 40, No. 8, pp. 102-116, August 2002.

[Ahl03] H.AhleHagh, W.R.Michalson, and D.Finkel, “Statistical characteristics of wireless network traffic and its impact on ad hoc network performance”, Advanced Simulation Technologies Conference April 2003, Orlando, USA, pp. 66-71.

[Bah00] P. Bahl, V. N. Padmanabhan, “RADAR: an in-building RF-based user location and tracking system”. Proceedings IEEE INFOCOM 2000., Apr. 2000, vol.2, p.775-84.

[Bas98] S. Basagni, I. Chlamtac, V.R. Syrotiuk, and B.A. Woodward, "A distance routing effect algorithm for mobility (DREAM)," in Proceedings of the ACM/IEEE International Conference on Mobile Computing and Networking (Mobicom), 1998, pp.76-84.

[Ber96] Berger, B., Kleinberg, J., and Leighton, T. “Reconstructing a three-dimensional model with arbitrary errors”. In Proceedings of the 28th ACM Symposium on Theory of Computing (1996).

[Beu99] J. Beutel, "Geolocation In A PicoRadio Environment." M.S. Thesis, ETH Zurich, Electronics Lab, 1999.

[Bro98] J. Broch, D. A. Maltz, D. B. Johnson, Y. C. Hu, and J. Jetcheva, “A Performance Comparison of Multi Hop Wireless Ad-Hoc Network Routing Protocols,” in Proc. of the Fourth Annual ACM/IEEE International Conference on Mobile Computing and Networking (MOBICOM ’98), Dallas, TX, October 1998.

[Cam02] Tracy Camp, Je. Boleng, Brad Williams, Lucas Wilcox, William Navidi "Performance Comparison of Two Location Based Routing Protocols for Ad Hoc Networks", INFOCOMM 2002

[Cor96] S. Corson, J. Macker, and S. Batsell, "Architectural considerations for mobile mesh networking," May 1996.

[Del80] J. M. Delosme, M. Morf, and B. Friedlander, "A linear equation approach to locating sources from time-difference-of-arrival measurements," in Proc. ZEEE Int. Con$ Acoustics, Speech, and Signal Processing (Denver, CO), 1980, pp. 818-824.

[Fee99] Feeney L.M. "A Taxonomy for Routing Protocols in Mobile Ad Hoc Networks" SICS Technical Report T99:07. Swedish Institute of Computer Science, Kista, Sweden, October 1999.

[Fri87] B. Friedlander, "A Passive Localization Algorithm And Its Accuracy Analysis," IEEE Trans. Ocean Engineering, Vol. OE-12, No. 1, pp. 234-245, 1987.

[Gup00] Piyush Gupta,"Design and Performance Analysis of Wireless Networks", Ph.D. Thesis, University of Illinois, August 2000

[Ko98] Y.Ko and N.H.V aidya, "Location-aided routing (LAR) in mobile ad hoc networks," in Proceedings of the ACM/IEEE International Conference on Mobile Computing and Networking (Mobicom), 1998, pp.66–75.

[Ho02] Wing Ho Yuen and Roy D. Yates, " Inter-relationships of Performance Metrics and System Parameters for Mobile Ad Hoc Networks ", Proc. IEEE MILCOM 2002

[Ho04] K. C. Ho, H. Parikh, L. Kovavisaruch, "Source Localization Using TDOA with erroneous receiver positions", IEEE International Symposium on Circuits and Systems, 23 May 2004 – 26 May 2004, Vancouver, Canada

[How01] A. Howard, M. J. Mataric, and G. S. Sukhatme. “Relaxation on a mesh: a formalism for generalized localization”. In Proc. IEEE/RSJ Int'l Conf. on Intelligent Robots and Systems (IROS01), pages 1055-1060, 2001.

[Lee00] Sung-Ju Lee. “Routing and Multicasting Strategies in Wireless Mobile Ad hoc Networks.” University of California, Los Angeles, Computer Science Department, September 2000.

[Lu] Y. Lu, Y. Zhong and B. Bhargava, “Packet Loss in Mobile Ad Hoc Networks”, Technical Report CSD-TR 03-009, Department of Computer Sciences, Purdue University.

[Lu03] Y. Lu, W. Wang, Y. Zhong and B. Bhargava, “Study of Distance Vector Routing Protocols for Mobile Ad Hoc Networks”, in Proceedings of IEEE International Conference on Pervasive Computing and Communications (PerCom), Dallas Fort Worth, Texas, Mar. 2003.

[Mau01] M. Mauve, J. Widmer, and H. Hartenstein. “A survey on position-based routing in mobile ad-hoc networks” In IEEE Network, November 2001.

[Mes] http://www.meshnetworks.com/

[Mic03] W.R.Michalson, H.AhleHagh, and I.Progri, "Dynamic Node Location in an Ad Hoc Indoor Communications and Positioning Network", in Proc. ION-GPS, Portland, OR, Sep. 2003.

[Mob] http://www.scires.com/mobileroute.htm

[Net] Network Simulator, ns-2, http://www.isi.edu/nsnam/ns/.

[Nov] http://www.bitpipe.com/detail/ORG/974220335_924.html

[Pah95] K. Pahlavan and Allen H. Levesque,"Wireless Information Networks", A Wiley-Interscience Publication,1995

[Par96] Parkinson and Spilker "Global Positioning System: Theory and Application II" Washington, D.C.: AIAA, 1996.

[Per94] C.E. Perkins and P. Bhagwat, "Highly Dynamic Destination-Sequenced DistanceVector Routing (DSDV) for Mobile Computers," ACM SIGCOMM: Computer Communications Review, vol.24, no.4, pp.234-244, October 1994

[Per02] C. E. Perkins, E. M. Royer, and S. R.Das, "Ad Hoc On-Demand Distance Vector (AODV) Routing," in draft-ietf-manet-aodv-10.txt, January, 2002

[Pri00] N. B. Priyantha, A. Chakraborty, H. Balakrishnan. "The Cricket Location-Support system." Proc. 6th ACM MOBICOM, Boston, MA, August 2000.

[Pri01] Nissanka B. Priyantha, Allen Miu, Hari Balakrishnan, Seth Teller, The Cricket Compass for Context-Aware Mobile Applications, Proc. 7th ACM MOBICOM, Rome, Italy, July 2001.

[Pri03] N. B. Priyantha, H. Balakrishnan, E. Demaine, and S. Teller, "Anchor-free Distributed Localization in Sensor Networks", Tech Report #892, April 15, 2003, MIT Laboratory for Computer Science, http://nms.lcs.mit.edu/cricket/

[Pro03] I.F. Progri, "An Assessment of Indoor Geolocation Systems", Ph.D. Thesis, Worcester Polytechnic Institute, (May 2003)

[Pun00] R. Punnoose, P. Nikitin, and D. Stancil, "Efficient Simulation of Ricean Fading within a Packet Simulator," in IEEE Vehicular Technology Conference, pages 764-767, 2000

[Obr98] K. Obraczka and G. Tsudik. “Multicast routing issues in ad hoc networks”. In Proc. of IEEE ICUPC, Oct 1998.

[Sam00] Samir R. Das, Charles E. Perkins, and Elizabeth M. Royer. “Performance Comparison of Two On-demand Routing Protocols for Ad Hoc Networks” Proceedings of the IEEE Conference on Computer Communications (INFOCOM), Tel Aviv, Israel, March 2000, p. 3-12

[Sav01] Savarese, C., Rabaey, J., AND Beutel, J. “Locationing in Distributed Ad-Hoc Wireless Sensor Networks.” In Proc. Of ICASSP (Salt Lake City, UT, May 2001), pp. 2037–2040.

[Sav02] Savarese, C., Rabaey, J., and Langendoen, K. “Robust Positioning Algorithms for Distributed Ad-Hoc Wireless Sensor Networks.” In USENIX Annual Technical Conference, General Track (Monterey, CA, June 2002), pp. 317–327.

[Savv01] A. Savvides, C. C. Han, and M. Srivastava. “Dynamic fine-grained localization in ad hoc networks of sensors”. In ACM/IEEE Int'l Conf. on Mobile Computing and Networking (MOBICON), July 2001.

[Savv02] A. Savvides, H. Park, and M. Srivastava. “The bits and flops of the n-hop multilateration primitive for node localization problems”. In 1st ACM Int'l Workshop on Wireless Sensor Networks and Applications (WSNA'02), pages 112-121, Atlanta, GA, Sept. 2002.

[Sch72] R.O. Schmidt, “A new approach to geometry of range difference location”, IEEE Trans. Aerosp. Electron. Syst., vol. AES-8, no. 6, pp. 821-835, Nov. 1972.

[Sch02] B. Schrick, M.J. Riezenman, "Wireless Broadband In A Box", Spectrum, pp. 38-43, June 2002.

[Shi01] E. Shih, S. Cho, N. Ickes, R. Min, A. Sinha, A. Wang, and A. Chandrakasan. “Physical layer driven protocol and algorithm design for energy-efficient wireless sensor networks.” In The seventh annual international conference on Mobile computing and networking 2001.

[Tak01] Mineo Takai, Jay Martin and Rajive Bagrodia “Effects of Wireless Physical Layer Modeling in Mobile Ad Hoc Network” Proceedings of the 2001 ACM International Symposium on Mobile Ad Hoc Networking & Computing (MobiHoc 2001*)*, October 2001. p. 87-94.

[Tan96] Tanenbaum, Andrew S., Computer Networks, Prentice Hall Inc, USA, 1996

[War97] Andy Ward, Alan Jones, Andy Hopper. A New Location Technique for the Active Office. In IEEE Personal Communications, Vol. 4, No. 5, October 1997. 42-47.

[War99] A. Ward, "Sensor-driven Computing," Ph.D. Thesis, Cambridge University, U.K., (May, 1999)